EGU Journal of Renewable Energy Short Reviews

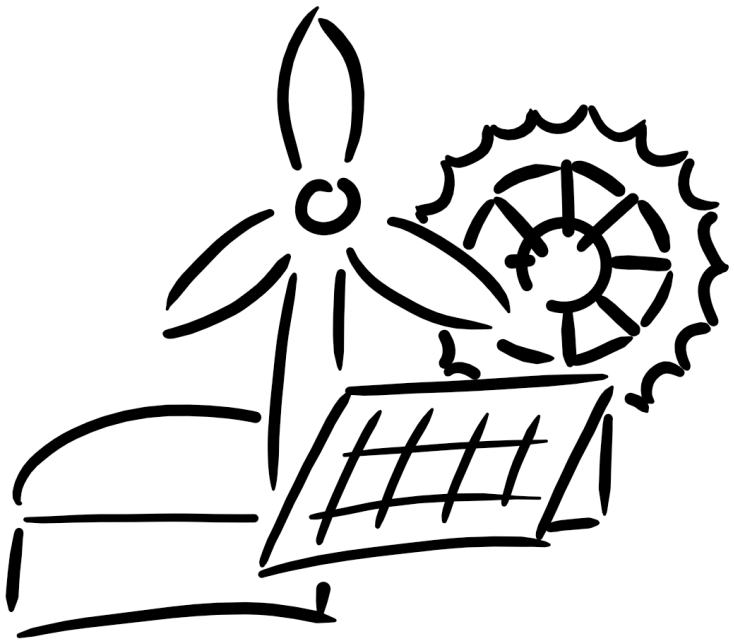

2021

Münster University of Applied Sciences

Preface

The *EGU Journal of Renewable Energy Short Reviews (EGUJRenEnRev)* is a teaching project rather that a regular scientific journal. To publish in this journal, it is a premise to take part in the master course *wind power, hydro power and biomass usage* at the faculty of Energy, Building Services and Environmental Engineering of the Münster University of Applied Sciences.

Students receive an equivalent of 2.5 credit points (European Credit Transfer and Accumulation System – ECTS) for their engagement in the course and for publishing a short review article of at most 3000 words in this periodical. The publication process closely mimics the typical publication procedure of a regular journal. The peer-review process, however, is conducted within the group of course-participants.

Although being just an exercise, we think that publishing the outcome of this course in a citable manner is not only promoting the motivation of our students, but may also be a helpful source of introductory information for researchers and practitioners in the field of renewable energies. We encourage students to write their articles in English, but this is not mandatory. The reader will thus find a few articles in German language. To further encourage students practicing English writing, perfect grammar is not part of the assessment.

We especially thank our students for working with LaTeX on Overleaf, although LaTeX is new to some of them. In this way, the editorial workload was reduced to a minimum. We also thank our students for sharing their work under the creative commons attribution licence (CC-BY). I appreciate their contribution to scientific information, being available to every person of the world, almost without barriers. I also thank the corresponding authors and publishers of the cited work, for granting permission to reuse graphics free of charge. All other figures had to be replaced or removed prior to publication.

Peter Vennemann and Christian Klemm in March 2021

https://doi.org/10.25974/ren_rev_2021_00

Contents

Hendrik Schmeinck

Impact of platform motion on the aerodynamic properties of FOWT 3

Jan-Niklas Linnenschmidt

Cost comparison between BOWT and FOWT 9

Dennis Tillenburg

Technical challenges of FOWT 13

Fiona Wagenknecht

Noise mitigation measures during offshore pile driving 19

Enno Tchorz

Review of sensorless MPPT systems 24

Joshua Steinigeweg

Review of the suitability of thermoplastic rotor blades in terms of the circular economy 30

Jurek Häner

Technologisches Lernen im Bereich Windenergie an Land 35

Alexander Hoge

Mitigating avian collision rates with wind turbines 42

Yannick Wittor

Electrostatic conversion of wind energy 48

Julian Speller

Self-build small wind turbines 53

Mark Scheffler

Low-Cost Hydropower Turbines for Developing Countries 57

Michael Hinse

The Wells turbine: state of the art 63

Niklas Olbertz

Sustainable hydro-power plants with focus on fish-friendly turbine design 67

Janik Budde

A comparison of PRO and RED 72

https://doi.org/10.25974/ren_rev_2021_00

Impact of wind and wave induced platform motion on the aerodynamic properties of floating offshore wind turbines

Hendrik Schmeinck *

Münster University of Applied Sciences, Stegerwaldstraße 39, 48565 Steinfurt, Germany

Abstract

With floating offshore wind turbines, new sources of wind energy can be used, which cannot be tapped into by bottom-fixed wind turbine systems. However, due to their design, they experience additional motion caused by wind and wave loads. The motions that are induced into the system have an oscillating course. This affects the aerodynamic properties of the wind turbine and leads to changes in the thrust force and power output of floating wind turbines compared to bottom-fixed wind turbines. Furthermore, the motions lead to an earlier breakdown of the helical wake structure behind the wind turbine and moreover lead to a decreased reliability of the rotor blades. Differences in the effects of wind and wave loads on the aerodynamic performance of floating offshore wind turbines supported by different platform systems were found.

Keywords: floating offshore wind turbine, unsteady aerodynamics, six-degree-of-freedom motions, failure probabilities, rotor blade reliability

1 Introduction

As part of the Green Deal the European Union has set itself the target of expanding the installed offshore wind power capacities to 60 GW by 2030 and 300 GW by 2050. In addition to bottom-fixed wind turbines, floating offshore wind turbines (FOWT) should also contribute to this [1]. With FOWT, wind energy can be harvested in areas with more than 40 to 50 m water depth, which cannot be reached by conventional bottom-fixed wind turbines [2]. Current floating platform systems are developed for water depth between 150 and 320 m [3–6]. They are therefore ideally suited to fully utilize the available capacities of shelf seas such as the North Sea. Nevertheless, Germany's EEZ[1] is less likely to come into question because here fixed systems are sufficient. But in other regions, such as Norwegian and British waters great potentials can be found. Altogether 66 percent of the North Sea water surface is located above water depths between 50 and 200 m [2]. However, the construction and operating of FOWT also creates new challenges. Through wind and wave loads the platforms experience translational (heave sway and surge) and rational (yaw, pitch and roll) motions [7]. These motions can have influence on the operating characteristics and the reliability of the rotor blades of FOWT. These review aims to summarize the effects of the influences. In particular, differences between different platform systems should also be noted.

2 Examined objects

2.1 Reference wind turbine

All studies which are mentioned in chapter 3 are based on the NREL[2] offshore 5-MW baseline wind turbine, which was defined by Jonkman et al. [8]. The main specifications of this wind turbine are listed in table 1.

Tab. 1: Specifications of the NREL 5-MW [8]

rated power	5 MW
hub height	90 m
shaft and hub tilt angle	5°
rotor orientation	upwind
number of blades	3
rotor diameter	126 m
control	variable speed, collective pitch
drivetrain	multiple stage gearbox
cut-in wind speed	3.0 m/s
rated wind speed	11.4 m/s
cut-out wind speed	25.0 m/s

*Corresponding author: hendrik.schmeinck@fh-muenster.de.

[1] Exclusive Economic Zone

[2] National Renewable Energy Laboratory

https://doi.org/10.25974/ren_rev_2021_01

2.2 Floating foundation

There are three primary floating platform constructions. One of them is the TLP[3], which is composed of an over-buoyant platform and moored by high tension lines. Due to the tension the system is dynamically stiff and can mitigate the dynamic stimuli from the wind and wave loads. Another system is the spar-buoy platform. It achieves its static stability due to its deep draft, combined with ballast weights. Furthermore, it is fixed by mooring lines to prevent drifting. The barge platform gets its stability from its large waterplane area and its distributed buoyancy. It is the cheapest and simplest system but due to its shallow draft is also the system with the greatest platform motions [7]. Another frequently examined platform type is, in addition to the three primary platform systems, the OC4[4] semi-submersible platform. It is made up of one main column on which the tower is attached. Three additional columns are attached to the main column with an offset of 120° through a series of pontoons and cross braces [5]. The three primary platform types and the OC4 platform are shown schematically in figure 1.

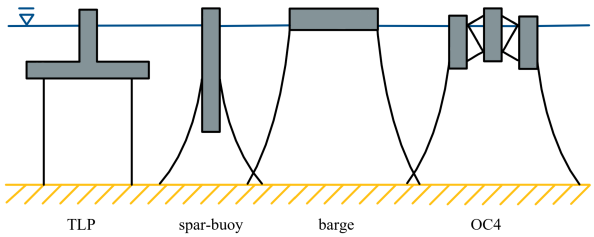

Fig. 1: Different types of floating foundations based on Lee and Lee [7] and Sebastian and Lackner [9]

3 Impact of platform motions

3.1 Impact on the aerodynamic performance

The waves on the sea exert direct forces on the platform. Simplified the waves are assumed to be periodic sinusoidal oscillations. Incoming waves pass on their periodic oscillations to the platform [7]. Due to the restrictions of the mooring lines the platform will oscillate around an equilibrium position [10]. Because platform, tower and wind turbine are rigidly connected, the motions of the waves have a direct influence on the aerodynamic performance. Just as the forces of the waves have a direct influence on the wind turbine, the forces of the wind, which are induced into the wind turbine, can also be transmitted through the tower to the platform. Here they also can lead to significant motions of the system. In comparison to the wave induced motions however, they are negligible [10]. As shown in figure 2, floating offshore wind turbine systems can experience six-degree-of-freedom motions (DoF) [7].

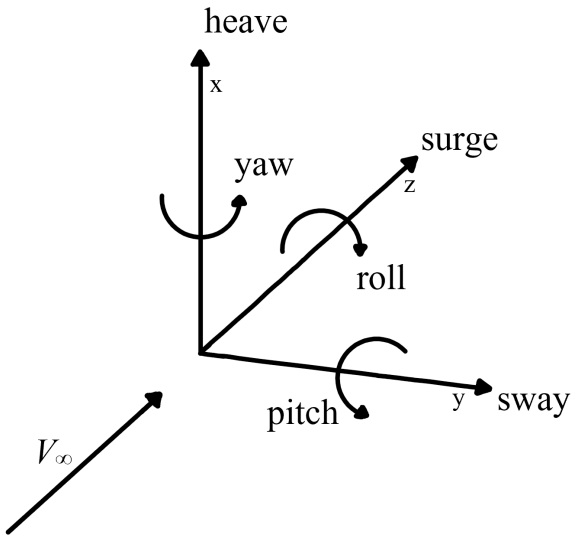

Fig. 2: Six-degree-of-freedom motions of a floating offshore wind turbine and direction of the incoming wind V_∞

Impacts of single DoF-motions

The first thing to consider is the impact of only a single DoF-motion on its own on the aerodynamic performance of a FOWT. The motions will be induced into the system at the bottom of the tower, 90 m below the hub. The focus is initially on the thrust force and the power output of the wind turbine. The examinations of Lee and Lee [7] show that only surge and pitch motions have a huge impact on the thrust force and power output of the wind turbine. In both cases the thrust force and the power output assume the sinusoidal function of the induced motions. The thrust force and power output of a FOWT under heave, sway, yaw and roll motions do not show significant differences to the thrust force and power output of a bottom-fixed wind turbine. Due to the surge and pitch motion, the power output fluctuates between the values listed in table 2. With the bottom-fixed wind turbine the power output is at a constant level of 2 MW.

Tab. 2: Fluctuation of the power output due to single DoF-motions based on Lee and Lee [7]

motion	power output
surge	0.6 MW - 3.8 MW
pitch	0.9 MW - 3.4 MW

[3] Tension Leg Platform
[4] Offshore Code Comparison Collaboration 4

https://doi.org/10.25974/ren_rev_2021_01

The examinations were done with the values from table 3 at a below-rated wind speed of 8 m/s. Moreover, a comparison of several induced motion amplitudes at the same frequency showed a linear relationship between the amplitudes of the motion and the amplitudes of the thrust force and power output. In a further step the impact of the single DoF motions on the wake structure was considered under the same conditions. Behind the rotor blades of a bottom-fixed wind turbine the wake structure develops in a form of a well-defined helical geometry. The structure remains over a distance of three times the rotor diameter, where it dissolves into turbulent wake. Due to the platform motions the helical geometry behind the rotor blades dissolves after a distance of 0.5 to 1.3 times the rotor diameter. In contrast to the thrust force and power output, all DoF motions show an significant influence on the wake structure [7].
The cause of the fluctuation of the thrust force and power output and the increase of the turbulent wake is that movements of the wind turbine in the opposite direction of the incoming wind increases the effective axial wind speed on the rotor blades. This increases the aerodynamic loads, thrust force, power output and wake vorticity. It reaches its maximum when the turbine moves with its maximum speed. If the wind turbine moves back in the opposite direction, the effect is correspondingly the other way around [7, 10].

Tab. 3: Amplitude and frequency of the induced single DoF-motions [7]

motion	amplitude	frequency
heave, sway, surge	4 m	0.1 Hz
yaw, pitch, roll	4°	0.05 Hz

Impact of multi DoF-motions

Sebastian and Lackner [9] determined the platform motions, which get induced into TLP, spar-buoy and barge platforms under realistic wind and wave conditions. A distinction was made between below- and above-rated wind speed cases. According to their analysis, pitch, surge and heave motions have a significant impact on barge platforms and pitch and yaw motions on spar-buoy platforms in both cases. The TLP is influenced by surge and pitch motions in the below-rated case. In the above-rated case the surge motion is the only motion with a significant influence. Due to the different designs with different centers of gravity and buoyancy and different mooring systems the wind and wave loads also result in different motion amplitudes and frequencies for each platform type. This is also reflected in the different results for the thrust force and power output of the FOWT which were examined by Lee and Lee [7]. Their study showed that the power output of a wind turbine supported by a TLP, spar-buoy or barge platform can fluctuate between the values given in table 4. In their results the higher static stability of the TLP and spar-buoy platform becomes clear. This is already evident in the values of the amplitudes of the motions that are induced in the platforms. Here the values of the barge platform are always higher than those of the other systems. The most significant deviations between the values of the amplitudes are shown in table 5. The two amplitudes for each motion originate from two superimposed oscillation functions that were used in the model of the present study.

Tab. 4: Fluctuation of the power output of wind turbines supported by different floating platforms under the influence of multi DoF-motions based on Lee and Lee [7] (the power output is given as a portion of the power output of a bottom-fixed wind turbine)

platform	power output
barge	40 % - 190 %
TLP and spar-buoy	90 % - 110 %

Tab. 5: Most significant differences in the amplitudes of the induced platform motions into different platform systems based on Lee and Lee [7]

motion	platform	amplitude 1	amplitude 2
pitch	spar-buoy	0.084°	0.016°
	barge	1.475°	1.630°
surge	TLP	0.436 m	0.222 m
	barge	0.752 m	0.442 m

The influence of multi DoF-motions on wind turbines supported by the semi-submersible OC4 platform were examined by Cheng et al. [10]. As with the barge platform, surge, pitch and heave are the main DoF-motions. With non-identical wind speed assumed, the results cannot be directly be compared with one another. But it can be said that the range of the fluctuation of the power output of the wind turbine is similar to the wind turbines supported by the TLP or barge platform. Accordingly, waves with a height of 3.66 m, which is two times the amplitude, and a frequency of 0.1 Hz[5] lead to a fluctuation of the power output between 4.5 MW and 4.9 MW.
Lee and Lee [7] also determined differences in the stability of the wake structure between the different platform types. Under realistic wind and wave conditions the well-defined helical geometry of the wake of a bottom-fixed wind turbine dissolves after a length of 1.3 times the rotor diameter behind the rotor blades. With wind turbines supported by floating platforms the well defined wake structure dissolves earlier. The corresponding results are shown in table 6.

In both studies, which are mentioned in this chapter

[5] original indication of the reference: wave period length in seconds

Tab. 6: Distance after which the well defined wake structure behind the rotor blades dissolves based on Lee and Lee [7]

platform	distance in times the rotor diameter
barge	0.5
spar-buoy	1.0
TLP	1.1

[7, 10] the pitch control keeps a constant pitch angle according to the velocity of the incoming wind.

3.2 Impact on the reliability of the rotor blades

The increase of the aerodynamic unsteadiness due to the multiple DoF platform motions can also lead to changes in the reliability of the rotor blades of FOWT in contrast to bottom-fixed offshore wind turbines. The causes and effects of the loss of reliability of an FOWT supported by an OC4 platform were investigated in a study of Liu et al. [11]. The examined causes of failure are

- blade root stress,
- flapwise motion of the blade tip and
- edgewise motion of the blade tip.

The resulting failure phenomena are listed in the first column of table 7. Liu et al. determined that the failure probabilities of all listed phenomena are higher on blades of FOWT than those of bottom-fixed wind turbines. The probability of failure results from the spread of the acting quantity and the spread of the resisting quantity, which are occurring in reality. In the area where the two distributions intersect, the components fail. Each occurrence of failure was examined in three different scenarios. This results in a total of nine investigations. The wind speed, wave height and peak period of wave spectrum of these scenarios are also listed in table 7. It should be noted that a wind speed of 11.4 $^{m}/_{s}$ correspondents to the rated wind speed and that a wind speed of 25.0 $^{m}/_{s}$ is equal to the cut-out wind speed of the wind turbine. The wind turbine in this study is still in operation at the cut-out wind speed. During the investigation at a wind speed of 51.5 $^{m}/_{s}$ the wind turbine is parked. The numbers of every investigation can also be found in figure 3. The absolute failure probabilities of a bottom-fixed wind turbine and a FOWT are compared here. Furthermore, the increase of the failure probabilities is shown. Particularly noteworthy is the increase in the failure probability due to stress overload of the blade root (no. 6 in figure 3). However, the high wind speeds examined in this scenario are extremely rare in the North Sea but can occur in individual gusts [12, 13].

The occurrence of ten-minute values of wind speed of an example location, about 100 km from the Dutch coast in the North Sea, can be seen in figure 4. The graphic is intended to provide a qualitative overview of the rarity of such an event. The increase of the failure probability due to structure fatigue of the blade root is also worth highlighting (no. 2 in figure 3). Under extreme wind conditions the probability of failure due to this cause can nearly be brought back to the level of a bottom-fixed offshore wind turbine through the cut-out of the wind turbine.
It can be assumed that the failure probability of an FOWT supported by a TLP or spar-buoy platform increases in a similar range as the failure probability of an FOWT supported by an OC4 platform, since they also achieved similar results in chapter 3.1.

Tab. 7: List of the examined failure phenomena and wind and wave scenarios in the study of Liu et al. [11]

event	wind speed $^{m}/_{s}$	wave height m	peak frequency[5] Hz	no.
structure	11.4	3.24	0.10	1
fatigue of the	25.0	6.02	0.09	2
blade root	51.5	12.90	0.07	3
stress over-	11.4	3.24	0.10	4
load of the	25.0	6.02	0.09	5
blade root	51.5	12.90	0.07	6
excessive dis-	11.4	3.24	0.10	7
placement of	25.0	6.02	0.09	8
the blade tip	51.5	12.09	0.07	9

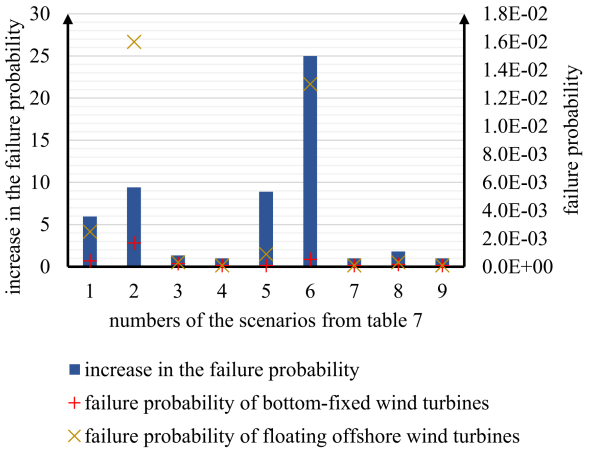

Fig. 3: Failure probabilities of rotor blades from bottom-fixed on floating offshore wind turbines based on Liu et al. [11]

4 Conclusion

In summary it can be said that the platform motions caused by wind and wave loads lead to a variety of

https://doi.org/10.25974/ren_rev_2021_01

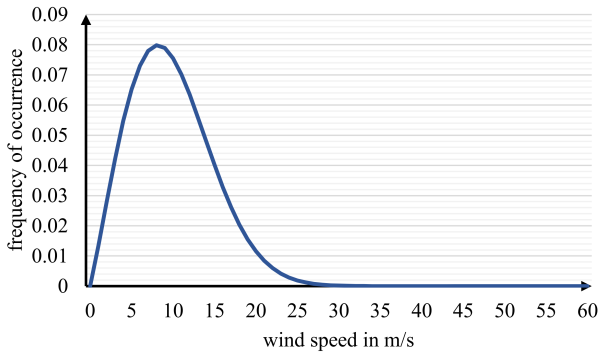

Fig. 4: Frequency of occurrence of ten minute mean values of wind speed in the north sea at location 53°13'04.0"N 3°13'13.0"E at a height of 74.8 m above the mean sea level based on Coelingh et al. [12]

changes in the operational properties of a FOWT. The following changes were noted in this review:

- The thrust force and power output of FOWT are fluctuating in the same frequency as the platform motions.
- The fluctuations of the thrust force and power output are almost exclusively based on surge and pitch motions of the platform.
- The TLP, spar-buoy and OC4 platform are less affected by wind and wave loads than the barge platform.
- Platform motions lead to an increase of the failure probability of the rotor blades of an FOWT compared to a bottom-fixed wind turbine.
- The wake structure behind the rotor blades of an FOWT is experiencing an earlier breakdown than the wake structure behind a bottom-fixed wind turbine.

The highly unstable wake might also lead to additional problems in floating offshore wind farms. Due to the unsteady wake the wind turbines, which are located downstream of another wind turbine are exposed to unsteady inflow conditions. This puts additional stress on their rotor blades [7]. Additional studies of how high these effects are would be desirable. Moreover, further studies on the failure probability of the FOWT rotor blades would be useful, as the data available so far is very limited.
All studies mentioned in this review, which take a critical look at the effects of platform motions are based in theoretical models. It can be assumed that practical data from current test systems will be added in the future.

5 Outlook

It is almost impossible to eliminate platform motions induced by wind and wave loads. Nevertheless, it is possible to decrease their influences on the operational properties of the wind turbine. Individual blade pitch control could be one possible solution. It was already shown that the power fluctuation of a FOWT, operating at above-rated wind speed conditions, supported by a barge platform, can be decreased by up to 44 % due to such a system. The pitch and roll motions were also decreased by 39 and 43 % respectively [14]. Further improvements could be reached due to a coating of a piezoelectric ceramic at the first quarter of the blade root, which is activated when root stress reaches its limitation. The failure probability due to the failure phenomena listed in table 7 could be decreased by up to 89 % [11].

References

[1] European Comission. *Communication from the comission of the European Union to the european parliament, the council, the european economic and social committee and the committee of the regions: An EU Strategy to harness the potential of offshore renewable energy for a climate neutral future*. Brussels. URL: https://ec.europa.eu/energy/sites/ener/files/offshore_renewable_energy_strategy.pdf.

[2] A. Arapogianni **et al.**. "Deep Water: The next step for offshore wind energy: a report by the European Wind Energy Association" (2013). Ed. by European Wind Energy Association. URL: http://www.ewea.org/fileadmin/files/library/publications/reports/Deep_Water.pdf.

[3] J. Jonkman. *Definition of the Floating System for Phase IV of OC3*. Tech. rep. National Renewable Energy Lab. (NREL), Golden, CO (United States), 2010. DOI: 10.2172/979456.

[4] D. Matha. *Model development and loads analysis of an offshore wind turbine on a tension leg platform with a comparison to other floating turbine concepts: April 2009*. Tech. rep. National Renewable Energy Lab.(NREL), Golden, CO (United States), 2010. DOI: 10.2172/973961.

[5] A. Robertson, J. Jonkman, M. Masciola, H. Song, A. Goupee, A. Coulling, and C. Luan. "Definition of the Semisubmersible Floating System for Phase II of OC4" (Sept. 2014). DOI: 10.2172/1155123.

[6] J. M. Jonkman. *Dynamics modeling and loads analysis of an offshore floating wind turbine*. Tech. rep. National Renewable Energy Lab.(NREL), Golden, CO (United States), 2007. DOI: 10.2172/921803.

[7] H. Lee and D.-J. Lee. "Effects of platform motions on aerodynamic performance and unsteady wake evolution of a floating offshore wind turbine". *Renewable Energy* 143 (2019), pp. 9–23. DOI: 10.1016/j.renene.2019.04.134.

[8] J. Jonkman, S. Butterfield, W. Musial, and G. Scott. *Definition of a 5-MW reference wind turbine for offshore system development*. Tech. rep. National Renewable Energy Lab.(NREL), Golden, CO (United States), 2009. DOI: 10.2172/947422.

[9] T. Sebastian and M. Lackner. "Characterization of the unsteady aerodynamics of offshore floating wind turbines". *Wind Energy* 16.3 (2013), pp. 339–352. DOI: 10.1002/we.545.

[10] P. Cheng, Y. Huang, and D. Wan. "A numerical model for fully coupled aero-hydrodynamic analysis of floating offshore wind turbine". *Ocean Engineering* 173 (2019), pp. 183–196. DOI: 10.1016/j.oceaneng.2018.12.021.

[11] L. Liu, H. Bian, Z. Du, C. Xiao, Y. Guo, and W. Jin. "Reliability analysis of blade of the offshore wind turbine supported by the floating foundation". *Composite Structures* 211 (2019), pp. 287–300. DOI: 10.1016/j.compstruct.2018.12.036.

[12] J. Coelingh, A. Van Wijk, and A. Holtslag. "Analysis of wind speed observations over the North Sea". *Journal of Wind Engineering and Industrial Aerodynamics* 61.1 (1996), pp. 51–69. DOI: 10.1016/0167-6105(96)00043-8.

[13] Deutscher Wetterdienst. *Orkantief ,,Anatol vom 3./4. Dezember 1999*. 1999. URL: https://www.dwd.de/DE/leistungen/besondereereignisse/stuerme/19991204_orkantief_anatol.pdf?__blob=publicationFile&v=4.

[14] H. Namik and K. Stol. "Individual blade pitch control of floating offshore wind turbines". *Wind Energy: An International Journal for Progress and Applications in Wind Power Conversion Technology* 13.1 (2010), pp. 74–85. DOI: 10.1002/we.332.

Cost comparison between bottom-fixed and floating offshore wind turbines

Calculating LCOE based on full hours of utilization and corresponding break-even points

*Jan-Niklas Linnenschmidt**

Münster University of Applied Sciences, Stegerwaldstraße 39, 48565 Steinfurt, Germany

Abstract

Originally this article was supposed to be a comparison between the technological differences of bottom-fixed offshore wind turbines (BOWT) and floating offshore wind turbines (FOWT). However, several authors already contributed to this topic and came to the conclusion that the higher levelized costs of energy (LCOE) prevent FOWTs from successfully entering the energy market [1, 2]. Multiple sources seem to agree on this conclusion but often do not provide the reader with further information regarding the LCOE. This is the reason why this article understands itself as an in depth cost comparison between BOWTs and FOWTs. For this purpose, individual LCOE are calculated for the upcoming FOWT technologies such as spar-buoy (SPAR), tension-leg platform (TLP) and semi-submersible platform (semi-sub) as well as conventional BOWTs using the wind turbines hours of full utilization (HOFU). The resulting functions are visualized graphically in order to determine break-even points between BOWTs and FOWTs. Finally, a sensitivity analysis is carried out to determine the influence of the weighted average costs of capital (WACC).

Keywords: cost comparison, bottom-fixed, floating, offshore wind turbines, LCOE, break-even point

1 Introduction

Bottom-fixed foundations have become established as the technical standard for offshore wind turbines. However, floating foundations have been emerging and are becoming more relevant. The different floating foundation types can be divided into three categories:

- spar-buoy (SPAR),
- tension-leg platform (TLP) and
- semi-submersible platform (semi-sub).

*Corresponding author: jl679273@fh-muenster.de.

Even though this article will not go into further detail regarding the technological differences between floating offshore wind turbines (FOWTs) and bottom-fixed offshore wind turbines (BOWTs), figure 1 gives a brief overview of the different foundation types.

All foundation types have their individual advantages and disadvantages. However, the upcoming FOWTs have a number of general advantages over the BOWTs:

- The possibility of using deeper waters increases the offshore wind power potential.
- Extended options for onshore pre-assembly lead to a reduced number of offshore operations, which are constrained to weather-windows and require expensive installation vessels [4].
- Instead of a solid foundation, a few cable attachment points are used, which reduces the irreversible environmental damage to the seabed and the noise pollution during installation.

However, these advantages are offset by higher levelized costs of energy (LCOE) which prevent FOWTs from successfully entering the energy market [1, 2]. Thus the question arises whether FOWTs will ever be able to compete with BOWTs from a cost point of view. To answer this question a procedure for calculating the LCOE for FOWTs and BOWTs and an afterwards carried out comparison with the goal of calculating break-even points based on the wind turbines hours of full utilization (HOFU) was developed and shall be explained in the now following chapter.

2 Material and Methods

2.1 Levelized costs of energy

For calculating the LCOE the following formula [5] was used:

$$LCOE = \frac{CAPEX + \sum_{t=1}^{n} \frac{OPEX}{(1+i)^t}}{\sum_{t=1}^{n} \frac{E}{(1+i)^t}} \quad (1)$$

https://doi.org/10.25974/ren_rev_2021_02

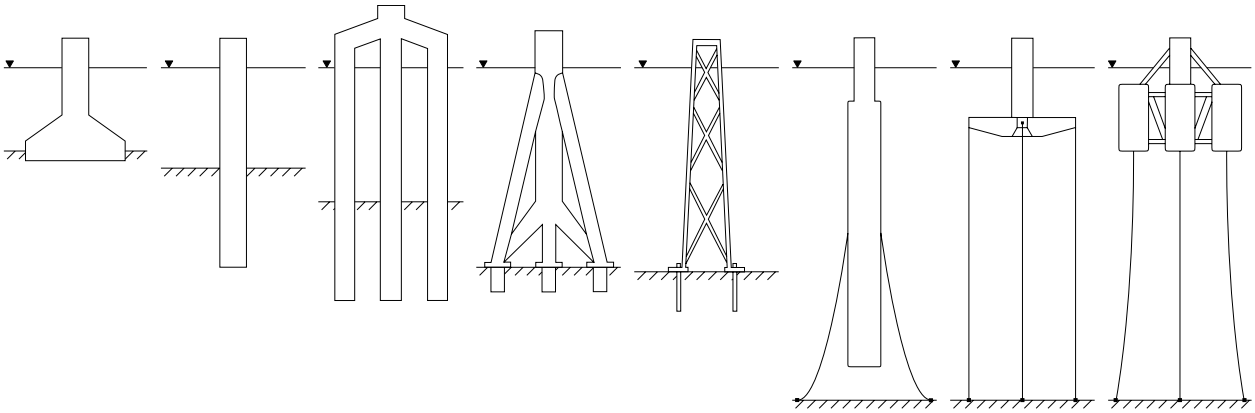

Fig. 1: BOWT and FOWT foundation types from left to right: gravity, monopile, tripile, tripod, jacket, SPAR, TLP, semi-sub (own illustration based on [3])

$LCOE$	levelized costs of energy in €ct/kWh
$CAPEX$	capital expenditures in €ct
$OPEX$	operational expenditures in €ct
E	generated energy in year t in kWh
i	weighted average costs of capital in %
n	operational lifetime in years
t	individual year of lifetime (1, 2, ... n)

Life cycle cost breakdowns show that the share of decommissioning expenditures in the total costs of an offshore wind turbine range from

- 1 % for BOWTs [6] up to
- 4-8 % for FOWTs [7].

Therefore, the decommissioning expenditures will not be taken into further consideration.

2.2 Costs of BOWTs

CAPEX and OPEX values according to [8] will be used for calculating the LCOE. A distinction is made between two possible scenarios:

- lower limit → best recent value (BRV)
- upper limit → global average (GA)

However, the different BOWT foundation types (figure 1) will not be further subdivided.

	BRV	GA	
CAPEX	2435	3485	k€/MW
OPEX	17.2	28.7	€/MWh

Tab. 1: CAPEX and OPEX values for BOWTs [8]

2.3 Costs of FOWTs

In contrast to BOWTs, FOWTs are not yet commercialized as many current projects are just in the pilot status. The different technical readiness levels (TRL) make a comparison between the LCOE for BOWTs and FOWTs difficult, since the TRL has a direct influence on the LCOE (compare figure 2).

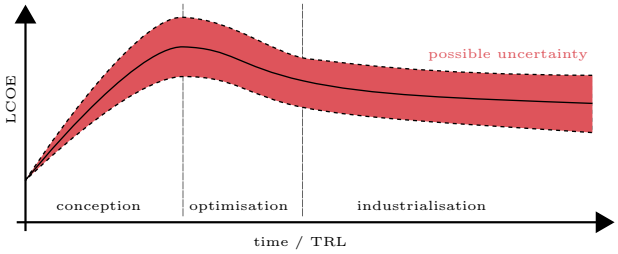

Fig. 2: schematic cost development through time (own illustration based on [4])

In order to answer the question if FOWTs will ever be able to compete with BOWTs from a cost point of view, the different TRLs of the two technologies must be adapted to each other. This can be accomplished by either adjusting the LCOE for BOWTs according to their already completed cost development or by estimating the future cost development for FOWTs. The latter approach was used in [4] for calculating CAPEX and OPEX values based on a list of several FOWT projects with different TRLs. Uncertainties and differences between the individual projects were taken into account using two possible scenarios:

- lower limit → minimal deviation (MIN)
- upper limit → maximum deviation (MAX)

The results, which will be used for calculating the LCOE, are shown in table 2. Different CAPEX values are available for the individual foundation types. The OPEX value, on the other hand, is identical for all technologies.

https://doi.org/10.25974/ren_rev_2021_02

		MIN	MAX	
CAPEX	SPAR	2860	3025	k€/MW
	TLP	2915	2970	
	semi-sub	2750	3080	
OPEX		88	121	k€/MW/a

Tab. 2: CAPEX and OPEX values for FOWTs [4]

2.4 Calculating the LCOE

The LCOE were calculated by inserting the following parameters into to formula 1:

- corresponding CAPEX and OPEX values according to the tables 1 and 2, [1]
- a constant value for $i = 7$ % (WACC), [2]
- as well as an operational lifetime of $n = 20$ a. [3]

The amount of generated energy E can be calculated by multiplying the wind turbines performance and the hours of full utilization (HOFU).

Since the wind turbines performance does not only affect the amount of generated energy E, but also has a direct influence on both CAPEX and OPEX (compare units in tables 1 and 2), the LCOE according to formula 1 do not change by varying the wind turbines performance. Any wind turbine performance can therefore be assumed for the calculation. However, varying the HOFU only affects the amount of generated energy E and therefore changes the LCOE. For this reason the LCOE were calculated as a function of the HOFU. The thus resulting functions for the individual floating foundation types are examined in more detail in the now following chapter.

3 Results

The calculated LCOE as functions of the HOFU are shown in the figures 3, 4 and 5. The lower and upper limit scenarios according to the chapters 2.2 and 2.3 are represented by the dotted curves, which result in partially overlapping price corridors. Out of the points that make up the dotted curves arithmetic mean values were formed and then connected to the solid curves in order to determine exact intersections and thus being able to calculate break-even points. Since the HOFU depend on the wind turbine installation site but usually move within a typical range, the x-axis was limited to 3000-5000 h/a for a better overview.

[1] However, the units were first converted to €ct by multiplying the CAPEX and OPEX values with the wind turbine performance or the amount of generated energy E.

[2] A sensitivity analysis to determine the influence of this initially assumed value is carried out in chapter 3.

[3] The here assumed time span is based on the German EEG law, which states that financial support by the government for renewable energies is limited to 20 years.

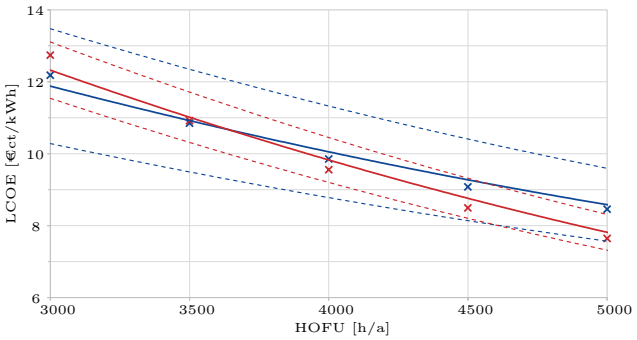

Fig. 3: comparing BOWT (blue) and SPAR (red)

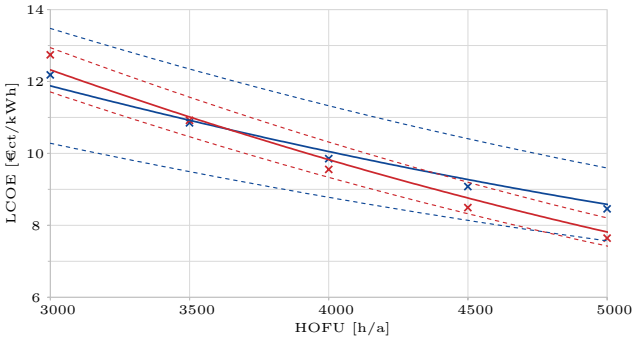

Fig. 4: comparing BOWT (blue) and TLP (red)

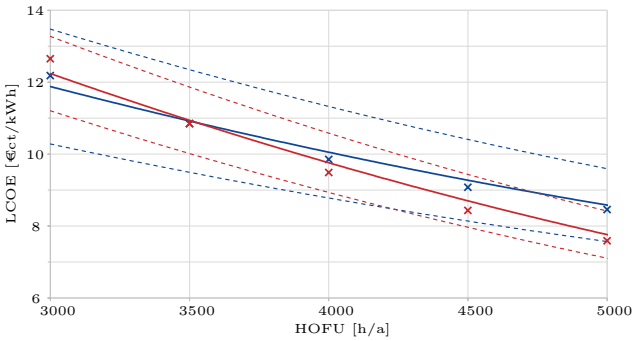

Fig. 5: comparing BOWT (blue) and semi-sub (red)

The break-even points for SPAR and TLP are on top of each other because the upper limit CAPEX value decreases by the same amount as the lower limit CAPEX value increases (compare table 2). Thus the TLP price corridor becomes tighter on both sides but the arithmetic mean stays the same.

Since the WACC depend on the market value of the company's equity and debt, a sensitivity analysis by calculating multiple break-even points for WACC values ranging from 4-10 % was carried out to take different financing structures into account (compare figure 6). The HOFU range from 3482 h/a up to 3656 h/a and are therefore subject to a relatively small change of 174 h/a. As expected, the LCOE are much more dependent on the WACC and therefore fluctuate between approximately 9-13 €ct/kWh.

https://doi.org/10.25974/ren_rev_2021_02

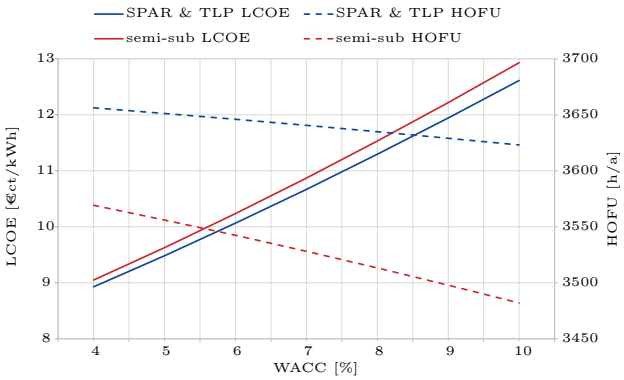

Fig. 6: influence of different WACC values on the break-even points

4 Conclusion

The figures 3, 4 and 5 can be used to carry out an initial rough economic comparison between BOWTs and FOWTs based on the HOFU achievable at the planned wind turbine installation site. A fundamental problem here, however, is that environmental impact scores lowly in regard to cost reduction potential [4].

Furthermore, the break-even points can be used to answer the initial question whether FOWTs will ever be able to compete with BOWTs from a cost point of view. However, this requires suitable figures for comparison. For this purpose the LCOE for German offshore wind energy was calculated by the Fraunhofer Institute for Solar Energy Systems and ranges from 7.5 €ct/kWh up to 13.8 €ct/kWh at 3200-4500 HOFU [9]. The in chapter 3 calculated break-even points overlap with this range, which shows that FOWTs will be able to compete with BOWTs in the future. However, this conclusion is based on an estimated cost development for FOWTs (compare chapter 2.3).

5 Outlook

In order to make the results of this article more useful for practical applications, further investigations will be necessary in the future. The following suggestions for improvement could serve as possible starting points:

- Instead of estimating a cost development for FOWTs, the already completed cost development of BOWTs could be used accordingly.
- Although the used procedure is sufficiently accurate, the result is only as good as the input data. A more in-depth analysis of the CAPEX and OPEX structures would lead to better results.
- In a few years the commercialization of the FOWTs will have progressed further and for projects that are currently being implemented more up-to-date data will be available with which the procedure can be repeated. This means that the results can be kept up to date and the uncertainties due to the estimated cost development can be reduced over time.

References

[1] A.-D. Maimon. “Brief review about floating offshore wind turbines projects”. *Annals of” Dunarea de Jos” University of Galati.* 41 (2018), pp. 49–62. DOI: 10.35219/AnnUGalShipBuilding.2018.41.08.

[2] M. Andersen. “Floating Foundations for Offshore Wind Turbines”. PhD supervisor: Professor Søren R.K. Nielsen, Aalborg University Assistant PhD supervisor: Associate Professor Peter B. Frigaard, Aalborg University. PhD thesis. 2016. DOI: 10.5278/vbn.phd.engsci.00175.

[3] “Foundations types and depth limits - Alternative solutions”. *Windpower Monthly* (2013). URL: https://www.windpowermonthly.com/article/1210054.

[4] R. James and M. C. Ros. “Floating offshore wind: market and technology review”. *The Carbon Trust* (2015). URL: https://www.carbontrust.com/de/node/958.

[5] R. Ebenhoch, D. Matha, S. Marathe, P. C. Muñoz, and C. Molins. “Comparative Levelized Cost of Energy Analysis”. *Energy Procedia* 80 (2015). 12th Deep Sea Offshore Wind RD Conference, EERA DeepWind’2015, pp. 108–122. DOI: 10.1016/j.egypro.2015.11.413.

[6] A. Ioannou, A. Angus, and F. Brennan. “A lifecycle techno-economic model of offshore wind energy for different entry and exit instances”. *Applied Energy* 221 (2018), pp. 406–424. DOI: 10.1016/j.apenergy.2018.03.143.

[7] C. Maienza, A. Avossa, F. Ricciardelli, D. Coiro, G. Troise, and C. Georgakis. “A life cycle cost model for floating offshore wind farms”. *Applied Energy* 266 (2020), p. 114716. DOI: 10.1016/j.apenergy.2020.114716.

[8] A. C. Levitt, W. Kempton, A. P. Smith, W. Musial, and J. Firestone. “Pricing offshore wind power”. *Energy Policy* 39.10 (2011). Sustainability of biofuels, pp. 6408–6421. DOI: 10.1016/j.enpol.2011.07.044.

[9] C. Kost, S. Shammugam, V. Jülch, H.-T. Nguyen, and T. Schlegl. “Stromgestehungskosten Erneuerbare Energien” (2018). URL: https://www.ise.fraunhofer.de/de/forschungsprojekte/stromgestehungskosten-erneuerbare-energien.html.

Technical challenges of floating offshore wind turbines

An overview

*Dennis Tillenburg**

Münster University of Applied Sciences, Stegerwaldstraße 39, 48565 Steinfurt, Germany

Abstract

Floating offshore wind (FOW) holds the key to 80 % of the total offshore wind resources, located in waters of 60 m and deeper in European seas, where traditional bottom-fixed offshore wind (BFOW) is not economically attractive. Many problems affecting floating offshore wind turbines (FOWT) were quickly overcome based on previous experience with floating oil rigs and bottom-fixed offshore wind. However, this technology is still young and there are still many challenges to overcome.

This paper shows that electrical failures are amongst the most significant errors of FOWT. The most common cause was corrosion. It is also stated that the control system is most often affected, and that the Generator is frequently involved. Material corrosion is also the key factor when it comes to the most common overall reason for failures. A particular attention must be paid to mooring line fracture. Mooring lines are especially vulnerable to extreme sea conditions and the resulting fatigue, corrosion, impact damage, and further risks. It must be stated that the primary challenge is that of economics. Over time technological costs will decline making FOW more competitive and hence attractive for greater depth.

Keywords: floating offshore wind power, challenges, wind turbine, mooring line, Windkraftanlage

Abbreviations

BFOW = Bottom-fixed offshore wind
CMA = Concept Marine Associates
TLP = Tension Leg Platforms
FOW = Floating offshore wind
FOWT = Floating offshore wind turbines
RPN = Risk Priority Number

*Corresponding author: dt828926@fh-muenster.de.

1 Introduction

Floating offshore wind (FOW) holds the key to an almost inexhaustible resource potential in Europe. 80 % of the total offshore wind resources in European seas is located within water depth of 60 m and deeper, where traditional bottom-fixed offshore wind (BFOW) is not economically attractive [1]. Many problems affecting floating offshore wind turbines (FOWT) were quickly overcome based on previous experience with floating oil rigs and bottom-fixed offshore wind. However, this technology is still young and there are still many challenges to overcome. This paper will combine information gathered from several studies to determine the most common causes of failure which FOWT experience and provide suggestions for possible solutions.

2 Specific technical challenges for floating offshore wind turbines

A floating offshore wind turbine is composed of many different system-relevant parts. This is why it make sense to categorize failures according to areas of occurrence.

2.1 Rotor-blades

Rotor-blades are the components with the highest chance of failure and also responsible for the highest percentage of a FOWT downtime. Many of these failures are due to structural failures and material fatigue. These failures are greatly due to the missing experiences associated with the heavier weather conditions floating wind-turbines experience compared with their fixed counterparts. Other failures include cracks, erosion and flaking. These usually occur around the edges of the wind-blades. One of the most common problems associated with wind-turbine-blades are failures in the yaw and pitch systems. These are used to control the blades angle in correspondence to the wind [2].

https://doi.org/10.25974/ren_rev_2021_03

2.2 Electrical components

Wiring is one of the biggest cost factors when it comes to FOWT. The connecting cables must be durable and flexible to be able to withstand constant movement. The biggest cost factor when it comes to faults in this category is caused by the generator and related parts. Generator faults may be caused by mechanical as well as electrical failures. Electrical issues are mainly caused by open-circuits or short-circuits within the rotor or overheating of the stator. Mechanical problems are due to corrosion and dirt [2].

2.3 Transmission system

The transmission system is composed of the coupling, main bearing and gearbox. The main bearing is used to control the torque during start and shutdown of the wind-turbine. The gearbox functions as a means to transform high-torque to low-torque or the low speed of the main bearing to the high speed to the generator. It is often damaged by sudden changes in wind-speed and the resulting shock as well as erosion [2].

2.4 Support system

The support system includes the nacelle, the tower and the foundation. The main reason for failures in the support-system are fatigue, corrosion, welding cracking and collisions with the hull. During extreme weather conditions movement and vibration of a FOWT can become so intense that the hull may be damaged more easily than with their fixed counterparts [2].

2.5 Mooring line

The amount and intensity of stress a mooring line endures is greatly dependent on the technology in use. The mooring lines of Tension Leg Platforms for example experience a continuous tension, while those of barge and spar-buoy foundations experience high tension only during extreme weather [2]. Mooring lines are also responsible for FOWT limits when it comes to water-depth. Although a theoretical 80 % of offshore resources lie within depth of over 60 m and are therefor too deep for conventional bottom-fixed offshore wind (BFOW), most of this area is momentarily too deep for FOWT as well. Currently most FOWT are being built within depth of less than 100 m. It would also be possible to install them in depth of around 200 m when using a special taut-leg (or semitaut) mooring design. However, the deeper the ocean, the more mooring line must be deployed. The mooring line and the foundation will have to endure greater traction and deployment, installation and maintenance costs will rise [3].

2.6 Auxiliary system

The auxiliary system consists of lightning protection, the hydraulic system and cooling system. Due to their height offshore wind turbines are likely to suffer from lightning strikes. These can burn electrical components, control systems and sensors. The hydraulic system provides the pressure needed to control the pitch and yaw systems. It can suffer from pressure loss, temperature errors, responsive issues and motor failure. In order to tackle overheating of generator, converter, hydraulic system and electronic components, a cooling system is required. So far wind-based cooling systems are in general use, but because offshore wind turbines are generally getting bigger, water-based cooling systems with higher thermal capacities are moving into focus [2].

3 Foundation types

Momentarily there are several different approaches to how the base of a FOWT should function. Each one of these designs has proven to hold different advantages and disadvantages over the other. To be seen in Fig. 3.

3.1 Ballast stabilized

Represented by the spar-buoy foundation, to be seen as the left FOWT in Fig. 1. A ballast stabilized foundation provides stability by using a below hanging central buoyancy tank as ballast, creating a correcting moment. It provides high inertia resistance to pitch and roll movement and usually enough draft to offset heave motion. Ballast-dominated designs are likely to heavier and therefor more expensive to build [4].

3.2 Mooring-line stabilized

The tension leg platforms (TLP) represent mooring-line stabilized foundations. To be seen as the central FOWT in Fig. 1. They rely purely on their updraft and mooring line tension to hold them in place. Due to this, they need considerably less mooring line length, but apply more traction on these and the anchors. Tension leg platforms have their base completely submerged [4].

3.3 Buoyancy stabilized

The barge FOWT seen on the right in Fig. 1 represents a buoyancy stabilized foundation. These kinds of foundations rely solely on their up drift. They float above the surface and stabilize thanks to their wide surface contact. Buoyancy-stabilized foundations are more likely to be subject to higher wind loading which in turn has a negative impact on the turbine's dynamics [4].

https://doi.org/10.25974/ren_rev_2021_03

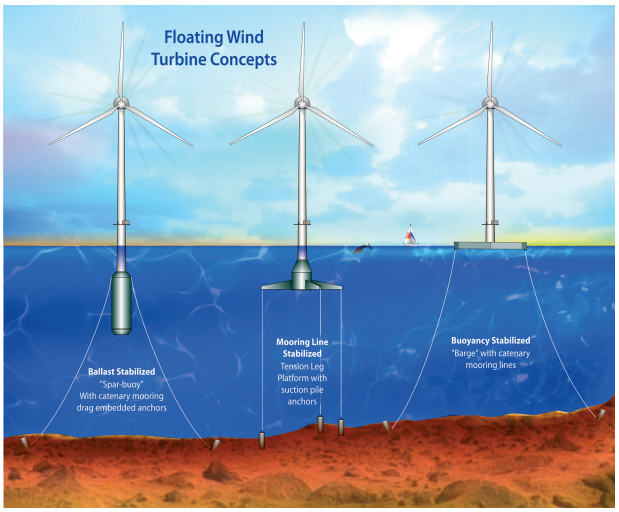

Fig. 1: Ballast-, mooring line-, and buoyancy stabilized FOWT. Image by: (Jonkman, 2009 [5])

3.4 Semi-submerged

Each of these platform types are to be considered idealized vessels with limited properties and each of them provides advantages over the other given specific circumstances. For example, the idealized spar buoy will have a tank with zero water surface friction while providing sufficient ballast below the waterline to offset the tower's movement. The mooring lines would only function to keep the construct in place. Similarly, the idealized TLP would be a weightless tank with zero surface friction and held only by the tension of the vertical mooring lines. Finally, the idealized barge would be weightless and moored only to prevent drifting. Its weighted water plane would be sufficient to stabilize the platform under static load conditions [4]. In practice, none of the above concepts are possible and not favoured in the first. Instead, combinations of the above have proven to provide the most benefits. One of the most popular models these days is a semi-submerged foundation, as seen in Fig. 2. Semi-submerged foundations benefit from both a buoyancy foundation's weighted water friction as well as a ballast foundation's weight stabilization and possibly mooring line tension [4]. Fig. 3 shows several different foundation-designs within the technology-triangle. To be seen are the single-technology designs, namely spar-buoy, barge and TLP. As well as the most commonly installed Concept Marine Associates (CMA) tension leg platform, a semi-submerged type foundation and the Dutch Tri-floater.

3.5 Design tools and methods

The complexity of the task of developing accurate modelling tools will increase with the degree of flexibility and coupling of turbine and platform. Usually this leads to faster response and movements counter-

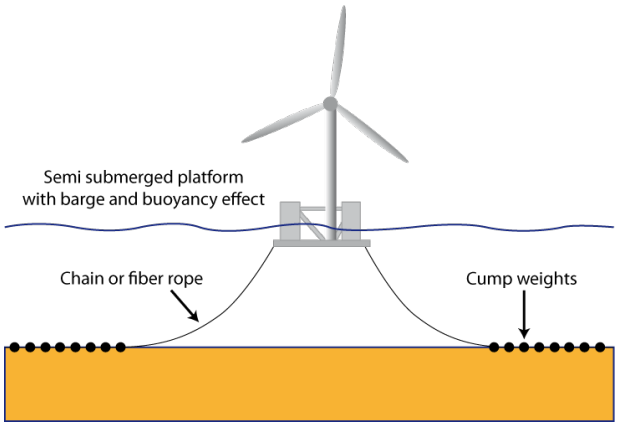

Fig. 2: Semi-submerged platform.

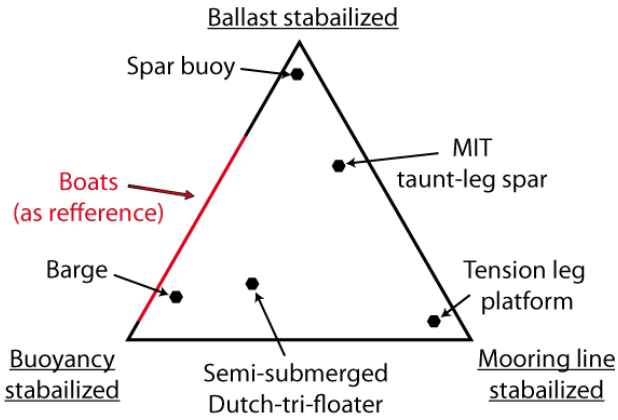

Fig. 3: Floating Platform Stability Triangle showing methods of achieving static stability. According to: (Butterfield et al., 2007 [4])

ing wave and wind loads. Predicting wave loads and dynamics for a relatively stable platform such as the TLP requires new analytical tools but is likely to be less of a problem than for platforms that are exposed to wave loading. Platforms like the barge, which have much of their structure near the free surface, encounter greater pitch, roll, and lift forces. A barge is likely to be more complex to model and validate. Spar concepts have smaller spire movements compared to the barge but can still be exposed to nonlinear wave forces that require more advanced tools.

Additionally, less predictable external influences such as floating debris must be calculated for, when developing design and modelling tools. This also counts for icebergs hitting the structure and marine growth [4].

Tab. 1 provides an overview of relative advantages and disadvantages of idealized platform types. Showing that most commonly the differences are but a matter of costs and are therefore dependent on the local conditions.

https://doi.org/10.25974/ren_rev_2021_03

Tab. 1: Platform design trade-offs for stability criteria. According to: (Butterfield et al., 2007 [4])

Platform design challenge	**Buoyancy barge**	**Mooring line TLP**	**Ballast spar**
Design Tools and Methods	-	+	-
Buoyancy Tank Cost/Complexity	-	+	-
Mooring Line System Cost/Complexity	-	+	-
Anchors Cost/Complexity	+	-	+
Load Out Cost/Complexity (potential)	+	-	
Onsite Installation Simplicity (potential)	+	-	+
Decommissioning and Maintainability	+	-	+
Corrosion Resistance	-	+	+
Depth Independence	+	-	-
Sensitivity to Bottom Condition	+	-	+
Minimum Footprint	-	+	-
Wave Sensitivity	-	+	+
Impact of Stability Class on Turbine Design			
Turbine Weight	+	-	-
Tower Top Motion	-	+	-
Controls Complexity	-	+	-
Maximum Healing Angle	-	+	-

Key: + = relative advantage; - = relative disadvantage; blank = neutral advantage

4 Risk assessment

One way to determine which parts of a Floating offshore wind turbine (FOWT) are most prone to damage is called risk assessment. This system has been used by (Kang et al., 2016 [2]) to analyse failures and rate them according to their severity (tab. 2), the frequency they appear (tab. 3) and how easy these failures can be detected (tab. 4). Tab. 5 provides a rating of categorized failures by multiplying their severity, occurrence and detection rate. This results in a so called risk priority number (RPN). For example a generator winding failure caused by flawed cable insulation is rated with severity 4, occurrence 8 and detection 5. Resulting in an overall RPN of 160.

4.1 Rating criteria

Tab. 2: Failure severity rating scale for FOWT. According to: (Kang et al., 2016 [2])

Scale	**Description**	**Criteria**
1	Minor	Electricity can be generated but urgent repair is required
2	Marginal	Reduction in ability to generate electricity
3	Critical	Loss of ability to generate electricity
4	Catastrophic	Major damage to the turbine as a capital installation

Tab. 3: Failure occurrence rating scale for FOWT. According to: (Kang et al., 2016 [2])

Scale	**Description**	**Criteria**
1-2	Unlikely	Probability of $< 0,01\,\%$
3-5	Remote	Probability of $\geq 0,01\,\%$
6-8	Occasional	Probability of $\geq 0,1\,\%$
9-10	Frequent	Probability of $\geq 1\,\%$

Tab. 4: Failure detection rating scale for FOWT. According to: (Kang et al., 2016 [2])

Scale	**Criteria**
1-2	Current monitoring methods almost always detect the failure
3-5	Good likelihood of detecting the failure
6-8	Low likelihood of detecting the failure
9-10	No known methods available to detect the failure

4.2 Overall rating

5 Results

Tab. 5 shows that electrical failures are amongst the most significant errors of FOWT. From a total of 4872 risk priority number (RPN), 1992 RPN are determined to have an electrical origin. Of these the most common cause was corrosion. It is also stated that the control system is most often affected, and that the generator is frequently involved. Material corrosion is also the key factor when it comes to the most common overall reason for failures.

https://doi.org/10.25974/ren_rev_2021_03

Tab. 5: Overall failure rating for FOWT. According to: (Kang et al., 2016 [2])

Scale	Criteria	RPN
Generator	Bearing deformation	676
	Overheat	396
	Winding failure	912
Electrical controls	Convert failure	630
	Transform winding failure	618
	Output voltage inaccuracy	411
	Yaw positioning inaccuracy	333
Support structure	Mooring line fracture	340
Auxiliary system	Cooling system failure	556

It is worth stating that structural components have a much lower failure rating than electrical components. Direct-driven generators have proven especially prone to damage. Giving it the highest RPN value among all sub-systems.

A particular attention must be paid to mooring line fracture. Mooring lines are especially vulnerable to extreme sea conditions and the resulting fatigue, corrosion, impact damage, and further risks. Large-scale wind turbines can be built to over 100 m in height, movement of the floating foundation may cause strong vibrations and swinging of the upper structure. This leads to high material stress on the blades, as well as the transmission and control system. Strongly dependent on the foundation design, determining the perfect balance of flexibility, strength and stiffness of mooring lines has proven to be challenging because even a minor failure could lead to serious consequences [2].

FOWT has only recently matured enough to seriously consider overcoming the technical challenges required to design successful machines. And while floating oil rig stations have provided FOWT with enough technology and experience to overcome these technical challenges, it must be stated that the primary challenge is that of economics [4]. It is technically possible to deploy FOWT in depth of over 200 m but mooring line, foundation support, deployment, installation and maintenance costs will rise. The later three not just because of the additional depth, instead costs will also increase due to the extra distance that has to be overcome when departing from shore. Over time technological costs will decline making FOWT more competitive and hence attractive for greater depth.

6 Solution approach

1. Material corrosion:
   This paper suggests strengthening the preservation layer of the equipment as an effective way to improve the systems reliability [2]. It is extreme important to not only choose the material and layout scheme of the mooring lines, but also optimize floating foundation design in order to minimize the impacts on the construct as well as the marine environment [2].

2. Electrical failures:
   Due to corrosion being the most frequent cause for electrical failures to appear, this issue should be addressed first. However, the control systems are shown to be the most affected and backup systems should be installed. The generator is shown to be involved in many instances of electrical failures which is most likely due to a FOWT encountering more vibration and swinging than their fixed counterparts. This paper recommends developing a more vibration dampening setup for FOWT.

3. Design tools and methods
   Further data must be gathered in regards to the influences of marine life, floating debris, icebergs or marine traffic on FOWT. While certain information gathered from bottom-fixed offshore wind (BFOW) and floating oil platforms can be obtained, FOWT might behave differently when encountering these issues. For example, a FOWT that has been in operation for over 15 years will have a different centre of gravity depending on where marine life has settled along the foundation and mooring lines. Improving the coating of these objects will reduce the influence this effect has on the turbine stability.

4. Maximum water depth
   Although at the moment it is technically only possible to deploy FOWT in depth of up to around 200 m, this is not a technical problem. There is simply no need in researching in this direction, as it would not make any economical sense at this point. Most FOWT are deployed in depth of up to 100 m as overall costs rise depending on water depth and there is still plenty of space in shallower waters. Prices for FOWT technology will decrease over time and once FOWT has become a competitive energy source, technologies for deeper deployment will be developed.

   These results could be useful for FOWT design improvement and maintenance optimization.

7 Outlook

When considering that many failures stand in direct correlation with each other, the system of RPN rating used in (Kang et al., 2016 [2]) seems rather imprecise. There are for example many electrical failures but focusing on improving the wiring might not be the

most effective solution to this issue. As many of these failures only occur due to the generator issues. Rather than concentrating on the symptoms the core problems should be addressed.

References

[1] *Floating Offshore Wind Vision Statement - June 2017*. WindEurope, 2017.

[2] J. Kang, L. Sun, H. Sun, and C. Wu. "Risk assessment of floating offshore wind turbines based on correlation-FMEA". *elsevier* 1 (2016), pp. 382–388. DOI: 10.1016/j.oceaneng.2016.11.048.

[3] K.-T. Ma, Y. Luo, T. Kwan, and Y. Wu. *Mooring System Engineering for Offshore Structures*. Elsevier, 2019. ISBN: 9780128185513. DOI: 10.1016/C2018-0-02217-3.

[4] S. Butterfield, W. Musial, J. J., and S. P. "Engineering Challenges for Floating Offshore Wind Turbines". *The National Renewable Energy Laboratory (NREL)* 1 (2007).

[5] J. Jonkman. "Dynamics of offshore floating wind turbines—model development and verification". *Wind Energy* 12 (2009), pp. 459–492. DOI: 10.1002/WE.347.

Assessment of noise mitigation measures during pile driving of larger offshore wind foundations

*Fiona Wagenknecht**

Münster University of Applied Sciences, Stegerwaldstraße 39, 48565 Steinfurt, Germany

Abstract

Wind energy is an important source of electricity generation, but the construction of offshore wind foundations causes high underwater sound pressure, harming marine life. In this context limiting values for underwater noise emissions were set to protect the marine flora and fauna. Therefore, noise mitigation measures during pile driving are mandatory to comply with these limits. Current development in the wind industry lead to increasing wind turbine sizes, requiring a larger pile diameter, which leads to higher underwater noise emissions. As a result, the state of the art noise mitigation systems might not be sufficient and a combination of different technologies is necessary. This article focuses on the issue of noise mitigation during pile driving with respect to large pile sizes. First, the most tested and proven noise mitigation techniques (big bubble curtain, hydro sound damper, and IHC-noise mitigation system) are described, following an analysis of noise reduction measurements in applications at different offshore wind farm projects. In the end the suitability of current noise mitigation systems for large monopiles is evaluated, regarding their effectiveness and practicability.

Keywords: Noise mitigation measures, Offshore wind foundations, Big bubble curtain, Hydro sound damper, IHC-noise mitigation system

1 Introduction

Renewable energies are developing rapidly and become more important as a source of energy generation and therefore, in reducing the use of fossil energy sources. One of these fast growing renewable energy technologies is wind power. New offshore wind parks are under construction around the world. The foundation of offshore wind turbines often consists of a steel monopile which is driven into the seabed by impact pile driving. This technique causes high underwater sound pressure harmful to the marine environment and threatening marine life. To protect the marine flora and fauna several governments set limiting values for underwater noise emissions. To comply with these values noise mitigation measures must be applied [1]. Due to larger wind turbines, pile sizes increase and a higher blow energy is needed, generating higher underwater sound levels. Therefore, an ongoing development of effective noise mitigation measures in regard to larger monopiles is necessary [2].

This article discusses the issue of noise mitigation concerning larger pile sizes due to larger turbines, while describing the effectiveness of existing noise mitigation measures, especially for larger monopiles. Parameters that influence the noise level are the pile diameter, water depth, soil structure and blow energy. The larger the pile diameter and the higher the blow energy, the less likely it is that existing noise mitigation measures are effective to meet noise standards [3].

2 Theoretical Background

In 2011 the German regulatory Federal Maritime and Hydrographic Agency of Germany (BSH), as first country worldwide, set limiting values for underwater noise,

- sound Exposure Level (SEL) = 160 dB (re 1 μPa^2s)
- Peak Level(LPeak) = 190 dB (re 1 μPa^2)

which must be complied within a distance of 750 m to the construction site [4]. The sound pressure level (SPL), measured in (dB) uses the logarithmic scale to represent the sound pressure of a sound relative to a reference pressure. The sound exposure level (SEL) characterises the underwater noise for pile driving, measured in decibels (dB). It is defined as the level of a continuous sound with 1 s duration and the same sound energy as the pile driving impulse. The peak level (LPeak) is the peak level of the sound pressure wave with no time constant applied. Measurements over the last years show that sound emission levels during pile driving, which are depending on many parameters (mostly blow energy and pile size), show values of

*Corresponding author: f.wagenknecht@fh-muenster.de.

https://doi.org/10.25974/ren_rev_2021_04

- up to 180 dB (SEL)
- up to 205 dB (LPeak)
- up to 210 dB (SPL)

in a distance of 750 m. [4] Therefore, noise mitigation measures must be applied during offshore construction to lower underwater noise. When the limiting values were established in 2011 noise mitigation technologies were a relatively new research area. Even though many solutions and prototypes existed, only a few were already tested offshore and near-shore studies did not correspond with offshore results [4]. In comparison to other types of offshore wind foundations, the most experience exists with monopiles when constructing offshore wind farms. Thus, monopiles are used for comparisons of different noise mitigation measurements. The most common installation method for monopiles is impact piling. This installation method comes with high impulse noise emissions as shown in figure 1, which can be harmful for the aquatic environment [5]. During pile driving sound levels mainly

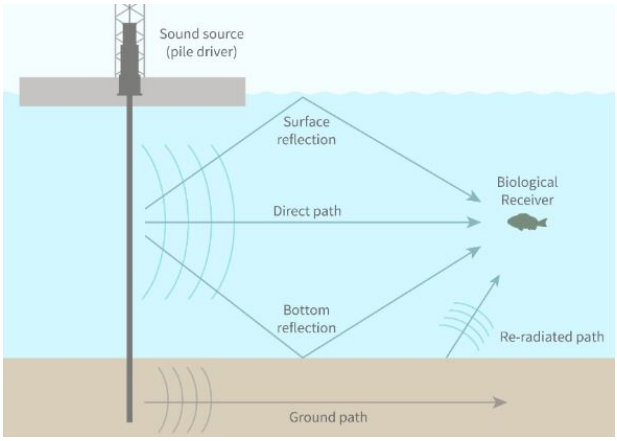

Fig. 1: Underwater sound emission paths associated with pile driving [6].

depend on the pile diameter and blow energy used. Moreover, the pile diameter can be used as key indicator of the expected noise emissions. Therefore, the required noise reduction mainly depends on the pile diameter. Measurements show, that a monopile with a diameter of 6 m can reach underwater noise levels of about 178 dB (SEL). To comply with the limits of the BSH a noise reduction of 18 dB (SEL) is necessary [4]. Currently, monopiles have a diameter of 7 to 8 m. For the next generation of wind turbines with 12 to 14 MW, the steel industry is ready to provides monopiles with a diameter of 10 to 12 m and a length of 100 m for greater water depth. Noise mitigation can be achieved by using two different principles:

1. by attenuating the generation of noise directly at the source (primary noise reduction)
2. by placing noise barriers (secondary noise reduction) [5].

3 State of the art noise mitigation systems

Several noise mitigation systems are available on the market. The following chapters summarize the noise mitigation measures, that are already proven systems under offshore conditions and considered as state of the art. These technologies use the principle of the secondary noise reduction, by placing a noise barrier.

3.1 Big Bubble Curtain (BBC)

A big bubble curtain (BBC) is a perforated hose lying on the seabed, positioned in a ring around the construction site, where the pile driving takes place. Air is pumped into the perforated hose and a bubble curtain is generated as shown in figure 2. Air bubbles change the water density, attenuating sound emissions due to pile driving [5]. The sound attenuating effect is caused by sound scattering and absorption on the air bubbles as well as the reflection at the transition from water to air. If a higher noise reduction is required, e. g. for large monopiles, a double bubble curtain (DBBC) can be deployed, where two perforated hoses are placed on the seabed in a specific distance to each other [7].

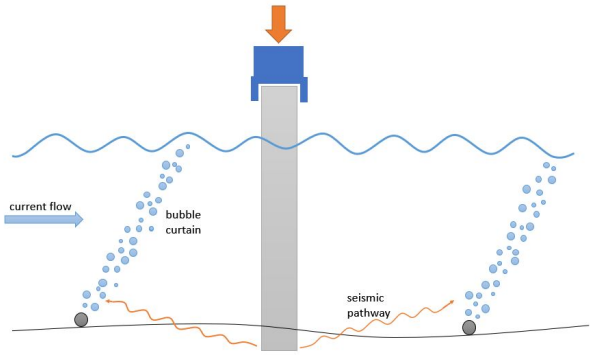

Fig. 2: Principle of the big bubble curtain

3.2 Hydro Sound Damper (HSD)

Hydro sound damper (HSD) are encapsulated resonator systems, which are gas filled elastic balloons or robust PE-foam elements. These are fixed to a net surrounding the pile in a short distance of around 5-6 m [8] as it is displayed in figure 3. The principle of noise attenuation of HSD elements is similar to that of a bubble curtain: Reflection of the sound waves as well as scattering, reflection and absorption due to resonance effects. In contrast to a conventional air bubble curtain the frequencies at which HSD provide a maximum noise reduction are adjustable by variations in balloon size and dissipation effects due to damping properties of the material [3]. A major

https://doi.org/10.25974/ren_rev_2021_04

advantage is the high control over different characteristics such as size of the bodies, effective frequency range, selected material, damping rate, number and distribution. Moreover, the HSD is not influenced by any current and unlimited by deep waters due to its static structure [2].

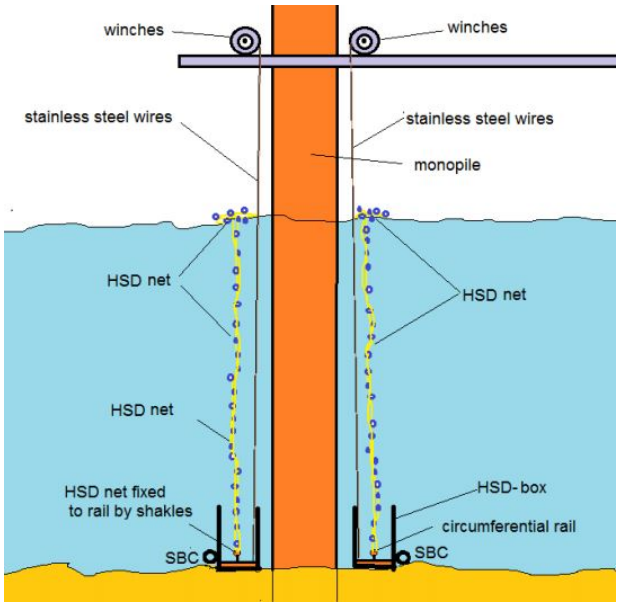

Fig. 3: Principle of the hydro sound damper [2].

3.3 IHC noise mitigation system (IHC-NMS)

The IHC noise mitigation system (IHC-NMS) is a shell-in-shell system, consisting of a double walled steel screen surrounding the pile as a tube, which is shown in figure 4. The space between the two walls is filled with air. In addition, the water column between pile an NMS can be supplied with air bubbles. Therefore, sound waves pass through two barriers, the bubble curtain as well as the air filled double wall screen, where the principle of noise attenuation is the reflection at phase transitions (air-steel-water) [7]

Fig. 4: IHC noise mitigation system, © Ørsted.

4 Results

The best studied and most regularly applied mitigation measure is the big bubble curtain in its various applications. Depending on the conditions at the construction site, noise reduction measurements can vary. Moreover, during pile installation some thousand blows per pile are necessary, also resulting in varying noise reduction results. Therefore a minimum and a maximum value of the noise reduction for each noise mitigation system were determined based on several projects [4]. Following, figure 5 and the two tables 1 and 2 show the measured reduction of sound exposure levels during pile driving at different water depths.

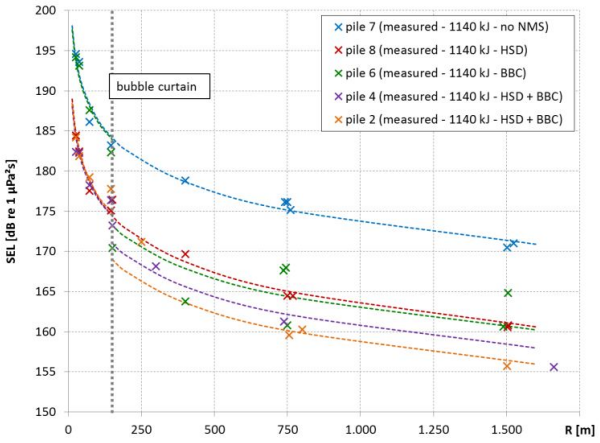

Fig. 5: Sound exposure levels measured in water depths around 20 m at different distances for piles with varying noise mitigation measures at 1140 kJ pile driving energy [9].

Tab. 1: Noise reduction measurements of varying noise mitigation systems in water depths of 30 m in a distance of 750 m [7].

noise mitigation system	**ΔSEL (dB)**	**piles**
BBC	10 - 15	≥ 300
DBBC	14 - 18	≥ 300
HSD	8 - 13	≥ 10
IHC-NMS	10 - 14	≥ 140
IHC-NMS +BBC	17 - 23	≥ 90
HSD+BBC	15 - 20	≥ 30
HSD+DBBC	14 - 22	≥ 20

Altogether the measurements show that noise mitigation measures reduce noise emissions significantly and the combination of tho different systems increases the effectiveness. A single noise mitigation system at 20 m water depth reduces sound levels by at least 9 dB at 750 m distance and the combination of two systems reduces noise emissions by at least 13 dB at 750 m. At water depth up to 30 m a single optimized

https://doi.org/10.25974/ren_rev_2021_04

Tab. 2: Noise reduction measurements of varying noise mitigation systems in water depths of 40 m in a distance of 750 m [5].

noise mitigation system	ΔSEL (dB)	piles
BBC	7 - 11	≥ 700
DBBC	15 - 16	
HSD	10 - 13	≥ 340
HSD+DBBC	18 - 24	

noise mitigation system can reduce noise levels by a minimum of 10 dB (SEL) and a maximum of 18 dB (SEL). For higher water depths up to 40 m the minimum is 7 dB (SEL) and the maximum 16 dB (SEL). Whereas a combination of two systems results in a minimum noise reduction of 14 dB (SEL) and maximum of 23 dB (SEL) in water depth of up to 30 m and for a water depth of 40 m the minimum is 18 dB (SEL) and the maximum 24 dB (SEL).

5 Conclusion

To protect the environment, reducing sound emissions during pile driving is of great interest. To date, several noise mitigation systems are available on the market, but only a few systems are commonly used and tested under offshore conditions. These systems are the BBC, HSD and IHC-NMS, which can be considered state of the art for water depths of up to 40 m and pile diameters of up to 8 m [4].

- The BBC is a proven technology with an independent installation process and the best tested noise mitigation system with potential for optimization with respect to effectiveness and handling. It was successfully applied in several projects where under certain environmental conditions the SEL of 160 dB can be met. With a DBBC or triple BBC, noise reduction increases and the system can be further combined with other noise mitigation measures such as HSD, IHC-NMS or reduced blow energy. However, the systems efficiency is impacted by the air volume stream pumped into the hose, strong currents, a sub-optimal configuration and it is highly dependent on water depth, making a project specific configuration necessary for a successful application. With regard to larger monopiles the greater water depth will make the combination with other noise mitigation systems necessary to achieve desired noise reduction.
- The IHC-NMS as well is a proven system, that is robust and reliable with no impact in installation time. At small and intermediate piles with shallow depth the SEL of 160 dB can be met. Moreover, the system is largely independent of water depth, but regarding lager monopiles more research is needed [5].
- HSD are an often used and tested noise mitigation technique. The system is lightweight and cost-efficient, with an easy handling causing no larger delays of the piling process and needs to be customized for each project. Even though the efficiency is independent of the water depth and currents, practicability and efficiency still need to be proven for larger water depths, but there are already concepts for large monopiles [2].

6 Outlook

The literature research revealed that noise mitigation systems are sufficient for water depth of up to 40 m and and pile diameters of up to 8 m. Large monopiles with diameters up to 12 m will cause higher noise emissions and greater water depth of over 40 m with higher hydro static pressure will cause further challenges in reducing underwater noise levels. Thus, more research concerning the successful application and noise reduction of noise mitigation systems to larger pile diameters at greater water depths is needed. Based on current project measurements, for large diameter monopiles the use of a single noise mitigation system will not be sufficient. To keep the limiting values for under water noise emissions, the combination of different noise systems will be mandatory. Alternative pile driving methods such as modification of the piling hammer and reducing the maximum blow energy are in the experimental stage of their development status, but are promising to reduce noise emission by an additional 1-4 dB [4]. Furthermore, noise mitigation concepts always need to be customized for each project. Factors such as local environmental conditions and the required degree of noise reduction need to be considered in the project specific evaluation. [9].

References

[1] E. Klages, J. von PEIN, S. Lippert, and O. Estorff. “Reducing offshore pile driving noise: Shape optimization of the impact hammer” (2019).

[2] K.-H. Elmer. “Effective Offshore Piling Noise Mitigation in Deep Waters”. *Journal of Civil Engineering and Architecture* 12 (2018), pp. 662–668.

[3] S. Koschinski and K. Lüdemann. “Development of Noise Mitigation Measures in Offshore Wind Farm Construction, report on behalf of BfN” (2013).

[4] M. A. Bellmann, J. Schuckenbrock, S. Gündert, M. Müller, H. Holst, and P. Remmers. "Is There a State-of-the-Art to Reduce Pile-Driving Noise?" (2017). Ed. by J. Köppel, pp. 161–172.

[5] S. Koschinski and K. Lüdemann. "Noise mitigation for the construction of increasingly large offshore wind turbines-Technical options for complying with noise limits, report on behalf of BfN" (2020).

[6] Z. Li and C. McPherson. "Rio Tinto Cape Lambert Port A Marine Structures Refurbishment Project. Acoustic Modelling of Impact Pile Driving for Assessing Marine Fauna Sound Exposures" (2018).

[7] M. A. Bellmann. "Overview of existing noise mitigation systems for reducing pile-driving noise". *Proceeding auf der Internoise* (2014).

[8] G. Glasbergen. "Underwater Noise: An analysis to the relevant criteria for positioning a bubble curtain" (2020).

[9] P. Stein, H. Sychla, J. Gattermann, and J. Degenhardt. "Hydro sound emissions during impact driving of monopiles using Hydro Sound Dampers and Big Bubble Curtain" (Oct. 2015).

https://doi.org/10.25974/ren_rev_2021_04

Sensorless maximum power point tracking systems in wind energy conversion systems

A review

*Enno Tchorz**

Münster University of Applied Sciences, Stegerwaldstraße 39, 48565 Steinfurt, Germany

Abstract

Wind energy conversion systems have attracted considerable attention as a renewable energy source due to depleting fossil fuel reserves and environmental concerns as a direct consequence of using fossil fuel and nuclear energy sources. The increasing number of wind turbines increases the interest in efficient systems. The power output of a wind energy conversion system depends on the accuracy of the maximum power tracking system, as wind speed changes constantly throughout the day. Maximum power point tracking systems that do not require mechanical sensors to measure the wind speed offer several advantages over systems using mechanical sensors. In this paper four different approaches that do not use mechanical sensors to measure the wind speed will be presented; the assets and drawbacks of these systems are highlighted, and afterwards the examined algorithms will be compared based on different characteristics. Finally, based on the analysis, an evaluation is made as to which of the presented algorithms is the most promising.

1 Introduction

The total installed capacity of wind power is growing tremendously in the global market. According to the statistics of the world wind energy association [1], the global wind power installation has reached 651 GW by the end of 2019. That is approximately double the amount of the wind power capacity by the end 2014, due to the increasing number of wind energy capacity the need of more efficient systems to determine the maximum power point (MPP) rises. Wind energy conversion systems (WECS) are usually equipped with mechanical sensors to measure wind speed, rotor shaft speed, generator position and speed for system monitoring, control and protection of the WECS. The use of this sensors increases the:

1. cost,
2. size,
3. weight,
4. hardware wiring complexity and
5. lowers the reliability of WECS [2].

Another drawback: anemometers typically used to measure wind speed from WECS are sensitive to icing. In many regions that have excellent wind resources but long winters, special models of anemometers with electrically heated shaft and cups are required [2]. To achieve high efficiency with MPPT systems in WECS, an accurate anemometer is required due to the gusts and turbulence of the wind. The use of an accurate anemometer adds extra cost to system, especially for small scale wind turbines [3]. The problems associated with using mechanical sensors to measure the wind speed can be solved by using sensorless maximum power point tracking (MPPT) systems.

2 Wind turbine modeling

The input of a wind turbine is wind and the output is mechanical power driving the generator rotor [4, 5]. The mechanical power can be expressed as:

$$P_m = \frac{1}{2}\rho A V^3 C_p(\lambda, \beta) \tag{1}$$

where P_m is the power extracted from the wind (in Watts), ρ is the air density (in kg/m^3), A is the area swept by the rotor (in m^2), V is the wind speed (in m/s) and C_p is the turbine power coefficient (dimensionless). The turbine power coefficient C_p describes the power extraction efficiency of the wind turbine [6]. It is a nonlinear function of both the tip speed ration (λ) and the blade pitch angle (β). While its maximum theoretical is approximately 0.59, in reality it is between 0.4 and 0.45 [7]. The tip speed ratio is a variable expressing the ratio of the linear speed of the

*Corresponding author: et839266@fh-muenster.de.

https://doi.org/10.25974/ren_rev_2021_05

blade tips to the rotational speed of the wind turbine [8–10], and can be expressed by Eq.2:

$$\lambda = \frac{R\omega_m}{V} \tag{2}$$

where ω_m is the velocity of the rotor. Numerous different versions of fitted equations for C_p have been used in previous studies. One way to express C_p is [11]:

$$C_p(\lambda,\beta) = 0,5176(\frac{116}{\lambda_i} - 0,4\beta - 5)e^{-\frac{21}{\lambda_i}} + 0,0068\lambda \tag{3}$$

with

$$\frac{1}{\lambda_i} = \frac{1}{\lambda + 0,08\beta} - \frac{0,035}{\beta^3 + 1} \tag{4}$$

3 MPPT control

3.1 Optimal Torque Control

The objective of the MPPT-Optimal Torque (OT) method is maximizing power extraction without wind speed measurements. This method is equivalent to tracking the maximum power conversion point of a filtered version for the wind, avoiding sudden changes of the torque, and consequently reducing mechanical stress in the shaft [12]. As shown in the block diagram Fig. 1, the OTC is reaching the maximum power point by adjusting the actual torque of the generator according to the reference torque. In order to determine the maximum power point without knowledge of the wind speed we substitute Eq.2 into Eq.1. The new expression yields:

$$P_m = \frac{1}{2}\rho\pi R^5 \frac{C_p}{\lambda^3}\omega_m^3 \tag{5}$$

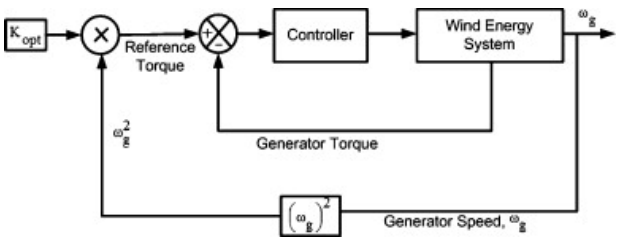

Fig. 1: Block diagram of the optimal torque control method [13]

If the rotor is running at $\lambda = \lambda_{opt}$, it will also run at $C_p = C_{Pmax}$. Thus Eq.5 also can be written as:

$$P_m = \frac{1}{2}\rho\pi R^5 \frac{C_{Pmax}}{\lambda_{opt}^3}\omega_m^3 = k_{opt}\omega^3 \tag{6}$$

Considering that $P_m = \omega_m T_m$, we reach our final expression:

$$T_m = \frac{1}{2}\rho\pi R^5 \frac{C_{Pmax}}{\lambda_{opt}^3}\omega_m^2 = k_{opt}\omega^2 \tag{7}$$

Eq.7 represents our analytical expression of the optimum torque curve, and Fig. 1, is a given as reference torque for the controller that is connect to the wind turbine.

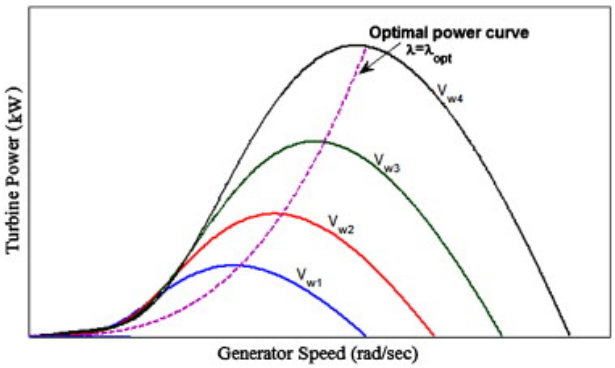

Fig. 2: Characteristics of turbine power as a function of the rotor speed for a series of wind speeds [13]

3.2 Hill Climb search

The hill-climb searching (HCS) method, is a mathematical optimization technique to determine the local maximum of a given function. Fig. 3 shows how the algorithm works. If the operating point of the function, in our case on the left side of the peak point P_{mpp}, the controller must move our operating point to the right so we can reach P_{mpp}. This happens with a perturbation of the control variable. If the perturb results in an increase of the power, the same perturbation is applied, otherwise the mathematical sign of the perturbation is reversed. To improve the efficiency and the accuracy of the conventional HCS method, modified variable step size algorithms have been proposed [13–15]. When using improved HCS algorithms, the step size is getting generated according the the operating point. When the system is far away from the tracking point, it speeds up the process by increasing the step size and speeding up the process of reaching the MPP. As the controller approaches the MPP, the step size decreases until it approaches zero. This way the oscillations occurring when using the conventional HCS algorithm are getting reduced. One way to increase efficiency and accuracy using an improved HCS algorithm is now explained. In the examined study [14], the distance from the actual generator speed (ω) to the optimal generator speed (ω^*),which is determined by the optimal power curve, was used to adjust the perturbation size at the end of each cycle[13].The Flowchart of the improved method can be found in [14]. There are three steps of operation. The features of the three modes are explained below:

- Mode 0: searching for k_{opt} to track the MPP. Once the initial conditions are satisfied, k_{opt} will

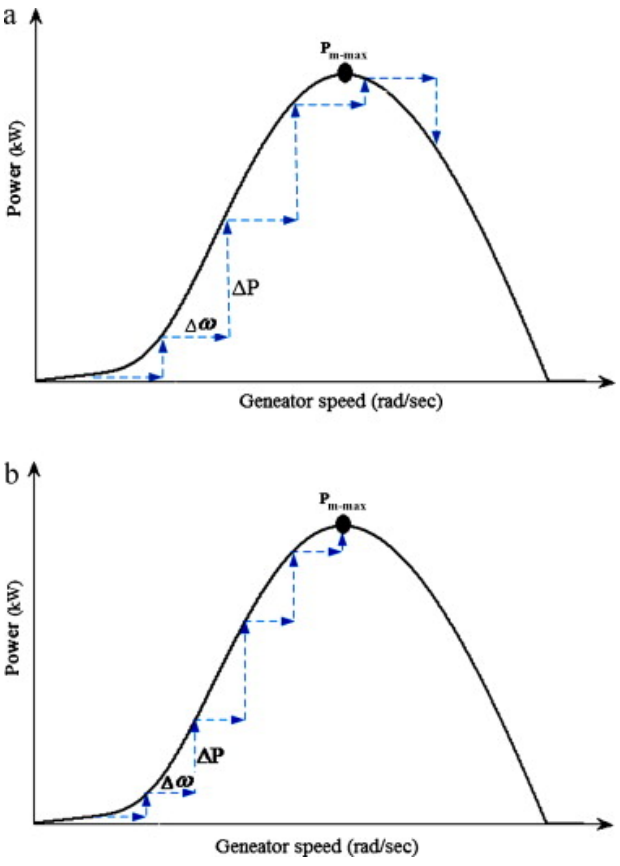

Fig. 3: HCS control (a) larger perturbation and (b) smaller perturbation [13].

be calculated through the measured power and rotational speed and the system is switched to Mode 1.

- Mode 1: the perturbation is set to zero to keep the system at the state reached in Mode 0. A change of wind speed is detected through change in rotor speed and leads to Mode 2.
- Mode 2: this mode implements the adaptive hill climbing according to the stored k_{opt}. The perturbation size is decided by the distance of the operating point from the $k_{opt} * w^3$ curve, shown in Fig. 2. It is not possible to track the MPP perfectly, but the controller moves the operating point very close to the peak power.

3.3 Neural Networks based MPPT-Algorithms

Artificial Neural Network (ANN) models, also called Neural Networks (NN), take their inspiration from the basic framework of the brain [16]. ANN consists of many nodes and connecting synapses. Nodes operate in parallel and communicate with each other through connecting synapses[17]. A NN consists of three layers:

- input,

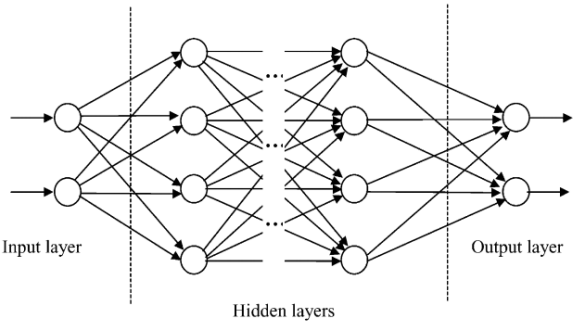

Fig. 4: Structure of a neural network [18]

- hidden,
- and output layers.

The layers are connected with nodes. The number of nodes in each layer varies dependent of the used model. The architecture of a NN is shown in Fig. 4

The input variables can be:

- pitch angle,
- terminal voltage,
- output torque,
- wind speed,
- rotor speed,

etc. or any combination of the variables [3]. The output is generally a reference signal:

- reference power,
- rotor speed,
- reference torque,

etc. that is used to drive the power electronic circuit of the wind turbine close to the MP [3]. There are numerous approaches using NN to determine the MPP [19–21].

4 Critical analysis and comparison

Although the OT algorithm is widely used in WECS, it requires the information of air density and turbine mechanical parameters, which vary in different systems. Moreover, the OT curve, which is mainly obtained via experimental tests, will change when the system ages [12, 22–24]. This will also affect the MPPT efficiency [3].

The HCS algorithm is the simplest MPPT algorithm that does not require any prior knowledge of the system or any additional sensor except the measurement

of the power which is subjected to maximization. That is the reason why the HCS algorithm can be used in any renewable energy system that exhibits a unique power maximum. Although these features should make HCS the top choice for MPPT in any renewable energy conversion system but in reality it is only feasible in the slow varying systems. For instance it is quite feasible for the PV energy systems where the sun's irradiance changes over the period of several minutes but not for the WECS where the wind may change quite fast in the matter of seconds.[25] However, the method deviates to trace the peak power point under sudden wind gusts. In order to overcome this drawback, there are many improved HCS methods presented in literature [3, 13, 14, 26].

ANN based control [27], [20] can be quite effective and robust only after it is sufficiently trained for all kinds of operating conditions. This is quite a tough requirement and requires a long offline training. Therefore, this MPPT control can be quite efficient when trained [3] for long time but this long offline training makes ANN quite unattractive for the real time practical applications. The ANN for its training requires wind velocity sensor additionally with the generator speed sensor which is again not a good feature.

4.1 Comparison and assets of the described algorithms

In other papers the presented methods have already been analyzed and compared. Nevertheless the authors used different criteria to compare the methods. Based on the above description and literature [3, 28, 29] comparing the different MPPT methods, Tab. 1 was compiled.

Tab. 1: Comparison of characteristics of the described MPPT algorithms

	HCS	Modified HCS	OTC	ANN-based
Complexity	Simple	Medium	Simple	High
Wind turbine characteristics	No	Yes	Yes	No
Convergence speed	Slow	Medium	Fast	Medium
Prior training/ knowledge	No	No	Yes	Yes
Perfomance under varying wind	Medium	Good	Medium	Very good
Wind speed measurement	No	No	No	No (dependent on the used NN)
Rotor speed measurment	Yes	Yes	Yes	Yes

5 Conclusion

Due to the increasing penetration of wind turbine power, it is necessary to get the maximum power from the wind. In some cases, the implementation of mechanical sensors is unfavorable, due to the reasons mentioned above. In this case, MPPT methods without mechanical sensors are the preferred technique. Due to their simplicity, HCS and OTC are promising methods to determine the MPP. Especially improved HCS methods have generated a great deal of interest lately because they overcome the drawbacks of the conventional HCS method by increasing the efficiency and accelerate the process of determining the MPP. ANN-based methods are of interest because of their good performance under varying wind speed. The main problem encountered when using ANN-based methods is the need of a long offline training. This problem has not been solved so far. Once the the long training time can be reduced, ANN-based methods can become the best choice for sensorless MPPT systems. Finally, it must be noted that none of the presented methods should be the preferred choice in any case. The assets and drawbacks are different and need to be considered before using the described systems in practical applications. This paper servers as a reference, to decide which sensorless MPPT system might be the most feasible for the given application. For instance, in areas with many sudden wind changes, the ANN-based algorithm should be the preferred choice. While the HCS algorithm could be considered a feasible method in areas with less varying wind speed due to the simplicity and the fact that no prior training is required for this algorithm.

References

[1] J.-D. Pittleoud (2019). [Online; accessed 28-December-2020]. URL: https://library.wwindea.org/global-statistics/.

[2] W. Qiao. "Intelligent mechanical sensorless MPPT control for wind energy systems". *2012 IEEE Power and Energy Society General Meeting*. IEEE. 2012, pp. 1–8.

[3] D. Kumar and K. Chatterjee. "A review of conventional and advanced MPPT algorithms for wind energy systems". *Renewable and Sustainable Energy Reviews* 55 (2016), pp. 957 –970. ISSN: 1364-0321. DOI: https://doi.org/10.1016/j.rser.2015.11.013. URL: http://www.sciencedirect.com/science/article/pii/S1364032115012654.

[4] Hui Li, K. L. Shi, and P. G. McLaren. "Neural-network-based sensorless maximum wind energy capture with compensated power coefficient". *IEEE Transactions on Industry Applications* 41.6 (2005), pp. 1548–1556. DOI: 10.1109/TIA.2005.858282.

[5] M. Karrari, W. Rosehart, and O. P. Malik. "Comprehensive control strategy for a variable speed cage machine wind generation unit". *IEEE Transactions on Energy Conversion* 20.2 (2005), pp. 415–423. DOI: 10.1109/TEC.2005.845525.

[6] M. Grimble and M. Johnson. "Optimal Control of Wind Energy Systems" (2008).

[7] Z. Chen, J. M. Guerrero, and F. Blaabjerg. "A review of the state of the art of power electronics for wind turbines". *IEEE Transactions on power electronics* 24.8 (2009), pp. 1859–1875.

[8] L. L. Freris and L. Freris. *Wind energy conversion systems*. Vol. 31. Prentice Hall New York, 1990.

[9] A. Abdelkafi and L. Krichen. "New strategy of pitch angle control for energy management of a wind farm". *Energy* 36.3 (2011), pp. 1470–1479.

[10] P. Nema, R. Nema, and S. Rangnekar. "A current and future state of art development of hybrid energy system using wind and PV-solar: A review". *Renewable and Sustainable Energy Reviews* 13.8 (2009), pp. 2096–2103.

[11] M Nasiri, J Milimonfared, and S. Fathi. "Modeling, analysis and comparison of TSR and OTC methods for MPPT and power smoothing in permanent magnet synchronous generator-based wind turbines". *Energy Conversion and Management* 86 (2014), pp. 892–900.

[12] S. Ganjefar, A. A. Ghassemi, and M. M. Ahmadi. "Improving efficiency of two-type maximum power point tracking methods of tip-speed ratio and optimum torque in wind turbine system using a quantum neural network". *Energy* 67 (2014), pp. 444–453.

[13] M. A. Abdullah, A. Yatim, C. W. Tan, and R. Saidur. "A review of maximum power point tracking algorithms for wind energy systems". *Renewable and sustainable energy reviews* 16.5 (2012), pp. 3220–3227.

[14] S. M. R. Kazmi, H. Goto, H.-J. Guo, and O. Ichinokura. "A novel algorithm for fast and efficient speed-sensorless maximum power point tracking in wind energy conversion systems". *IEEE Transactions on Industrial Electronics* 58.1 (2010), pp. 29–36.

[15] A. C.-C. Hua and B. C.-H. Cheng. "Design and implementation of power converters for wind energy conversion system". *The 2010 International Power Electronics Conference-ECCE ASIA-*. IEEE. 2010, pp. 323–328.

[16] E. Alpaydin. *Introduction to machine learning*. MIT press, 2020.

[17] Y. S. Murat and H. Ceylan. "Use of artificial neural networks for transport energy demand modeling". *Energy policy* 34.17 (2006), pp. 3165–3172.

[18] S. A. Kalogirou. "Artificial neural networks in renewable energy systems applications: a review". *Renewable and sustainable energy reviews* 5.4 (2001), pp. 373–401.

[19] M. Pucci and M. Cirrincione. "Neural MPPT control of wind generators with induction machines without speed sensors". *IEEE Transactions on Industrial Electronics* 58.1 (2010), pp. 37–47.

[20] J. Thongam, P Bouchard, R Beguenane, and I Fofana. "Neural network based wind speed sensorless MPPT controller for variable speed wind energy conversion systems". *2010 IEEE Electrical Power & Energy Conference*. IEEE. 2010, pp. 1–6.

[21] L. Shanzhi, W. Haoping, T. Yang, and A. Aitouche. "A RBF neural network based MPPT method for variable speed wind turbine system". *IFAC-PapersOnLine* 48.21 (2015), pp. 244–250.

[22] S. Morimoto, H. Nakayama, M. Sanada, and Y. Takeda. "Sensorless output maximization control for variable-speed wind generation system using IPMSG". *IEEE Transactions on Industry Applications* 41.1 (2005), pp. 60–67. DOI: 10.1109/TIA.2004.841159.

[23] M. Shirazi, A. H. Viki, and O. Babayi. "A comparative study of maximum power extraction strategies in PMSG wind turbine system". *2009 IEEE Electrical Power Energy Conference (EPEC)*. 2009, pp. 1–6. DOI: 10.1109/EPEC.2009.5420931.

[24] H. Camblong, I. M. de Alegria, M. Rodriguez, and G. Abad. "Experimental evaluation of wind turbines maximum power point tracking controllers". *Energy Conversion and Management* 47.18 (2006), pp. 2846 –2858. ISSN: 0196-8904. DOI: https://doi.org/10.1016/j.enconman.2006.03.033. URL: http://www.sciencedirect.com/science/article/pii/S0196890406001245.

[25] S. M. R. Kazmi, H. Goto, H. Guo, and O. Ichinokura. "Review and critical analysis of the research papers published till date on maximum power point tracking in wind energy conversion system". *2010 IEEE Energy Conversion Congress and Exposition*. 2010, pp. 4075–4082. DOI: 10.1109/ECCE.2010.5617747.

[26] B. Meghni, D. Dib, A. T. Azar, and A. Saadoun. "Effective supervisory controller to extend optimal energy management in hybrid wind turbine under energy and reliability constraints". *International Journal of Dynamics and Control* 6.1 (2018), pp. 369–383.

[27] H. Li, K. Shi, and P. McLaren. "Neural-network-based sensorless maximum wind energy capture with compensated power coefficient". *IEEE transactions on industry applications* 41.6 (2005), pp. 1548–1556.

[28] M. Cheng and Y. Zhu. "The state of the art of wind energy conversion systems and technologies: A review". *Energy Conversion and Management* 88 (2014), pp. 332–347.

[29] H. Abouobaida **et al.**. "New MPPT control for wind conversion system based PMSG and a comparaison to conventionals approachs". *2017 14th International Multi-Conference on Systems, Signals & Devices (SSD)*. IEEE. 2017, pp. 38–43.

https://doi.org/10.25974/ren_rev_2021_05

Review of the suitability of thermoplastic rotor blades in terms of the circular economy

Joshua Steinigeweg[*]

Münster University of Applied Sciences, Stegerwaldstraße 39, 48565 Steinfurt, Germany

Abstract

Wind energy has steadily gained importance in the generation of renewable energy over the last 25 years. A wind turbine has an average life expectancy of about 25 years. After that, thermoplastic composite materials from the rotors, among other things, accumulate and have to be recycled. Previous methods, such as landfilling, incineration and pyrolysis, have not yet proven to be effective in terms of the circular economy because the recycled material cannot be reused for equivalent products. The use of thermoplastic materials can be a sensible alternative, as thermoplastic resins can be recycled almost without loss of value due to their properties. Recycling of fibreglass is also possible with less loss of stiffness. In the future, it will be crucial to scale up thermoplastic rotor blades and create a market for the recycled material.

Keywords: Wind power, Recycling, Thermoplastic rotor, Solvolysis, Circular economy

1 Introduction

Wind power plants are of great importance for the energy turnaround and in the fight against climate change. After about 20 to 25 years they have to be shut down and dismantled because they have reached the end of their design life. Here, the experience with onshore plants is much greater than with off-shore plants [1].

In order to achieve the goal of closed material cycles, the materials must be recycled. Success can already be seen in the tower, hydraulics, generator and gearbox, while the neodymium (NdFeB) magnets, nacelle and rotors are still considered problematic. Especially the rotors are problematic because they are made of composite materials consisting of epoxy resin, fiberglass and balsa wood. For this reason, only incineration and subsequent landfilling of these components has so far been an economical method of exploitation, since alternatives such as pyrolysis, oxidation in fluidized bed and treatment with chemicals are very costly and only possible with a high energy input [2].

In the USA, recyclate is obtained from shredded rotor blades and then used as an aggregate for polyresin for the production of railway tracks, subway rails and masts. Since the rotor blades are additionally shredded in this process, recovery of the raw materials resin and fiberglass after use is almost impossible [3].

Therefore, this paper will first take a closer look at the current recycling of rotor blades and then discuss to what extent thermoplastics are suitable for the production of rotor blades and whether recycling without downcycling can be achieved through their use. The recycling of the other material flows is not considered in this review, because they are not as critical as the composite materials or already functioning recycling technologies.

2 Existing recycling methods for thermoset rotors

A wind farm consists mainly of different metals, such as iron, copper and aluminum. Composite materials made of wood, resin and fiberglass represent another large fraction. Other components are NdFeb magnets, various oils, electronic components and batteries. Recycling for these different material streams has been worse for some materials and better for others. For example, the tower, hydraulics, generator and gearbox are considered relatively easy to recycle, while the rotor blades, made of composite materials, are the most difficult to recycle. Table 1 gives an overview of the typical material composition of a 60 MW wind farm.

2.1 Recycling of composites

Composite materials are mainly found in the rotor blades and nacelles. The recycling of these materials is very difficult due to the complex material structure. In addition, the rotors will grow from a length of 15 to 20 m to a length of 75 to 80 m. It is crucial to have the right technology and a market for the recycled products [2].

[*]Corresponding author: j.steinigeweg@fh-muenster.de.

https://doi.org/10.25974/ren_rev_2021_06

Tab. 1: Material components of a 60 MW wind farm [2]

Type of Material	Mass [kg]
Ferrous metal	6 560 000
Aluminium	104 000
Composite Materials	660 000
Lubricating oil	30 000
Electronics	124 000
Batteries	36 000
Fluorescent lamps	3 800
NdFeB magnet	40 000
Copper	292 000
Balsa Wood	29 000
Polyethylene	32 000
Polypropylene	6 600
Polyvinylchloride	6 000
Miscellaneous	-
Total	7 923 400

2.1.1 Mechanical recycling and thermal utilization

The composite materials are shredded. However, it is almost impossible to separate the resin from the material. Therefore, it is only possible to use these materials as landfill materials. But this is prohibited in Germany, which is why incineration and subsequent disposal of the ashes is preferred [2].

In the USA the company Global Fiberglass Solutions Inc. cooperates with the Environmental Protection Agency (EPA) to jointly issue recycling certificates. Here the rotor blades are also processed to a recyclate by shredding. Poly resin is added to this recyclate and new products for infrastructure, such as railroad sleepers, subway sleepers and bollards are produced. This products did not show disadvantages compared to conventionally made products [3].

2.1.2 Pyrolysis

The pyrolysis process requires temperatures in a range of 450 °C to 700 °C. The process is divided into two sub-steps, each of which takes place in rotating ovens. An oxygen-free atmosphere is required in the first oven [2]. The resin becomes steam and can be used to generate electricity [3]. In the second rotating oven oxygen is present. This removes the remaining impurities on the surface of the fiberglass [2]. The company ReFiber from Denmark is well known for this process, but a commercial use is not yet being made [2, 3].

2.1.3 Chemical

By adding a solvent to the composite stopper, the glass fiber is released without mechanical damage. The resin can be partially recovered by chemical solvolysis [4].

2.2 Problems

High costs of the recycling processes, a lack of market for the recycled products and a general lack of business model are the main problems of current recycling in all processes [2].

2.2.1 Mechanical recycling and thermal utilization

The rotor blades are shredded into 15 mm to 25 mm long pieces [2], which makes reuse almost impossible, since the fiberglass has very poor mechanical properties [3]. In addition, only an incomplete separation of resin and fiberglass is possible, since a resin residue remains on the fiberglass [2, 3]. In addition, fiberglass dust can be released during the shredding process, which can lead to health problems for the workers[3].

After incineration, about 60 % remains as ashes [2], depending on anaorganic pollutants. Further treatment of the ashes may therefore become necessary [4]. Small glass fibre components in the flue gas can also cause clogging of the filter system. This can lead to the release of toxic flue gases [4]. Both mechanical crushing and combustion represent downcycling in the waste hierarchy, which is why these processes should not be the methods of choice [2].

2.2.2 Pyrolysis

The disadvantage of the pyrolysis process is that the glass fiber has a much lower strength after the process. Because the glass fiber cannot be reused for the production of new rotor blades, downcycling takes place. In addition, the resin cannot be recovered, but can only be burned as pyrolysis gas to generate electricity and heat [4]. However, the energy yield of this process is low [3].

2.2.3 Chemical

Problems with this process are the use of toxic and aggressive chemicals and the extremely high costs [3, 4].

3 Thermoplastic blades

As the results from chapter 2 demonstrate, no suitable process has yet been found that meets the requirements of a circular economy, since the conventional recycling processes for rotors made of composite materials are very costly and energy-intensive, in some

https://doi.org/10.25974/ren_rev_2021_06

cases toxic chemicals are required and in some cases materials are withdrawn from the material cycles. This chapter will therefore examine whether rotors made of thermoplastic composite material are suitable for replacing the rotors made of thermoset composite material used to date, since the thermoplastic composite material has significantly better recycling properties [5]. For this purpose, two rotor blades of identical shape, which differ in the use of thermoplastic composite material in one rotor blade and thermoset composite material in the other, are first compared in terms of their mechanical properties. Recycling techniques for the rotors with thermoplastic composite material are then presented.

3.1 Comparison between thermoset and thermoplastic rotor blades

In the following, two 13 m long test rotor blades, one made of a composite material with thermoplastic resin and the other made of a composite material with thermosetting resin, are compared with regard to their mechanical properties. The rotor blade was developed and validated for another National Rotor Testbed (NRT) project. The aerodynamic behavior is comparable to that of a rotor blade for 1.5 MW wind turbines [6].

Both rotors have the same shape and the same balsa wood core. Hexion epoxy resin was used for the thermoset composite rotor. The manufacturer of the fiberglass is Nippon Electric Glass, which is woven by Vectopryl in unidirectional and biaxial directions. For the rotor made of thermoplastic composite material, Elium thermoplastic resin was used. The fiberglass is from Johns Manville. Due to density and weight differences, different numbers of layers of fiberglass had to be used for the rotors. However, computer simulations showed that the effect on stiffness was not significant [6].

The molds for both rotors were produced using 3D-printing. The individual blade components were produced by vacuum assisted resin transfer (VARTM) and then glued together. Polymethyl metacrylate adhesive was used for the thermolastic components and a special epoxy adhesive for the thermoset composite rotor. It is necessary to limit the temperature to below 80 °C for the exothermic reaction during the production of the rotor components made of thermoplastic composite material, otherwise there will be negative effects on the material. A control agent must therefore be added. But this has no influence on the material properties. In the manufacture of the thermoset composite rotor, the resin was poured into a mold and then kept at a temperature of 70 °C for a period of 4 hours [6].

3.1.1 Measurement methodology

As Figure 1 shows, the static load is simulated at the positions 4.60 m, 7.55 m and 10.85. At the 4.60 m point, a static ballast weight is mounted and at the other two points, the force is applied by an overhead crane, with a force redirection performed by a turning plate on the floor and the two points connected by a stirrup. At all points, the forces are transmitted by stirrups attached to the rotor. The deflection is measured by string potentiometer at positions 4 m, 7 m and 11.25 m respectively. Load is applied at a rate of 45 N/s over a period of 30 s. The load is applied up to the design limit [6].

To simulate fatigue loads, the weights on the saddles are adjusted. Fatigue test moments are achieved Resonance Excitation actuators at damped natural frequency [6].

Fig. 1: 13 m thermoplastic blade at the test stand (c) Ryan Beach [7]

3.1.2 Results

In terms of static response, the thermoplastic rotor has a displacement at the 4 m measuring point that is 11 % greater than that of the thermoset rotor. At the 11 m measuring point, the deflection of the thermoplastic rotor is only 3 % greater. The small difference near the outer edge of the rotor indicates that there is only a small difference in stiffness between the two materials. The small differences can be attributed to the use of fibreglass from different manufacturers and the use of different adhesives, as the adhesive for the thermoplastic components has a higher elasticity [6].

The fatigue behaviour of the two different composites is good, with less than 0.5 % deviation in compliance after each of 1 000 000 cyclic runs compared to the first run [6].

The same test set-up as for the fatigue test was used to determine the structural damping. The results show that the thermoplastic rotor has 0.70 % of the

critical damping and the thermoset rotor 0.13 % of the critical damping in the flatwise direction. In the edgewise direction, the thermoplastic rotor has 1.34 % of the critical damping and the thermoset rotor 0.21 % of the critical damping. In both directions, the values of the thermoplastic rotor exceed those of the thermoset rotor by at least five times. One possible reason for this is the use of different adhesives; however, this can be neglected as the proportion of adhesive is very small in relation to the total mass. The main cause can be seen in the different material matrix of thermoplastics and thermosets. Due to the higher damping, the reaction of the rotor to dynamic changes may be reduced, thus increasing stability. [6].

3.2 Recycling

The main recycling processes for thermoplastic rotor blades are thermal treatment by pyrolysis, mechanical shredding, thermal forming and chemical solvolysis. As the pyrolysis and mechanical treatment processes do not differ significantly from the processes for the treatment of thermoset rotor blades presented in chapters 2.1.1 and 2.1.2, only thermal reshaping and chemical solvolysis are discussed below [7].

3.2.1 Thermoforming

The thermoforming process for thermoplastics has meanwhile matured. First, the material must be heated to the glass transition of the respective polymer. Then it can be formed into other shapes. Even after cooling, the material remains dimensionally stable. However, this process has so far only been established for granulated material. For composite materials, there is little experience available so far. One possible procedure could be the division of large rotors into smaller segments, which are then heated and shaped into new shapes. For example, building boards or skateboards could be produced in this way [7].

3.2.2 Chemical

The chemical process used is solvolysis. In this process, the covalent bonds of the polymer matrix are broken by a reactive solvent. This process requires high temperatures and pressures, which results in a high energy input. However, there have been recent developments that have shown promising results in a low energy process. In the solvolysis process, both the polymer and the glass fibre can be reused, as the stiffness of the fibre has only been reduced by 12 %. So far, however, there is also limited experience with composite materials [7].

4 Evaluation

The discussion of existing recycling processes for thermoplastic rotors has shown that there is currently no technology available that can be used to recycle the rotor blades in the sense of closed cycles. Therefore, a comparison between a 13 m long rotor blade made of thermoplastic composite material and a rotor made of thermoset composite material was presented. In the static test the results only differ slightly. The deflection of the rotor blade made out of thermoplastic composite material is slightly higher in comparison to the one made out of thermoset composite material. The more than 5 times higher damping can have the effect of increasing the stability of the system, as it reacts less to dynamic changes. In addition, after solvolysis almost complete recycling of the thermoplastic composite material is possible. The reduction in the stiffness of the fibreglass is low at 12 %, which means that further use is possible.

This clearly shows that a thermoplastic rotor can be a promising replacement for the existing thermoset rotors; also in the sense of the increasingly important closed raw material cycles.

5 Outlook

In the future, it will be important to gain more experience with thermoplastic rotors. Especially the scale-up will be crucial. Then it will be necessary to check whether cost reductions can be realised through technology on a large scale, because currently this is still more expensive for the rotors used in chapter 3. It will also have to be checked whether a cost advantage can be realised through self-heating due to the exothermic reaction [6]. In addition, a further development of the existing recycling methods is necessary to reduce the costs. It is important that markets are created for recycled materials, because only then it will be possible for them to displace raw materials [7].

References

[1] M. M. Luengo and A. Kolios. “Failure Mode Identification and End of Life Scenarios of Offshore Wind Turbines: A Review”. *Energies* 8.8 (2015-08-01), pp. 8339–8354. ISSN: 1996-1073. DOI: 10.3390/en8088339.

[2] J. P. Jensen. “The path towards sustainable energy”. *Wind Energy* 22.2 (2019), pp. 316–326. ISSN: 1095-4244. DOI: 10.1002/we.2287.

[3] N. Sakellariou. “Current and potential decommissioning scenarios for end-of-life composite wind blades”. *Energy Systems* 9.4 (2018), pp. 981–1023. ISSN: 1868-3967. DOI: 10.1007/s12667-017-0245-9.

[4] K. Larsen. "Recycling wind turbine blades". *Reinforced Plastics* 53.1 (2009), pp. 20–25. ISSN: 0034-3617. DOI: 10.1016/S0034-3617(09)70043-8.

[5] J. Garate, S. Solovitz, and D. Kim. "Fabrication and Performance of Segmented Thermoplastic Composite Wind Turbine Blades". *International Journal of Precision Engineering and Manufacturing - Green Technology* 5.2 (2018-04-01), pp. 271–277. ISSN: 2288-6206. DOI: 10.1007/s40684-018-0028-3.

[6] R. E. Murray, R. Beach, D. Barnes, D. Snowberg, D. Berry, S. Rooney, and et al. "Structural validation of a thermoplastic composite wind turbine blade with comparison to a thermoset composite blade". *Renewable Energy* 164 (2021), pp. 1100–1107. ISSN: 0960-1481. DOI: 10.1016/j.renene.2020.10.040.

[7] D. S. Cousins, Y. Suzuki, R. E. Murray, J. R. Samaniuk, and A. P. Stebner. "Recycling glass fiber thermoplastic composites from wind turbine blades". *Journal of Cleaner Production* 209 (2019), pp. 1252–1263. ISSN: 0959-6526. DOI: 10.1016/j.jclepro.2018.10.286.

Technologisches Lernen im Bereich Windenergie an Land

*Jurek Häner**

Münster University of Applied Sciences, Stegerwaldstraße 39, 48565 Steinfurt, Germany

Abstract

Diese Arbeit befasst sich mit Kostentrends in Zusammenhang mit technologischem Lernen von Windenergie an Land in den USA, in Deutschland und weltweit. Ziel dieser Arbeit ist es, eine Lernkurve für Windenergie an Land zu bestimmen. Dafür wurden Daten zu Stromgestehungskosten (LCOE) und Kosten für die Installation (COP) von Windenergieanlagen (WEA) im Zeitraum von 1983 bis einschließlich 2020 gesammelt, grafisch dargestellt und weitergehend ausgewertet. Die grafische Darstellung der Datenlage verdeutlicht die zeitliche Entwicklung der Technologie. Zur Beschreibung dieser Lernkurven wurden die Progress Ratio (PR) und Learning Rate (LR) in fünf unterschiedlichen Modellen bestimmt. Anhand derer sich in Kombination mit der zukünftig installierten Leistung von WEA eine Prognose über zukünftige Kosten ableiten lässt. Die ermittelten LR bewegen sich zwischen 13 % und 28 %, woraus sich LCOE im Jahr 2030 zwischen 44,03 US$/MWh und 61 US$/MWh ergeben.

Keywords: Wind energy, Technological Learning, renewable energy, Levelized cost of energy

1 Einleitung

Mit dem erwarteten Anstieg des weltweiten Energiebedarfs durch die fortschreitende wirtschaftliche Entwicklung und das Bevölkerungswachstum in Entwicklungsländern könnten sich negative Umweltauswirkungen verstärken. [1] Zur Verringerung der Treibhausgasemissionen, die größtenteils durch die Nutzung von Energie erzeugt werden, sollte die Entwicklung emissionsarmer Energietechnologien priorisiert werden.[2] Der Einsatz von Windenergieanlagen (WEA) zur Bereitstellung erneuerbarer Energie gilt als wichtiger Bestandteil zukünftiger Energiesysteme [3–5]. Gleichzeitig wurden technologische Fortschritte bei der Konstruktion von WEA erzielt [6]. Angefangen bei Konstruktionen mit einer Vertikal-Achse um ca. 200 v. Chr., welche nahe der Persisch-Afghanischen Grenze gefunden wurden, über niederländische Windmühlen bis hin zu großtechnischen Anlagen zur Energieerzeugung, wie sie heute verfügbar sind [7]. Diese Entwicklungen lassen sich ebenfalls in Zusammenhang mit technologischem Lernen darstellen. Technologisches Lernen bzw. Lernkurven sind eine Methode, die besonders in der dynamischen Umwelt- und Klimamodellierung Anwendung findet. Außerdem werden sie unterstützend in politischen Entscheidungsprozessen verwendet [8]. „Das Konzept der Lernkurven beschreibt die empirische Feststellung, dass die Kosten eines industriell gefertigten Gutes bei jeder kumulierten Verdopplung seines produzierten Volumens um einen mehr oder weniger konstanten Prozentsatz sinken.“ [9] Als mögliche Einflussfaktoren werden: Effekte durch die Skalierung, den technischen Fortschritt, das Lernen von ausführenden Stellen und die Rationalisierung der Prozesse benannt.[9] In der Vergangenheit wurden diverse Kostenanalysen für Windenergie an Land durchgeführt und in weiteren Studien zu Lernkurven zusammengefasst. Die Betrachtungen umfassen unterschiedliche Zeiträume oder beziehen sich auf verschiedene Regionen [10]. Daher besteht das Ziel der vorliegenden Arbeit darin, diese Studien zu sammeln, auszuwerten und eine Lernkurve für diese Technologie zu ermitteln.

2 Material und Methoden

Im nachfolgenden Kapitel werden die in dieser Arbeit verwendeten Daten und Methoden dargestellt.

2.1 Datengrundlage

Die verwendeten Daten zur Ermittlung einer Lernkurve werden in Fig. 1 in Anlehnung an Yao, Xu und Sun (2020) dargestellt [11]. Zur Ermittlung der Kosten für die Stromerzeugung durch WEA wurden Publikationen ausgewertet, die ebenfalls das Thema technologsiches Lernen im Bereich Windenergie haben, oder die Kosten für die Stromerzeugung aus erneuerbaren Quellen betrachten.

In den Veröffentlichungen wird eine Aussage über die Stromgestehungskosten (engl. Levelised cost of energy, kurz LCOE) getroffen und/oder die mit der Installation von WEA auftretenden Kosten, im Verhältnis zur installierten Leistung (COP) in US$/kW dargestellt. [11–24] Darüber hinaus werden die hier verwendeten

*Corresponding author: haener@fh-muenster.de.

https://doi.org/10.25974/ren_rev_2021_07

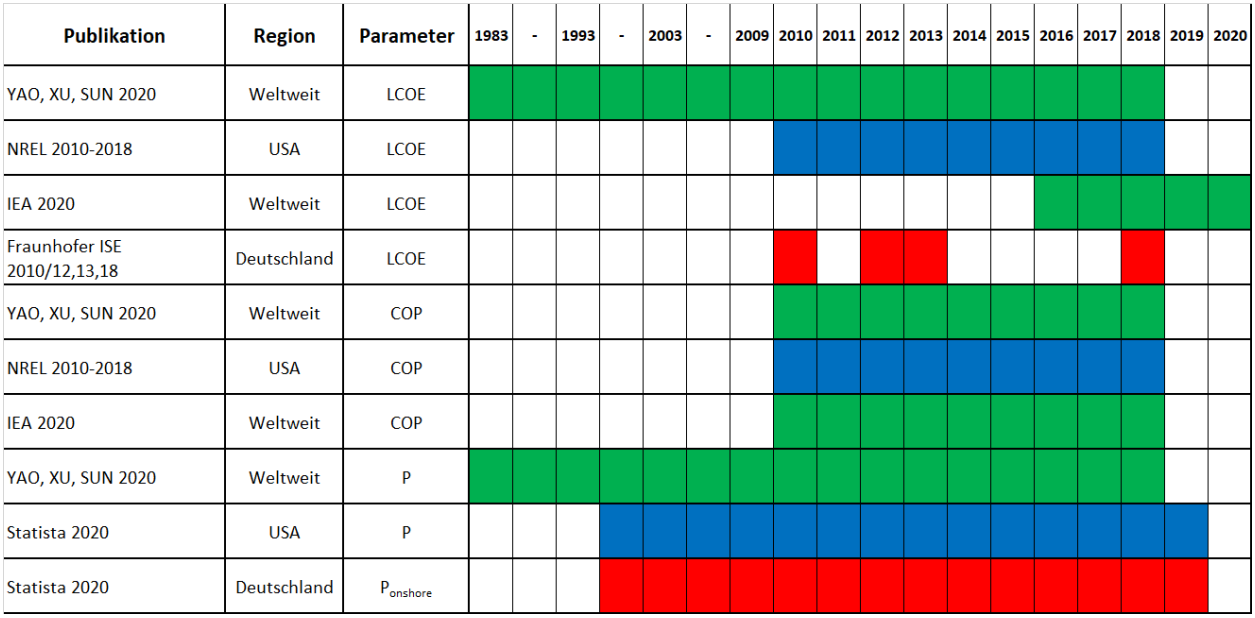

Fig. 1: Verwendete Datengrundlage

Daten zur installierten Erzeugungsleistung von Windenergie in unterschiedlichen Jahren, in den USA, in Deutschland und weltweit in Fig. 1 dargestellt [11, 25, 26].

2.2 Berechnung der Progress Ratio und Learning Rate

Neben der grafischen Darstellung der Relation zwischen Kostenreduktion und produzierter Menge eines Produkts lassen sich die eintretenden Kostenreduktionen ebenfalls durch die Faktoren Progress Ratio (PR) und Learning Rate (LR) darstellen. Diese Parameter dienen dem Vergleich unterschiedlicher Lernkurven bzw. Technologien [27]. Das bei technologischem Lernen zu beobachtende "Korrelationsphänomen", wie es von Neij (1999) beschrieben wird, von sinkenden Kosten bei steigenden kumulierten produzierten Einheiten lässt sich durch folgende Formel 1 vereinfacht beschreiben [28]:

$$C = C_0 \cdot ACC^{-E} \tag{1}$$

Eingang in (1) finden mit C die Kosten für ein Produkt zum Zeitpunkt X, mit C_0 die Kosten für ein Produkt zum Anfangszeitpunkt, mit ACC die kumulierte Menge hergestellter Produkte zum Zeitpunkt X und mit E, der sogenannte Lernparameter. Daraus leiten sich die in Formel 2 und 3 dargestellten Parameter ab. [9]

$$PR = 2^{-E} \tag{2}$$

Die Progress Ratio (PR) trifft eine Aussage über die Höhe der Kosten eines Produkts bei Verdopplung der kumulierten Produktion eintreten. [9, 29]

$$LR = 1 - (2^{-E}) \tag{3}$$

Ähnliches gilt für die Learning Rate (LR), mit dem Unterschied, dass die LR die Höhe der Kostenreduktion quantifiziert. [9, 29] Die Berechnung des Lernparameters E erfolgt durch die umgeformte Formel 1. Sie ergibt sich nach Junginger, Faaij und Turkenburg (2005) sowie nach van Sark und Alsema (2010) wie in Formel 4 dargestellt [29, 30].

$$log(C) = log(C_0) + E \cdot log(ACC) \tag{4}$$

Entsprechend der Struktur der Formel 4 lässt sich, wie auch durch Pieper (2001) empfohlen, bei doppeltlogarithmischer Auftragung der Kostenparameter gegenüber ACC eine Ausgleichskurve ermitteln, dessen Steigung dem Lernparameter E entspricht. Im darauffolgenden Schritt lassen sich dann die PR und LR mit Hilfe der Formeln 2 und 3 bestimmen. [9]

Für die Anwendung dieser Systematik auf den Bereich Windenergie werden für die Parameter C und C_0 die LCOE bzw. die COP verwendet und ACC entspricht hier der installierten Leistung (P). Gleichzeitig ergibt sich dadurch die Möglichkeit, verschiedene Kostenarten auf unterschiedliche Parameter (Installierte Leistung weltweit (P_{ww}) oder auf installierte Leistung in einem Land) zu beziehen. Es wird erwartet, dass sich hier verschiedene PR und LR ergeben. Die Darstellung der LCOE und COP erfolgte in der Vergangenheit in Form unterschiedlicher Währungen. Die Umrechnung von Euro (€) in US-Dollar (US$) erfolgte mit dem durchschnittlichen Umrechnungsfaktor (2010-2018) von 1,228 US$/€ [31]. Tabelle 1 zeigt die ausgewählten Kombinationen anhand der Modelle 1-5.

https://doi.org/10.25974/ren_rev_2021_07

Tab. 1: Ausgewählte Modelle zur Beschreibung des Technologischen Lernens im Bereich Windenergie

Nr.	Kostenart	Bezug	Zeitraum
1	LCOE (Mittelwert)	P_{ww}	1983-2018
2	LCOE (Mittelwert)	P_{ww}	2010-2018
3	COP (Mittelwert)	P_{ww}	2010-2018
4	$LCOE_{DE}$	P_{DE}	2010-2018
5	$LCOE_{US}$	P_{US}	2010-2018

2.3 Prognose

Die ermittelten LR und die PR treffen eine Aussage über die Kosten von Windenergie in der Zukunft. Sie beziehen sich jedoch auf die kumulierte installierte Leistung. Trifft man eine Annahme zum Ausbau der Windenergie zu unterschiedlichen Zeiten, lassen sich die dann erreichten Kostenreduktionen einzelnen Jahren zuordnen.
In einem moderaten Szenario gehen Sawyer et al. (2016) von einer weltweit installierten Leistung für Windenergieanlagen im Jahr 2030 von ca. 1.675 GW (PW1) aus. Ein weiteres Szenario ("advanced scenario") derselben Publikation gibt eine installierte Leistung 2.110 GW (PW2) an.[32] Bezogen auf Deutschland ist im Jahr 2030 von einer installierten Leistung zwischen 69,6 GW (PDE1) und 80 GW (PDE2) auszugehen [33, 34]. Anhand dieser Daten und der ermittelten Lernkurven werden die Kosten für Windenergie in Deutschland und weltweit im Jahr 2030 berechnet.

3 Ergebnisse

Fig. 2 zeigt die LCOE in US$ pro erzeugter Megawattstunde (MWh) in den Jahren 1983 bis 2020. Außerdem gibt IEA (2020) einen Ausblick über zukünftige Kosten für Windenergie in den Jahren 2021 - 2025. Die unterschiedlichen Markierungstypen der Datenpunkte sind den verschiedenen Publikationen zugeordnet. Zu Beginn der Kurve liegen die LCOE im Jahr 1983 bei 303 US$/MWh und sinken in den fortlaufenden 20 Jahren auf 104 US$/MWh (2003). Seit dem Jahr 2010 treffen auch die Publikationen neben Yao, Xu, Sun (2020) eine Aussage über die Kosten für Windenergie. ISE (2020) stellt die LCOE für Windenergie an Land für einen küstennahen, einen durchschnittlichen Standort und einen windschwachen Standort in Deutschland dar.

In Fig. 3 werden die LCOE in US$/MWh in den Jahren 2000 bis 2018 dargestellt. Im Jahr 2010 liegen die LCOE zwischen 71 US$/MWh (NREL) und 91,75 US$/MWh (ISE, windschwach). Ähnlich wie im Jahr 2010 werden durch NREL (2018) für das Jahr 2018 die geringsten LCOE in Höhe von 42 US$/MWh und durch ISE (2018) für windschwache Standorte die

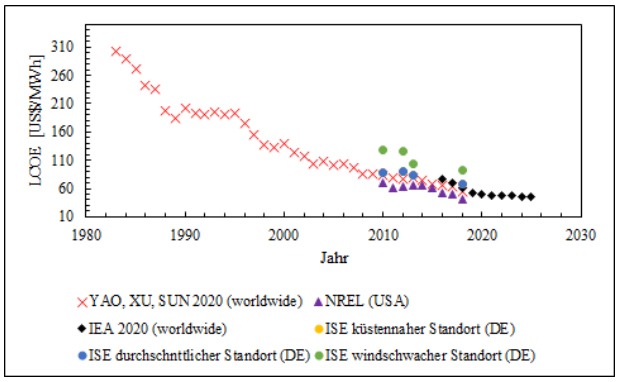

Fig. 2: LCOE von Windenergie in den Jahren 1983 bis 2020 und Ausblick bis 2025

höchsten LCOE von 127,72 US$/MWh. Die Mittelwerte der betreffenden Jahre liegen bei 88,47 US$/MWh (2010) und 62 US$/MWh (2018). Die höchsten LCOE (139 US$/kWh) in den Jahren von 2000 bis 2018 lassen sich entsprechend der aus dem Lernkurvenmodell abgeleiteten Erwartung dem Jahr 2000 zuordnen. Außerdem fällt auf, dass eine Wertereihe deutlich über den anderen liegt. Dies lässt sich dadurch begründen, dass hier von einem windschwachen Standort in Deutschland ausgegangen wird und damit bei vergleichbaren Installationskosten weniger Energie produziert wird. Gleichwohl ist zu diskutieren, ob diese hoch signifikante Abweichung der LCOE darauf beruht. Außerdem fällt auf, dass die letzten vier von der NREL publizierten LCOE für Windenergie an Land im Vergleich zu denen der anderen Publikationen stärker fallen.

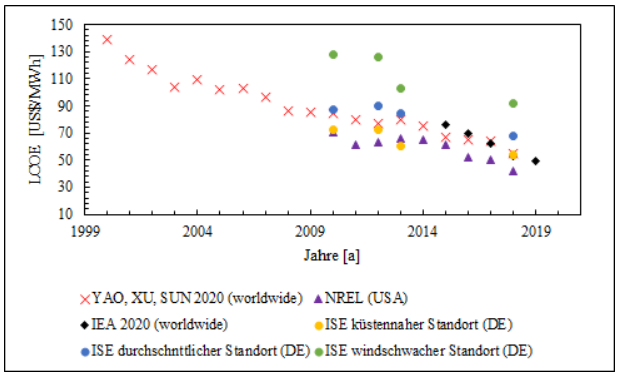

Fig. 3: LCOE von Windenergie in den Jahren 2010 bis 2018 in Abhängigkeit zur weltweit installierten Leistung

Die in Fig. 4 dargestellten Kosten für die Installation von Windenergieanlagen in den Jahren 2010-2018 unterschiedlicher Quellen bilden einen ähnlichen Verlauf ab. Beginnend mit COP von 1.730,5 US$/kW bis 2.155 US$/kW im Jahr 2010 fallen die Kosten auf durchschnittlich 1.444 US$/kW in 2018. Gleichzeitig verkleinert sich die Spannbreite der genannten COP, sodass im Jahr 2018 die geringsten Investitionskosten bei 1.363,5 US$/kW und die höchsten bei 1.498,5 US$/kW liegen.

https://doi.org/10.25974/ren_rev_2021_07

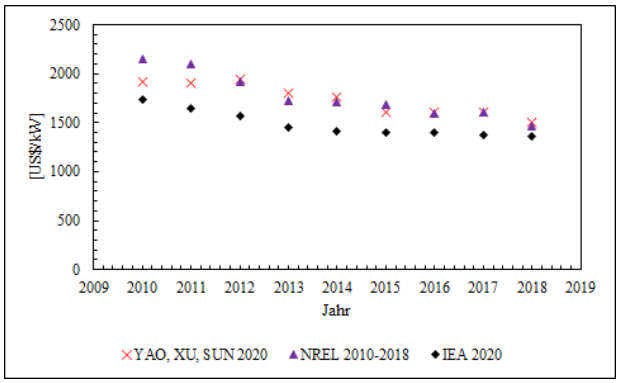

Fig. 4: Kosten für die Installation von Windenergieanlagen in den Jahren 2010-2018

Wie in Kapitel 2.2 hergeleitet und beschrieben, lassen sich durch die doppelt-logarithmische Darstellung der in diesem Kapitel präsentierten Daten die zugehörigen linearen Ausgleichskurven bestimmen, wodurch wiederum E, PR und LR berechnet werden können. Tab. 2 stellt diese Ergebnisse zusammenfassend dar und trifft außerdem eine Aussage über das Bestimmtheitsmaß R^2 der ermittelten Ausgleichskurven.

Tab. 2: Anwendung der vorgestellten Systematik auf die gesammelten Daten entsprechend der Modelle 1-5 (Werte auf drei Nachkommastellen gerundet)

	M1	**M2**	**M3**	**M4**	**M5**
E	0,206	0,272	0,225	0,411	0,478
R^2	0,982	0,828	0,963	0,919	0,694
PR	87 %	83 %	86 %	75 %	72 %
LR	13 %	17 %	14 %	25 %	28 %

Die Modelle 1-5 liefern wie erwartet unterschiedliche Ergebnisse. Die Lernraten bewegen sich zwischen 13 % und 28 %. Damit treffen sie die Aussage, dass die LCOE für Windenergie bei Verdopplung der Erzeugungsleistung auf maximal 72 % bzw. minimal 87 % der bisherigen Kosten fallen. Das Bestimmtheitsmaß von M5 liegt lediglich bei 0,694, sodass hier von einer unzureichenden Korrelation ausgegangen wird und dieser Ansatz nicht zur Ermittlung zukünftiger LCOE für Windenergie verwendet wird. Anhand der Modelle 2 und 3 wurde eine LR von 17 % und 14 % berechnet. Das Bestimmtheitsmaß von M2 wurde zu $R^2 = 0{,}828$ berechnet und ist damit geringer als R^2 von M3. Das Modell mit dem längsten Bilanzzeitraum (M1) liefert eine LR von 13 % und weist die höchste Bestimmtheit mit R^2=0,982 auf.
Anhand der Szenarien PW1-2 und PDE1-2 werden die LCOE und COP für Windenergie im Jahr 2030 ermittelt. Die Ergebnisse werden in Tab. 3 und Tab. 4 dargestellt.
Die in Tab. 3 dargestellten Ergebnisse beruhen auf Daten, die als weltweit gültige Kosten für Windenergie veröffentlicht wurden. Daher wurde wie auch

Tab. 3: $LCOE_{weltweit}$ und $COP_{weltweit}$ für Windenergie an Land im Jahr 2030

	M1	**M2**	**M3**
Parameter	LCOE	LCOE	COP
Einheit	US$/MWh	US$/MWh	US$/kW
PW1	51,92	46,88	1114,39
PW2	49,51	44,03	1058,03

Tab. 4: $LCOE_{DE}$ für Windenergie an Land im Jahr 2030 (durchschnittlicher Standort)

	M4
Parameter	LCOE
Einheit	US$/MWh
PDE1	61,49
PDE2	58,07

schon bei der Ermittlung der LR und PR den Modellen M1 bis M3 die Szenarien PW1 und PW2 zugeordnet. Die ermittelten LCOE belaufen sich anhand der getroffenen Annahmen im Jahr 2030 auf 46,88 US$/MWh bis 51 US$/MWh. Die Kosten für die Installation von WEA sinken bei einer Lernrate von 17 % von 1.443,99 US$/kW auf 1.114,39 US$/kW bzw. 1.058,03 US$/kW im Jahr 2030.
Die Szenarien PDE1 und PDE2 liefern, anhand der in M4 ermittelten LR, LCOE in Deutschland für durchschnittliche Standorte von 58,07 US$/kWh bis 61 US$/kWh.

4 Diskussion

Primäres Ziel dieser Arbeit ist es ist es, eine Lernkurve für Windenergie an Land zu bestimmen. Die dafür gesammelten Daten beziehen sich größtenteils auf den Zeitraum 2010-2018. Die Datenlage zu den Kosten für Windenergie an Land vor 2010 basiert lediglich auf einer Veröffentlichung und ist damit weniger aussagekräftig. Gleichwohl finden sich auch innerhalb der Datenreihen mit Bezug auf den Zeitraum 2010-2018 Unregelmäßigkeiten. Darunter fallen beispielsweise die von der NREL aufgerufenen LCOE. Hier war eine vergleichsweise starke Minderung der Kosten zu beobachten. Diese Beobachtung ist möglicherweise damit zu erklären, dass die Ermittlung der LCOE anhand eines jährlich variierenden und durch die Autoren ausgewählten Referenzprojekts durchgeführt wurde [16–23]. Dementsprechend ändern sich bei diesen Referenzprojekten auch die äußeren Umstände. Darüber hinaus ist zweifelhaft, ob die anhand eines Projekts ermittelten Kosten für Windenergie an Land in den USA für die gesamte Region repräsentativ sind. Im Vergleich dazu stehen die Veröffentlichungen des Fraunhofer ISE für Windenergie in Deutschland. Hier wurde einerseits eine weitere Kategorisierung in windstarke,

https://doi.org/10.25974/ren_rev_2021_07

windschwache und durchschnittliche Regionen vorgenommen und andererseits die Rahmenbedingungen der Kostenermittlung weitgehend konstant gehalten [12–15]. Außerdem fiel bei der Darstellung und Beschreibung der Lernkurven auf, dass die LCOE für windschwache Standorte in Deutschland deutlich über den übrigen LCOE liegen. Es wird jedoch davon ausgegangen, dass diese Daten plausibel sind, da die Datenpunkte dieser Reihe dem Trend der anderen Publikationen folgen und damit in sich schlüssig sind. Darüber hinaus wurden die LCOE für durchschnittliche Standorte in Deutschland mit der selben Systematik ermittelt und die LCOE für durchschnittliche Standorte entsprechen denen der anderen Publikationen.

Die bereits bei der grafischen Darstellung beobachteten Abweichungen bezüglich der NREL-Daten schlagen sich auch in der Ermittlung der PR und LR nieder. Die Daten wurden im Modell 5 verwendet und auf die in den USA installierte Leistung von WEA bezogen. In Modell 5 wurde die höchste LR (28 %) und gleichzeitig das geringste Bestimmtheitsmaß (0,694) ermittelt. Es ist anzunehmen, dass auch dies durch die oben beschriebenen Zusammenhänge zu begründen ist. Im Gegensatz dazu steht die hohe Bestimmtheit im Modell 1, was durch den Umfang der verwendeten Daten zu erklären ist. Fig. 5 stellt die Ergebnisse dieser Arbeit mit Bezug auf die LCOE als Kostenparameter im Vergleich zu den von Yao, Xu und Sun (2020) ermittelten Werten in Anlehnung an Rubin et al. (2015) dar [10]. Wie Fig. 5 zeigt, konnte

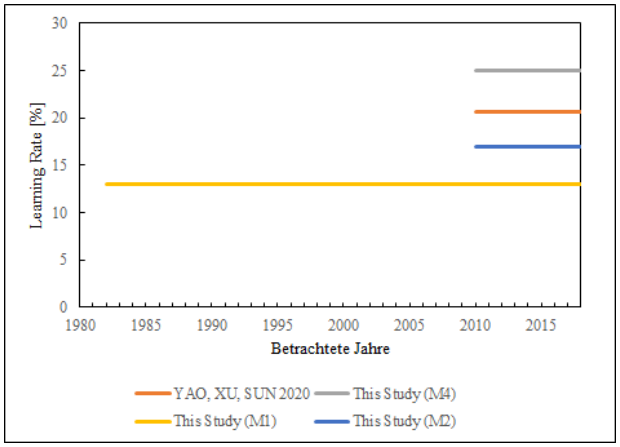

Fig. 5: Vergleich der Ergebnisse mit LCOE als Kostenparameter [11]

lediglich eine Studie im Zeitraum 2010-2018 gefunden werden, die ebenfalls $LCOE_{global}$ als Kostenparameter verwendet. Gleichzeitig ist diese Veröffentlichung auch Teil der Datengrundlage in dieser Arbeit. Die Abweichung zwischen der ermittelten LR von Yao, Xu und Sun (2020) und M2 dieser Arbeit ergibt entspricht ca. 3 %. Dies ist damit zu erklären, dass in M2 ebenfalls Daten der IEA (2020) eingeflossen sind. Außerdem erscheint die LR von M4 bei Betrachtung der anderen Ergebnisse und vor dem Hintergrund, dass in Deutschland bereits seit vielen Jahren der Bau von WEA gefördert wird, vergleichsweise hoch. Hier wurden die von ISE (2010,12,13,18) LCOE für Windenergie in Deutschland an durchschnittlichen Standorten der Jahre 2010, 2012, 2013 und 2018 verwendet und die PR und LR in Abhängigkeit zur in Deutschland installierten Leistung der betreffenden Jahre gesetzt. Verwendet man anstelle der in Deutschland installierten Leistung die weltweit installierte Leistung ergibt sich eine Lernrate von 15,7 % bei R^2=0,8. Damit läge die LR in Deutschland unterhalb der ermittelten weltweiten LR in M2, was als plausibler bewertet wird.
Fig. 6 stellt LR der Gesamtkosten für die Installation von WEA unterschiedlicher Veröffentlichungen im Vergleich zu den Ergebnissen des M3 in Anlehnung an Rubin et al. (2015) dar [10].

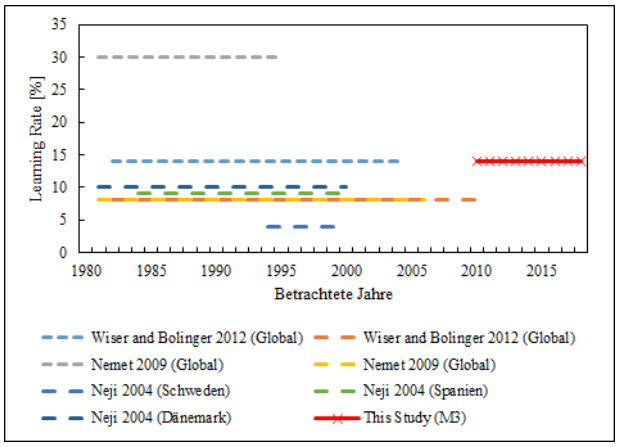

Fig. 6: Vergleich der Ergebnisse mit COP als Kostenparameter [10, 35]

Ausgehend von Rubin et al. (2015) und Neji (2004) wurden sieben weitere LR für die Gesamtkosten der Installation von WEA identifiziert [10, 35]. Ein Vergleich mit den Ergebnissen ist auch hier vage, da die Betrachtungszeiträume der betreffenden Studien nicht dem dieser Arbeit entsprechen. Die Mehrzahl der genannten LR liegt im Bereich zwischen 8 % und 14 %, worunter auch die Ergebnisse von M3 fallen. Es wird daher gemutmaßt, dass die durch M3 ermittelte LR plausibel ist, obwohl sich die Zeiträume der Studien unterscheiden.

Die Prognose für LCOE und COP von WEA im Jahr 2030 wurde anhand der ermittelten LR und zwei möglichen Szenarien für den Ausbau der Windenergie weltweit und in Deutschland getroffen. Demnach werden die genannten Werte auch nur eintreten sofern die Kostenreduktion in den folgenden Jahren der bisherigen entspricht und die Ausbauziele tatsächlich erreicht werden. Trotz der hohen LR in M4 werden im Zeitraum von 2018 bis 2030 geringere Kostenreduktionen als in M2 erreicht. Die Ursache liegt darin, dass die Annahme für die weltweit installierte Leistung in 2030 dem 3,1/3,9-fachen

https://doi.org/10.25974/ren_rev_2021_07

der installierten Leistung in 2018 entspricht. In Deutschland entspricht die Annahme der installierten Leistung in 2030 dem 1,3/1,5-fachen der in 2018 installierten Leistung, sodass trotz einer höheren LR geringere Kostenreduktionen erzielt werden. Daraus wird gefolgert, dass die genannten Werte für die LCOE und COP im Jahr keine absoluten Werte darstellen, sondern als richtungweisend zu betrachten sind.

5 Zusammenfassung und Ausblick

Das primäre Ziel dieser Arbeit war es, eine Lernkurve für Windenergie an Land zu bestimmen. Dafür wurden Daten zu LCOE und COP von WEA in unterschiedlichen Zeiträumen für die Regionen USA, Deutschland und Weltweit gesammelt und grafisch dargestellt. Die grafische Darstellung der Datenlage verdeutlicht die zeitliche Entwicklung der Technologie. Zur Beschreibung dieser Lernkurven wurden die PR und LR in fünf unterschiedlichen Modellen bestimmt, anhand derer sich in Kombination mit der zukünftig installierten Leistung von WEA eine Prognose über zukünftige Kosten ableiten lässt. Die ermittelten LR im Betrachtungszeitraum 2010-2018 bewegen sich zwischen 14 und 28 %, woraus sich LCOE im Jahr 2030 zwischen 44,03 US$/kWh und 61 US$kWh ergeben. Für die Zeitspanne zwischen 1983-2018 und unter Inbezugnahme der weltweiten LCOE wurde eine LR von 13 % ermittelt. Die erzielten Ergebnisse zeigen auf, dass in vergangenen Jahren nachweisbare Kostenreduktionen erreicht wurden. Daraus lässt sich folgern, dass sich eine weitere Kostenreduktion in der Zukunft über kurz- bis mittelfristige Zeiträume ergeben wird. In dieser Arbeit nicht betrachtet sind die Ursachen für die zu beobachtenden Kostenreduktionen. Sie könnte auf unterschiedliche Faktoren, wie technologischer Fortschritt, gezielte Forschung oder das wachsende Know-how der ausführenden und planenden Stellen in unterschiedlichem Umfang zurückzuführen sein. Eine differenziertere Darstellung als das in dieser Arbeit verwendete Modell (One-Factor-Learning) gibt beispielsweise das Multi-Factor-Learning, in welches neben der installierten Erzeugungsleistung auch Parameter, wie angemeldete Patente in einem Land, die Größe der Anlagen oder die Ausgaben für Forschung und Entwicklung im Bereich Windenergie in einer Region einfließen können [10, 11, 36].
Die in dieser Arbeit erzielten Ergebnisse zeigen auf, dass in den vergangenen Jahren nachweisbare Kostenreduktionen erreicht wurden und in Abhängigkeit der installierten Leistung quantifizierbar sind. Daraus lässt sich folgern, dass sich eine weitere Kostenreduktion in der Zukunft über kurz- bis mittelfristige Zeiträume ergeben wird.

References

[1] S. A. A. Suganthi L. "Energy models for demand forecasting — A review". *Renewable and Sustainable Energy Reviews* 16 (2012), pp. 1223–1240. DOI: https://doi.org/10.1016/j.rser.2011.08.014.

[2] N. Stern. *The Economics of Climate Change: The Stern Review*. Ed. by Cambridge University Press. New York, 2007.

[3] K. Fung, R. Scheffler, and J. Stolpe. "Wind Energy - A Utility Perspective". *IEEE Transactions on Power Apparatus and Systems* PAS-100.3 (1981), pp. 1176–1182. ISSN: 0018-9510. DOI: 10.1109/TPAS.1981.316586.

[4] E. Sesto and C. Casale. "Exploitation of wind as an energy source to meet the world's electricity demand". *Journal of Wind Engineering and Industrial Aerodynamics* 74-76 (1998), pp. 375–387. ISSN: 01676105. DOI: 10.1016/S0167-6105(98)00034-8.

[5] A. Palzer and H.-M. Henning. "A Future German Energy System with a Dominating Contribution from Renewable Energies: A Holistic Model Based on Hourly Simulation". *Energy Technology* 2.1 (2014), pp. 13–28. ISSN: 21944288. DOI: 10.1002/ente.201300083.

[6] G. M. Joselin Herbert, S. Iniyan, E. Sreevalsan, and S. Rajapandian. "A review of wind energy technologies". *Renewable and Sustainable Energy Reviews* 11.6 (2007), pp. 1117–1145. ISSN: 13640321. DOI: 10.1016/j.rser.2005.08.004.

[7] J. K. Kaldellis and D. Zafirakis. "The wind energy (r)evolution: A short review of a long history". *Renewable Energy* 36.7 (2011), pp. 1887–1901. ISSN: 09601481. DOI: 10.1016/j.renene.2011.01.002.

[8] G. F. Nemet. "Interim monitoring of cost dynamics for publicly supported energy technologies". *Energy Policy* 37.3 (2009), pp. 825 –835. ISSN: 0301-4215. DOI: https://doi.org/10.1016/j.enpol.2008.10.031.

[9] F. Pieper. "Das Konzept von Lernkurven im Energiesektor — Beschreibung, Modellierung und Aggregation". Diplomarbeit. Potsdam: Technische Universität Berlin, 2003. URL: https://www.pik-potsdam.de/members/edenh/theses/masterpieper.pdf.

[10] E. S. Rubin, I. M. Azevedo, P. Jaramillo, and S. Yeh. "A review of learning rates for electricity supply technologies". *Energy Policy* 86 (2015), pp. 198–218. ISSN: 03014215. DOI: 10.1016/j.enpol.2015.06.011.

[11] Y. Yao, J.-H. Xu, and D.-Q. Sun. "Untangling global levelised cost of electricity based on multi-factor learning curve for renewable energy: Wind, solar, geothermal, hydropower and bioenergy". *Journal of Cleaner Production* (2020), p. 124827. ISSN: 09596526. DOI: 10.1016/j.jclepro.2020.124827.

[12] Kost, Christoph, Schlegl Thomas. *Studie Stromgestehungskosten Erneuerbare Energien*. Ed. by Prof. Dr. Eicke R Weber. Freiburg, 2010.

[13] C. Kost, T. Schlegl, J. Thomsen, S. Nold, and J. Mayer. *Studie Stromgestehungskosten Erneuerbare Energien*. Ed. by Prof. Dr. Eicke R Weber. Freiburg, 2012.

[14] C. Kost, J. N. Mayer, J. Thomsen, N. Hartmann, C. Senkpiel, S. Phillips, S. Nold, Lude Simon, and T. Schlegl. *Studie Stromgestehungskosten Erneuerbare Energien*. Ed. by Prof. Dr. Eicke R Weber. Freiburg, 2013.

[15] Kost, Christoph, Shammugam, Shivenes, V. Jülch, H.-T. Nguyen, and Schlegl Thomas. *Studie Stromgestehungskosten Erneuerbare Energien*. Ed. by Prof. Dr. Hans-Martin Henning and Dr. Andreas Bett. Freiburg, 2018.

[16] S. Tegen, M. Hand, B. Maples, E. Lantz, P. Schwabe, and A. Smith. *2010 Cost of Wind Energy Review*. Golden, Colorado, 2011.

[17] S. Tegen, E. Lantz, M. Hand, B. Maples, A. Smith, and P. Schwabe. *2011 Cost of Wind Energy Review*. Golden, Colorado, 2013.

[18] C. Moné, A. Smith, B. Maples, and M. Hand. *2013 Cost of Wind Energy Review*. Golden, Colorado, 2015.

[19] C. Moné, T. Stehly, B. Maples, and E. Settle. *2014 Cost of Wind Energy Review*. Golden, Colorado, 2015.

[20] T. Stehly, D. Heimiller, and G. Scott. *2016 Cost of Wind Energy Review*. Golden, Colorado, 2017.

[21] C. Moné, M. Hand, M. Bolinger, J. Rand, D. Heimiller, and J. Ho. *2015 Cost of Wind Energy Review*. Golden, Colorado, 2017.

[22] D. H. Tyler Stehly and G. Scott. *2018 Cost of Wind Energy Review*. Golden, Colorado, 2019.

[23] T. Stehly, P. Breiter, D. Heimiller, and G. Scott. *2017 Cost of Wind Energy Review*. Golden, Colorado, 2018.

[24] IEA. *Renewables 2020*. 2020. URL: https://www.iea.org/reports/renewables-2020.

[25] Statista. 2020. URL: https://de.statista.com/statistik/daten/studie/180543/umfrage/installierte-windenergie-in-den-usa-seit-2000/.

[26] Statista. 2020. URL: https://de-statista-com.ezproxy.fh-muenster.de/statistik/daten/studie/20113/umfrage/installierte-leistung-der-anlagen-fuer-windenergie-in-deutschland-seit-1993/.

[27] T. Wiesenthal, P. Dowling, J. Morbee, C. Thiel, B. Schade, P. Russ, S. Simões, E. Peteves, K. Schoots, and M. Londo. *Technology Learning Curves for Energy Policy Support*. 2012. DOI: 10.2790/59345.

[28] L. Neij. "Cost dynamics of wind power". *Energy* 24.5 (1999), pp. 375–389. ISSN: 03605442. DOI: 10.1016/S0360-5442(99)00010-9.

[29] M. Junginger, A. Faaij, and W. Turkenburg. "Global experience curves for wind farms". *Energy Policy* 33.2 (2005), pp. 133–150. ISSN: 03014215. DOI: 10.1016/s0301-4215(03)00205-2.

[30] W. van Sark and E. A. Alsema. "Potential errors when fitting experience curves by means of spreadsheet software". *Energy Policy* 38.11 (2010), pp. 7508–7511. ISSN: 03014215. DOI: 10.1016/j.enpol.2010.06.053.

[31] Statista. 2020. URL: https://de-statista-com.ezproxy.fh-muenster.de/statistik/daten/studie/200194/umfrage/wechselkurs-des-euro-gegenueber-dem-us-dollar-seit-2001/.

[32] S. Sawyer, S. Teske, L. Fried, and S. Shukla. *Global Wind Energy Outlook 2016*. Oct. 2016.

[33] International Renewable Energy Agency. *GLOBAL RENEWABLES OUTLOOK: Energy Transformation 2050*. 2020. URL: www.irena.org/publications.

[34] G. Corbetta and European Wind Energy Association. *Wind energy scenarios for 2030: A report by the European Wind Energy Association - August 2015*. 2015. URL: https://www.ewea.org/fileadmin/files/library/publications/scenarios/EWEA-Wind-energy-scenarios-2020.pdf.

[35] L. Neij. *Experience curves: A tool for energy policy assessment*. Vol. 40. IMES/EESS report. Lund: Environmental and Energy Systems Studies, Univ, 2003. ISBN: 91-88360-56-3.

[36] N. Odam and F. P. de Vries. "Innovation modelling and multi-factor learning in wind energy technology". *Energy Economics* 85 (2020), p. 104594. ISSN: 01409883. DOI: 10.1016/j.eneco.2019.104594.

Measures for mitigating avian collision rates with wind turbines

Determining an effective technique regarding effort and effect

*Alexander Hoge**

Münster University of Applied Sciences, Stegerwaldstraße 39, 48565 Steinfurt, Germany

Abstract

Because of the rapid expansion and widespread application of wind energy the overall environmental impacts of wind power plants have increased as well. For the further development of wind power, methods to lessen the adverse effects wind power has on avian populations have to be implemented. This review aims to find effective methods to reduce avian collision rates with wind turbines and that therefore can reduce bird fatality rates.

For the assessment the different mitigation methods, for which concrete data was found, are compared with each other regarding the hypothetical effort of implementation and effectiveness in reducing avian collision rates with wind turbines.

These methods are:

- Coloring of rotor blades
- Coloring of the tower base
- Ultraviolet/violet lightning
- Temporary shut-down of wind turbines
- Auditory warning signals
- Repowering

All of the mentioned methods report influence on reducing avian collision rates or at least the behavior of birds in flight.

This review found the following three methods to be most effective:

- Coloring of rotor blades
- Temporary shut-downs of wind turbines
- Repowering

The most effective method to reduce avian collision rates at horizontal axis wind turbines is to paint one of the rotor blades black and consequently increasing the visibility of the rotor blades. The presented study [1] reports 71,9 percent reduction of found carcasses of birds at the treated turbines. For this method the effort of implementation is low while the effectiveness is high.

The effectiveness of the found mitigation methods has been proven and they are suited for application. The method of using lightning or sound fields require more testing to determine their effectiveness. Another topic for research could be how different mitigation methods interact with each other. Is there a significant advantage to be had if multiple mitigation methods are applied at the same wind power plant or turbine? Furthermore the environmental impacts of wind turbines are not limited to birds. Other animals like bats are affected too and might require different methods of mitigation.

Keywords: wind turbine, wind energy, birds, collisions, mitigation

1 Preliminary note

The following chapter gives an introduction to the subject and explains the purpose of this review. In addition the methods that were used to gather the information as well as the criteria for choosing literature are acknowledged.

1.1 Introduction

Wind energy has undergone an rapid development in order to combat global warming. But with the numbers of wind turbines increasing, so does the severity of environmental impacts. Prominent among these impacts is the influence wind turbines have on avian population. All kind of different types of birds get affected. Soaring raptors might collide with the rotor

*Corresponding author: alexander.hoge@fh-muenster.de.

https://doi.org/10.25974/ren_rev_2021_08

blades. So do migratory bird. The same risk consist for residential birds who also might suffer from habitat loss.

The fear of severe avian population decline leads to financial burden, causes delays and can restrict the further development of wind power. Hence it becomes obvious, that bird-strikes are costly for both the wildlife and the expansion of wind power production.Therefore, measures to reduce avian collision rates with wind power turbines have to be developed and applied.

The aim of this review is to determine the state of scientific knowledge on reducing avian collision rates with wind turbines and to develop a recommendation for the implementation in practice through evaluation of the different methods.

An ideal method would be highly effective in reducing collision rates while also not be detrimental to the power production of the affected wind turbine and have a low effort of application.

1.2 Methodology

The contents of this review were acquired through a literature research using the internet. The search engines Google and Google Scholar were used to obtain sources. In addition the search for literature was expanded onto the library of the University of Applied Sciences Muenster using their own search engine FINDEX.

For the search different keywords where used. Both in German and English language. Among others, searches were started with the following terms:

- Innovative mitigation tools for avian conflicts with wind turbines
- Bird protection at wind turbines
- Ecological risks of onshore wind power
- Methods to reduce bird strikes on wind turbines
- Mitigation of avian impacts with wind turbines

The focus during the search for articles was to find those, that not only enumerate mitigation options, but also give concrete figures for a certain method. Preferably numbers about bird mortality before and after a certain method was applied.

2 Measures of mitigation

In the following subsections the different measures that have been found will be presented. No evaluation of the individual methods will be given yet.

2.1 Coloring of rotor blades

One method for reducing avian collisions with wind turbines is to increase the visibility of the rotor blades.

One study carried out by the Norwegian Institute for Nature Research from the 19th of February 2020 examined the effect of painting one of the three rotor blades black to reduce motion smear and therefor increase visibility. The painting was done during August of 2013 at four wind turbines in the Smøla wind-power plant in Norway (Fig.1). Four neighboring wind turbines where used as a control group. To assess the effect of the measures, searches for bird carcasses were performed at regular intervals in a radius of 100 meters around the wind turbines. These numbers were than compared to numbers of found carcasses determined before treatment. The experiment and the searches ran for seven and a half years pre- and three and a half years post-treatment. During the study the number of carcasses that have been found at the control turbines increased. From 7 before treatment to 18 after. At the treated turbines these numbers decreased from 11 to 6. The authors report that there has been an average 71.9 percent reduction in the annual fatality rate after the painting was conducted [1].

Fig. 1: Wind turbine in the Smøla wind-power plant with painted rotor blade (c) Roel May [1]

https://doi.org/10.25974/ren_rev_2021_08

2.2 Effect of tower base painting

Besides from colliding with the rotor blades, birds do also collide with the tower base of wind turbines.

In a study from the Norwegian Institute for Nature Research the effect of tower base painting on the collision rates of willow ptarmigan with the tower base is examined. The study was carried out in a very similar manner to the previous mentioned study done by the same institute. The study itself is from the 23rd of November 2019. Four wind turbines had the lower 10 meters of their tower base painted black in mid-August 2014. Unaltered, adjacent turbines were used as an control group. In mid-July 2015 another six wind turbines had their tower bases painted in the same pattern. To determine the effect of the painting, the carcasses found before and after treatment were compared. The study includes the findings of the searches for carcasses from 2006 to 2017. During this time 474 carcasses were found with the species willow ptarmigan being recorded 194 times. For the 10 control turbines the number of carcasses increased from 11 pre-treatment to 19 post-treatment. While at the treated turbines the numbers decreased from 25 to 14. The authors report an 48 percent reduction of recorded ptarmigan carcasses per search at the painted turbines relative to the control turbines [2].

2.3 Avian response to (ultra)violet lighting

Another method to increase visibility besides painting is to illuminate the wind turbines. Which is especially useful during periods of low natural lightning like during the night or bad weather. Normal paint-jobs are not sufficient then.

A study conducted by the Norwegian Institute for Nature Research from 2017 tested if birds in flight respond to violet and ultraviolet lighting. The basic idea for this experiments is, that especially many birds that collide with off-shore wind turbines are sensitive to ultraviolet light. The experiments were conducted outside with wild birds near a wind power plant. Two UV LED lights were placed vertically on top of a 2.5 meter high mast. One light emitted violet light with a wavelength of 400 nm (nanometer) and the other light emitted ultraviolet light with a wavelength of 365 nm. Over the duration of an week, the lighting was alternated between the two lights. Ultraviolet lightning was used during Tuesdays and Saturdays, while violet lightning was used on Wednesdays and Fridays. The days in between were used as control-days without any lighting. The experiment was run from March to May during 2014. The movement of the birds were recorded 24/7 using a special modulated radar. The author reports that relative to the control nights, the flight activity of the birds was reduced by both types of lighting. There was a 27 percent reduction when the ultraviolet light was on and a 12 percent reduction with the violet light on. In addition, a vertical displacement was present, with the birds increasing their average flight altitude by seven meters [3].

2.4 Temporary shut-down of wind turbines

Many birds that collide with wind turbines, do collide with the moving rotor blades. The most obviously method to reduce, if not completely prevent any collisions, is to shut down the wind turbine when birds are in the immediate proximity. Naturally, this would also lead to a decline in total power produced for a wind turbine.

The Department of Ethology and Biodiversity Conservation from Seville in Spain, among others, conducted a study at 13 wind farms in Tarifa, Cadiz, Spain before and after when selective turbine stopping programs were implemented. These programs would stop wind turbines when vultures were observed nearby. To determine the effectiveness of these programs in reducing avian collisions, the number of dead griffon vultures that were found near the wind turbines were recorded. The searches for carcasses were performed before the stopping programs were implemented from 2006 to 2007 and after implementation from 2008 to 2009. In total 244 wind turbines of 10 wind parks were equipped with the stopping programs. The authors recorded a reduction in the vulture mortality rate by 50 percent with a consequent reduction in total energy production by 0.07 percent per year [4].

2.5 Auditory warning signals

Another method to reduce bird-strikes on wind turbines or buildings in general is to alert the bird to the presence of an obstacle by means of an auditory signal.

A study by the Biology Department of the Institute for Integrative Bird Behavior Studies of the College of William and Mary in Williamsburg, USA, examined the impact of a warning signal on birds in flight. The authors suggested that one reason for avian collisions with man-made structures is, that birds in cruising flight do not pay adequate attention to the area directly in front of them. When the body and head of birds are aligned to reduce drag during flight, their visual gaze is directed downwards. The authors tested captive zebra finches that were trained to fly down a corridor and through an opening in an wooden frame. A net with large enough gaps for the bird to be able to fly through was installed in the opening. The birds now had to fly through the corridor once without a warning signal and once while being exposed to an sound field projected in front of the net up to a

distance of 1.5 meters. The experiment showed that the birds reduced their flight speed approximately 20 percent more when the sound field was present. In addition the only time where the birds avoided the net occurred when the sound field was active. The authors concluded that, the birds where only able to completely avoid the net when they got a acoustic warning signal, but they also reduced their flight speed significantly. Translated to free-roaming birds, this would mean that even when the birds would not be able to avoid the obstacle, the force of the collision would be reduced and so the severity of an potential injury. Furthermore the authors recommend that, when using this method on large buildings such as wind turbines, the warning signal should be audible more than 30 meters from the strike surface [5].

2.6 Repowering

Replacing old wind turbines with newer, more efficient and often larger models, is common practice. These projects are also met with concerns, that new-generation wind turbines on taller towers and with an larger rotor diameter would result in a higher fatality rate for birds. But one study suggested that increasing the tower high might actually reduce the bird mortality by over 70 percent [6].

K.S. Smallwood et al. [7] published a study, in which the authors examined the effect that repowering of wind turbines had on the fatality rates of birds. In the study they compared estimates of fatality rates from between 1998-2003 and 2005-2007 and between a repowered wind project and old-generation wind turbines. The wind turbines were part of the Altamont Pass Wind Resource Area (APWRA) in California, USA. The authors found that, although the fatality rates caused by the repowered wind turbines where not lower than the replaced turbines, they were 66 percent lower for all birds compared to the old-generation wind turbines. The authors concluded that lowering the mean annual fatality rates by 65 percent for all birds could be possible at APWRA by repowering the old-generation wind turbines while also more than doubling the annual energy production.

It should be mentioned, that in the repowering project vertical axis turbines were replaced by horizontal axis turbines (Tab.1). Which lead to an insignificant rise in fatalities for specific bird species [7].

3 Assessment

In the following table (Tab.2) the different mitigation methods that where introduced in chapter two are compared with each other regarding the hypothetical effort of implementation and effectiveness in reducing avian fatalities. An reduction in bird fatalities equal or greater than 50 percent is considered to be of high effectiveness.

The coloring of one rotor blade is a simple and highly effective method. The study [1] proves that this method is universally applicable for horizontal axis turbines and should lead to similar results no matter the location of the wind power plant.

Painting the tower base of a wind turbine is a reasonable effective method considering it only affects specific bird species [2]. But at locations where those bird species are present, it can be applied with low effort.

Although lightning is easy to install and the study [3] reports an respond of the birds to the lightning, its exact effect on bird collisions at wind turbines still has to be determined. In addition, illuminating wind turbines with violet-lightning could lead to conflict with local residents if the wind turbines are close to human settlements.

The study [4] chosen to represent the method of temporary shut-downs reports promising results: minimal loss of energy production while significant reduction in avian fatalities. The use of temporary shut-downs and also auditory warning signals requires additional effort, because a system to identify approaching birds has to be included. And the effectiveness of this system to correctly identify birds also influences the possible reductions of bird moralities.

The data presented to determine the effectiveness of auditory signals come from an controlled environment. In reality, the birds would move with an higher travel speed and could also be distracted by different kind of signals. But considering that in the study [5] the birds would completely avoid the obstacle only with the sound field present leads to the assumption that this method could also be of use in a realistic scenario. Similar to the installation of lightning, loud auditory signals might be unacceptable near human settlements.

In addition to the study by K.S. Smallwood et al., which reported a significant decrease in bird mortality after repowering [7], other studies came to different conclusions. One study found that replacing horizontal axis turbines with larger horizontal axis turbines lead to a similar collision risk [8].Another study even reported that taller turbines towers increase the mortality rates of birds and recommended that repowering of older wind farms with griffon vulture populations nearby, should avoid placing turbines on hills with gentle slopes [9]. This leads to the conclusion that in certain situations repowering can reduce the mortality rates or at least does not lead to an increase of fatalities. Although repowering can be considered to be the method with the highest effort and to be the most costly one, it also leads to a significant increase in power production. This might result in an indirect reduction in bird fatalities because the higher

https://doi.org/10.25974/ren_rev_2021_08

Tab. 1: Attributes of wind turbines involved in the Diablo Winds Energy Project, which repowered 21 megawatts (MW) of rated capacity in the Altamont Pass Wind Resource Area, California, USA, in February 2005 [7]

Attribute	Repowered Flowind[a] vertical-axis turbines		New Vestas[b] horizontal axis turbines	
Model	F-17	F-19	V47	V47
No. turbines	105	21	24	7
Rated output/turbine (MW)	0.15	0.25	0.66	0.66
No. of blades	2	2	3	3
Rotor diam (m)	17.2	19.1	47	47
Rotor speed (revolutions/min)	66.3	59.7	28.5	28.5
Hub ht above ground (m)			50	55
Highest blade reach above ground (m)	29.5	32.3	73.5	78.5
Lowest blade reach above ground (m)	4	4	26.5	31.5
Inter-turbine spacing within rows (m)	51	51	104	104

[a] FloWind Corp., San Rafael, California, USA.
[b] Vestas Wind Systems A/S, Randers, Denmark.

Tab. 2: Comparison of mitigation methods

Method	Effort	Effectiveness
Coloring blades	Low	High
Tower painting	Low	Medium
UV/Violet-Lightning	Low	Low
Temp. shut-down	Medium	High
Auditory signals	Medium	Medium
Repowering	High	High

efficiency could make other, old-generation wind turbines obsolete.

4 Results

The three methods with the highest effectiveness are:

- Coloring of rotor blades
- Temporary shut-downs of wind turbines
- Repowering

The coloring of rotor blades can be considered to be the preferable method. The effort of implementation is low while the effectiveness is high. Because it is effective for different species of birds it can be implemented at wind power plants regardless of location.

5 Outlook

Minimising environmental impacts should be a part of wind energy projects. Application of mitigation methods can vary depending on the specific location of wind power plants and the occurrence of specific bird species. The effectiveness of the mentioned mitigation methods has been proven and they are suited for wide spread application. The method of using lightning or sound fields require more testing to determine their effectiveness. A further question could be, if the combination of different mitigation methods would result in an greater reduction of bird collision rates then the methods would achieve individually. Furthermore the environmental impacts of wind turbines are not limited to birds. Other animals like bats are affected too and might require different methods of mitigation.

There are also mitigation methods that were not included in this review. These reason for this is, that for these methods no concrete data could be found. These methods include:

- Micrositing of wind turbines
- Dummy wind turbines
- Noise to deter birds

References

[1] R. May, T. Nygård, U. Falkdalen, J. Åström, Ø. Hamre, and B. G. Stokke. "Paint it black: Efficacy of increased wind turbine rotor blade visibility to reduce avian fatalities". *Ecology and evolution* 10.16 (2020), pp. 8927–8935.

[2] B. G. Stokke, T. Nygård, U. Falkdalen, H. C. Pedersen, and R. May. "Effect of tower base painting on willow ptarmigan collision rates with wind turbines". *Ecology and Evolution* ().

[3] R. May, J. Åström, Ø. Hamre, and E. L. Dahl. "Do birds in flight respond to (ultra) violet lighting?" *Avian Research* 8.1 (2017), p. 33.

[4] M. De Lucas, M. Ferrer, M. J. Bechard, and A. R. Muñoz. "Griffon vulture mortality at wind farms in southern Spain: Distribution of fatalities and active mitigation measures". *Biological Conservation* 147.1 (2012), pp. 184–189.

https://doi.org/10.25974/ren_rev_2021_08

[5] J. P. Swaddle and N. M. Ingrassia. "Using a sound field to reduce the risks of bird-strike: an experimental approach". *Integrative and Comparative Biology* 57.1 (2017), pp. 81–89.

[6] K. S. Smallwood and C. Thelander. "Bird mortality in the Altamont Pass wind resource area, California". *The Journal of Wildlife Management* 72.1 (2008), pp. 215–223.

[7] K. S. Smallwood and B. Karas. "Avian and bat fatality rates at old-generation and repowered wind turbines in California". *The Journal of Wildlife Management* 73.7 (2009), pp. 1062–1071.

[8] K. L. Krijgsveld, K. Akershoek, F. Schenk, F. Dijk, and S. Dirksen. "Collision risk of birds with modern large wind turbines". *Ardea* 97.3 (2009), pp. 357–366.

[9] M. De Lucas, G. F. Janss, D. P. Whitfield, and M. Ferrer. "Collision fatality of raptors in wind farms does not depend on raptor abundance". *Journal of applied ecology* 45.6 (2008), pp. 1695–1703.

https://doi.org/10.25974/ren_rev_2021_08

Harvesting wind energy through electrostatic wind energy conversion

Comparison with common wind turbines and future possibilities

*Yannick Wittor**

Münster University of Applied Sciences, Stegerwaldstraße 39, 48565, Steinfurt, Germany

Abstract

Despite their important role in our energy system, common wind turbines have some disadvantages. Mainly, those disadvantages are connected to the intermediate conversion of wind energy in rotational energy. The resulting effects include maintenance costs and social acceptance problems. There are different technological approaches, that convert wind energy to electrical energy without its conversion to kinetic energy. As one of those technologies, the electrostatic wind energy conversion is to be discussed in this article. For this discussion, the historical development of this technology is presented. There are three important projects which will be presented to explain the technology and its different technological approaches. Those projects are the Wind Power Charged Aerosol Generator (WPG), the Electrostatic Wind Energy Converter (EWICON) and the Solid State Wind Energy Transformer (SWET). Furthermore the results of those different experimental projects are collected and analyzed. On the basis of this analysis it is discussed, whether or not the electrostatic wind energy conversion could be of importance in a future energy system. Therefore the technology is set in relation to modern wind turbines. Also, important factors that influence the efficiency and energy output of those systems are outlined for further research. Due to different technological approaches a suggestion is made for the most promising system setting.

Keywords: electrostatic wind energy, wind energy, solid state wind energy, electrohydrodynamics, bladeless wind generator

List of abbreviations

WPG	Wind Power Charged Aerosol Generator
EWICON	Electrostatic Wind Energy Converter
SWET	Solid State Wind Energy Transformer
LCOE	Levelized cost of energy

*Corresponding author: yw090223@fh-muenster.de.

1 Introduction

Common wind turbines have a central role in our current energy system. In 2018, on- and offshore turbines produced 111,6 TWh of electrical energy in Germany. With an overall electricity demand of 594,9 TWh in 2018, 18,8 % were produced by wind turbines [1]. They transform wind energy into rotational energy, which then is used to generate electrical energy. As an intermediate step in the energy conversion, this rotational movement leads to wear and tear causing maintenance costs. Furthermore, the head of the wind turbine and its rotors can be turned in and out of the wind. Three other negative aspects of wind turbines are environmental impacts [2–4]:

- noise
- shadow flicker
- avian fatalities

The shadow flicker effect refers to the shadow, that the rotor of the wind turbine causes on the ground while turning. The noise is also caused by the rotation. While rotors rotate, they possibly strike flying animals causing avian fatalities. As we can see, the conversion of wind energy in rotational energy is accompanied by the main flaws of this wind energy harvesting technology. Therefore this paper will pay attention to a comparatively novel technology, which generates electric energy from the wind without moving parts. There are different methods in this field of energy production, but this paper will focus on the principle of electrostatic wind energy conversion. A descriptive illustration is given in Figure 1. The idea behind this concept is that charged particles are emitted by an emitter. These particles are carried against the force of an electric field by the kinetic force of the wind, thus increasing the electric potential of the particle. When the particle reaches the collector, the circuit is closed through the load resistance and the additional energy is ready to be used. There are different experimental approaches that work on the basis of this concept. In chapter 4 it will be answered,

https://doi.org/10.25974/ren_rev_2021_09

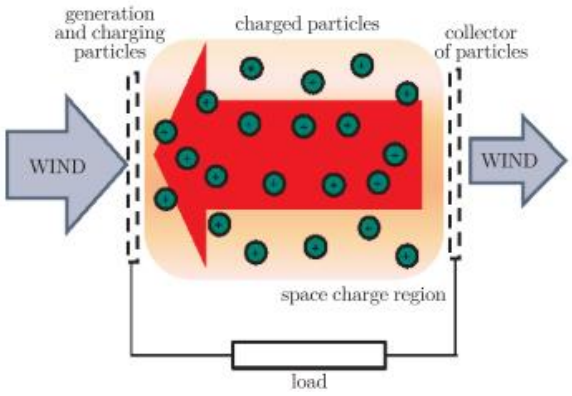

Fig. 1: Scheme of electrostatic wind energy generation [2]

whether or not this technology and its development could be of importance for the sustainable wind energy production in the future. Furthermore possible fields of application will be discussed.

2 Materials and methods

This paper examines practical and theoretical results obtained by researchers in this field throughout the years. Furthermore those results are compared and important findings or evaluations from the research are outlined. Parameters of interest are the net power output, the process efficiency and the specific power output per area. Moreover calculations of scaled up systems and the outlooks the researchers give are of interest. In this chapter, all analyzed projects are presented in a short timeline. The results of those projects are then presented in the chapter three. Due to the differences between the results of the different systems, they won't be represented in tabular form. In Figure 2 the WPG is shown. The WPG was developed by Alvin M. Marks and a final report was written for the Solar Energy Research Institute in 1980 [5]. The research of his team began in the 1940's and lead to a patent [6]. The WPG by Marks is an aerosol

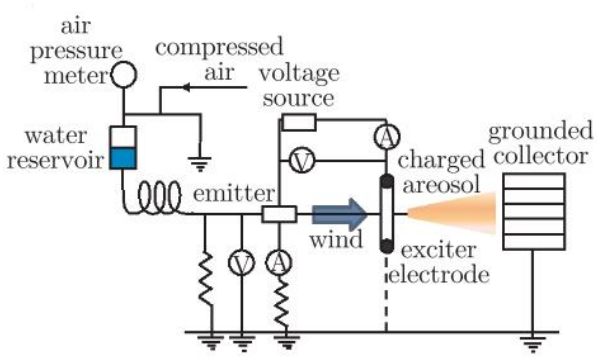

Fig. 2: Scheme of a WPG from [2] based on [5]

based energy converter. It uses water or other fluids to produce charged particles. To achieve this, pressure is applied to a water tank through compressed air. The water flows through a thin tube and is charged by the emitter. Electrostatic wind energy systems can differ in the creation method of charged particles. In this case the charging method is induction. Then the water issues through a very small orifice (25 to 100 µm) while the exciter electrode creates the electric field. Now, the wind carries the spray of charged water droplets out of the electric field. If the particles reach the collector a current flows through the load resistance. An external voltage source provides the energy to charge particles and creates the electric field. All in all, the presented WPG is a small scale experimental apparatus. Another aerosol based system is the EWICON. The EWICON was developed and tested at the Delft University of Technology where it was researched by Djairam et al. from 2005 to 2014 [3, 7]. The assembling presented in Figure 3 is an experimental apparatus. It is considered to be the most promising technical solution by the researchers. A huge aspect of the TU Delft research were new tech-

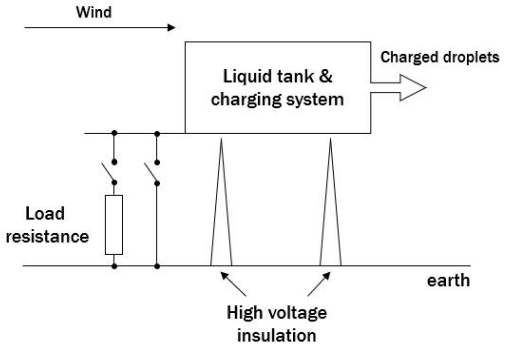

Fig. 3: Scheme of the final EWICON system adjusted from [3]

nological possibilities to create charged droplets of an aerosol. This paper will not elaborate those developments but will examine the maximal output results later on. A special spraying and charging system creates charged particles and the electric field. Again the wind carries the particles out of this electric field. The EWICON system doesn't need an additional collector. The earth acts as such. To assure the current through the load resistance the charging system needs to be insulated. The last and newest considered project is the SWET by Richard Epstein [8]. In 2019 Epstein published an article in the journal Applied Physics Letters where he presented the SWET as a proof of concept. It proves that a system for electrostatic wind energy conversion doesn't need an aerosol but works by charging air molecules. A design for the SWET is shown in Figure 4. The emitter consists of two wooden masts with a height of 8,5 m. They are erected 8 m apart from one another. Between

https://doi.org/10.25974/ren_rev_2021_09

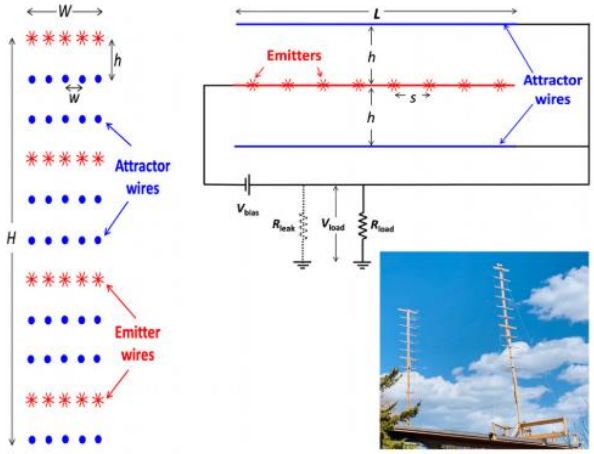

Fig. 4: Design of a SWET with H = 5m, W = 1m and L = 7m [8]

these masts, 35 attraction wires and 20 emitter wires are installed. Both attraction and emitter wires are aluminium wires. Additionally there are small tufts of carbon fiber attached to the emitter wires. Now a negative voltage is biased to the emitter wires and a positive voltage to the attraction wires. If this voltage is high enough, it leads to coronal discharge at the emitter points. Coronal discharge means an ionization of the dielectric surrounding of the emitter due to a high electric field strength. At the same time, the field strength is not high enough to create an electrical arch. This concept is another possibility for charging particles [9]. Now, the wind carries away the charged air ions. The earth acts as collector for those ions and a current through the load resistance is the result.

3 Results

In this chapter the main results of the above described modules are outlined and summarized. Due to the large differences between the projects the results for aerosol- and ion-based systems are examined separately.

3.1 Results for aerosol-based systems

Marks et al. [5] achieved a net power output of 1 mW per aerosol orifice. The hydraulic input power for applying the water pressure was 1,3 mW. Furthermore, the system needed 0,05 mW for particle charging and the electric field. An electric efficiency of 75% to 97% was measured in a wind tunnel. Also an important theoretical finding was made. While increasing the number of orifices n_a the output power scaled with the factor n_a^2 and the input power with n_a. Based on this, he calculated a theoretical large scale version with a power output density of 400 W/m² aperture area. Therefore 36.000 orifices/m² were needed . In comparison, a modern 10 MW wind turbine with a rotor diameter of 193 m achieves around 340 W/m² [10]. Regarding the optimization potential of such a system, Marks et al. outlined the significance of the droplet charge density in an aerosol. Djairam et al. [3] paid further attention to the creation of a charged aerosol. The best results were obtained through the method of electrohydrodynamic atomization. In this way, their water-based system reached a power output density of 2,3 W/m². They calculated 3 charging systems /m² thus a power output density of 767 mW/charging system was reached. The system efficiency in this case was 6,9 %. The researchers calculated the power coefficient of 2,3 %. This power coefficient is the relation between achieved efficiency and Betz limit. While the Betz limit is 59,3%, power coefficients of modern wind turbines are around 50% [11]. Furthermore Djairam and his team calculated a scaled up system as well with the following assumptions:

- wind velocity: 10 m/s
- constant homogeneous electric field: 50 kV/m
- droplet diameter: 10 µm
- droplet charge: 5,0 * 10^{-12}
- no evaporation

Under these assumptions a theoretical power output density of roundabout 100 W/m² is achieved. For that, a multi array of 900 nozzles/m² is required.

3.2 Results for ion-based systems

As main finding, Epstein et al.[8] proved that harnessing wind energy through movement of charged air particles in an electric field is possible. The SWET concept achieved a small power output density of 1,4 mW/m³. The systems width has 5 parallel lines of wire, resulting in power output density/m² equal to 0,28 mW/m². This result is the maximal power output of the system. It produced 50 mW of electric energy with a wind velocity between 10 to 12 m/s and an input voltage of 7 kV. A roughly optimized load resistance of 5 GΩ was chosen. Based on this, a larger scale system was estimated which could deliver 40 kW/km. But in using air-ions instead of a charged aerosol, Epstein points out one problem. Air-ions are much lighter than a charged aerosol. Because of this, more force is needed to push the air ions out of the electric field.

4 Discussion

The superfluity of rotating parts leads to less wear and tear and thus to less maintenance effort. Even flaws of common wind turbines as stated above don't

https://doi.org/10.25974/ren_rev_2021_09

matter. On the other hand, there are negative aspects as well. As seen above, the specific energy output as well as the exploitation of kinetic wind energy in comparison to modern wind turbines is up until today very low. D. Djairam argues that the efficiency is not the only aspect that matters, but also the Levelized cost of energy (LCOE). Additionally, in 2014 he saw a potential to increase the power coefficient 20% to 30% in the next 5 to 10 years [3]. But with increasing power capacities for common wind turbines in the future, their LCOE will decrease, too. According to an expert survey on future wind energy costs, published in Nature Energy LCOE, are expected to decrease by 24-30% in 2030 and 35–41% in 2050, assuming a medium development [12]. An additional advantage of this new method of wind energy conversion is the lower down time. The critical wind speed for common wind turbines is 20 to 25 m/s [11]. A theoretical analysis of an aerosol-based wind energy converter by Minardi et al. [13] shows that the system withstands up to 44 m/s. It is a fence-like scaled up construction with a power capacity of 2,25 MW, a height of 60 m and a length of 400 m. This would be of interest mainly for offshore applications. Additionally, total estimated investment costs were calculated for this system. These costs are 23.073.000 $. This resulted in specific investment costs of circa 10.250 $/kW at that time. Back then, typical wind turbines had specific investment costs of 3.000 to 3.500 €/kW [14]. Considering historical exchange rates between $ and DM and a simplifying exchange rate of 1 € = 2 DM, the specific investment costs comprised a range of 2780 $/kW to 3240 $/kW. The huge cost difference between both technologies might be the reason for the domination of common wind turbines. Nonetheless, concerning system costs, a system similar to the ion-based SWET would be less expensive. Regarding energy conversion, the ion-based method has an advantage over the aerosol-based. The system is less complex and therefore more cost efficient. Additionally, aerosols need to be environmentally friendly. They limit the field of application. For example, water-based systems cannot operate in freezing conditions. On the contrary, in an electric field aerosols are easier mobilized by the wind than charged air molecules. The SWET concept is not complex and therefore suggests extensive optimization opportunities [8]. The fence-like structure of the SWET is a restriction on the field of application because of the wind direction. The optimum point of operation is reached if the wind blows vertically to the structure. Another drawback is the very little energy output of the SWET compared to the aerosol-based systems. Finally regarding costs and complexity, systems without an additional collector seem to have an advantage over systems with additional collectors. This also improves the system applicability because an extra collector has to be aligned with the emitter in the wind flow. If it's possible to further increase the power coefficient, the electrostatic wind energy conversion could only be of interest in the rather distant future. One example of an innovative concept where the EWICON technology will be implemented in a larger scale is the Dutch Windwheel. It is a 174 m high architectural structure financed by development funds. The purpose of this project is the creation of a sustainable living space under implementation of renewable energies. A start of service is planned for 2025 in Rotterdam [2, 15].

5 Outlook

Further research should focus on the optimization of the ion-based SWET concept, because the system is less complex and therefore more cost efficient. As stated by Epstein, a possible optimization of the system could be a more concentrated assembling, with emitter and attraction wires installed closer together. Additionally, it also could be effective to investigate a different construction of the whole system. A fence-like system is dependent on the wind direction. Possibly, a tower of round horizontally stacked emitting and attracting discs would not be. Concerning it's safety, it should be investigated if the coronal discharge has negative effects on the environment. Also further investigations concerning the maximization of the air molecule charge density are of interest.

References

[1] U. Fahl and M. Blesl. "Energiewirtschaftliche Gesamtsituation". *BWK - Das Energie-Fachmagazin* 71 (2019), pp. 20–32.

[2] H. Nowakowska, M. Lackowski, T. Ochrymiuk, and R. Szwaba. "Novel electrostatic wind energy converter: An overview". *Task Q* 19.2 (2015), pp. 207–218.

[3] D. Djairam, P. H. Morshuis, and J. J. Smit. "A novel method of wind energy generation-the electrostatic wind energy converter". *IEEE Electrical Insulation Magazine* 30.4 (2014), pp. 8–20.

[4] S. Wang and S. Wang. "Impacts of wind energy on environment: A review". *Renewable and Sustainable Energy Reviews* 49 (2015), pp. 437–443.

[5] A. M. Marks. *Wind Power Charged Aerosol Generator*. Tech. rep. National Renewable Energy Lab.(NREL), Golden, CO (United States), 1980.

[6] A. M. Marks. *Charged aerosol power conversion device and method*. US Patent 3,518,461. 1970.

https://doi.org/10.25974/ren_rev_2021_09

[7] D Djairam, A. Hubacz, P. Morshuis, J. Marijnisen, and J. Smit. "The development of an electrostatic wind energy converter (EWICON)". *2005 International Conference on Future Power Systems*. IEEE. 2005, 4–pp.

[8] R. I. Epstein. "A solid-state wind-energy transformer". *Applied Physics Letters* 115.8 (2019), p. 083901.

[9] E. D. Fylladitakis, M. P. Theodoridis, and A. X. Moronis. "Review on the history, research, and applications of electrohydrodynamics". *IEEE Transactions on Plasma Science* 42.2 (2014), pp. 358–375.

[10] 2019. URL: https://www.siemensgamesa.com/newsroom/2019/01/new-siemens-gamesa-10-mw-offshore-wind-turbine-sg-10-0-193-dd.

[11] H. Watter. "Windenergie". *Regenerative Energiesysteme*. Springer, 2019, pp. 55–102.

[12] R. Wiser, K. Jenni, J. Seel, E. Baker, M. Hand, E. Lantz, and A. Smith. "Expert elicitation survey on future wind energy costs". *Nature Energy* 1.10 (2016), pp. 1–8.

[13] J. E. Minardi and M. O. Lawson. *Conceptual design of an electrofluid dynamic wind energy system. A subcontract final report*. Tech. rep. Dayton Univ., OH (USA). Research Inst., 1984.

[14] J. K. Kaldellis and D. Zafirakis. "The wind energy (r) evolution: A short review of a long history". *Renewable energy* 36.7 (2011), pp. 1887–1901.

[15] *Dutch Windwheel: PNO ist Servicepartner des Projektes*. 2018. URL: https://www.pnoconsultants.com/de/neuigkeiten/dutch-windwheel/.

https://doi.org/10.25974/ren_rev_2021_09

Self-build small wind turbines

A review

*Julian Speller**

Münster University of Applied Sciences, Stegerwaldstraße 39, 48565 Steinfurt, Germany

Abstract

Self-build small wind turbines are used for rural electrification in the developed and developing world as well as for educational purposes. To give an overview about self-build small wind turbines a systematic literature review was conducted. The identified literature deals with two different vertical and horizontal axis turbine designs. The vertical axis turbines are both prototypes while one of the horizontal axis designs, the design by Piggott is widely used in rural electrification projects. Different papers dealing with the optimization of the Piggott design exist. In retrospect the conduction of a holistic review was not possible due to limited resources and length of this review. Nevertheless it can give a quick overview and a starting point for further research.

Keywords: small wind turbines, self-build, horizontal axis, vertical axis,

1 Introduction

Small wind turbines (SWT) are often used for off-grid electrification in rural areas of developing countries but also in isolated regions in the developed world [1]. Beside commercial turbines manuals for self-build turbines are available. These manuals are used in electrification projects of different associations as engineers without borders or even for educational purposes (e.g. the project windmobil in Luxemburg). This review paper summarizes published technical reports and manufacturing manuals in connection with small self-build wind turbines found by a systematic literature review. The aim of this paper is to give an overview about the variety of different types of self-made wind turbines and their documented optimizations. As an initial point this paper can help non-profit organizations as well as individual persons or education institutions to identify relevant literature.

*Corresponding author: js978529@fh-muenster.de.

2 Methods

To collect the data, a systematic literature search according to the snowballing approach described by Wohlin [2] was conducted. Relevant literature was identified using the search engine of the authors host university called "FINDEX". Included studies have to be a manual or illustrate the results of an modification on a small wind turbine or a component of it. Some relevant literature was published in Spanish and is therefore not included in this review. To begin the snowballing process the search string *("locally manufactured" OR "self build" OR "self made") AND "small wind turbines"* was used. The starting set included 13 papers.

Afterwards the identified literature is classified by axis of rotation, summarized and evaluated shortly.

3 Results

The ten papers identified by the systematic literature review are shown in Table 1. Afterwards the papers are shortly presented in subsections in respect to the axis of rotation. Literature in respect to horizontal axis of rotation mainly focuses on the manual of Hugh Piggott. Even it is not published in an academic outlet this manual is additionally included.

Tab. 1: Publications dealing with self-build small wind turbines identified by systematic literature review

Axis of rotation	SWT model	Ref
3***Vertical**	Al-Bahadly	[3]
	Venetica M1	[4]
	Venitica M1	[5]
8***Horizontal**	Piggott manual	[6]
	Piggott rotor	[7]
	Piggott rotor	[8]
	Piggott rotor	[9]
	Piggott generator	[10]
	Piggott generator	[11]
	homebrew	[12]

https://doi.org/10.25974/ren_rev_2021_10

3.1 Vertical axis small wind turbines

The publications in connection with vertical axis turbines deal with two different designs. Al-bahadly presented a turbine based on the Savonius rotor driven by drag forces. The design published by Bassett is based on an hybrid design which is driven by lift and drag forces. A more detailed construction manual of this design called Venecia M1 is online available [13].

Design Al-Bahadly [3]
The rotor is made out of two cut in half and stacked 44 gal drums. The rotor is 1.5 m tall with a diameter of 0.65 m. To reach the needed generator speed a transmission from rotational axis to generator is needed. The support frame is constructed out of galvanized steel. The calculated power output is 27 Watts and 0.65 kWh per day at a average wind speed of 10 m/s. The author estimated construction costs of $NZ 500.

Design Bassett (Venetica M1)[4]
The rotor consists of three blades out of a pine profile wrapped in sail cloth material. It is 1.524 m tall with a diameter of 0.927 m (fig. 2). The generator connected directly to the rotational axis is based on a design by Hugh Piggott. A transmission is not needed. The calculated power output is 100 Watts at 10 m/s. The results of trials show an output of 45 Watts at 10 m/s wind speed [13]. Additionally the author proofed the possibility of blade production with 3D-printing for this turbine in another research paper [5].

3.2 Horizontal axis small wind turbines

Literature focuses mostly on the design of Hugh Piggott [6]. Only one of the evaluated papers [12] focuses on another design called homebrew design [14]. This manual was not available in the library of the authors home university. Due to the missing basic literature the paper of Louie [12] is excluded in this study.

The manual published by Piggott is often used in rural electrification projects [1]. The evaluated papers mainly focus on the optimization of rotor or generator of the turbine. The general design is presented in fig. 3. Therefore this chapter is subdivided according to this focuses.

Rotor
The original manual by Piggott describes different rotor diameters from 1.2 m (rated power 200 Watts) to 4.2 m (rated power 1000 Watts) and tip speed ratios between 5 and 7. The blade with a complex twisted airfoil is carved out of wood. Hosmann [7] constructed a turbine with 1.8 m rotor diameter according to the manual, analysed its characteristics, implemented a new untwisted airfoil (NACA4412) and repeated the tests. The new blades led to a 11 % higher rotor efficiency but higher noise production at low wind speeds of 4 m/s. At higher wind speeds the efficiency improvement decreases from 5.2 % at 5 m/s to 1.2 % at about 8 m/s. Melendez-Vega et al. [9] replaced the original Piggott 1.2 m blades with ones made out of PVC pipes. This configuration slightly lowered the performance at wind speed under 6 m/s but increased it at higher wind speed. At 10 m/s the modified turbine had a 30 % higher performance. Latoufis et al. [8] examined the influence of eroded edges of an 2.4 m turbine after 18 months of use. The noise produced by the turbine increased significantly at all wind speeds while the output power was stable under 8 m/s wind speed and decreased at rated wind speed of 11 m/s about 23,7 %.

Generator
The original manual presents different coreless generator configurations for each rotor size described earlier and system voltages of 12 V, 24 V and 48 V. Sumanik-Leary et al. [10] changed the neodymium magnets (class N40) of the 48 V generator connected to 2.4 m turbine to ferrite magnets (class F8) which have a lower magnetic field strength but are cheaper and less sensitive to corrosion. Generally at higher rotational speeds from around 240 rpm the neodymium magnets had an approximately 5 % higher overall efficiency in the laboratory tests. Field test were only realized with the neodymium generator so no comparable data of a ferrite generator was generated. For probably the same generator size with neodymium magnets Shea and Ludois [11] added ferrous fillings into the stator windings. This led to a 50 % lower magnet thickness maintaining the electrical power output.

4 Conclusions

4.1 Vertical axis

Al-Bahadly [3] evaluation
The paper presents the planning of the turbine step by step and indicates the general theoretical background. Although the generator properties are not shown as well as the devided costs by parts. Therefore it is not transparent how the author considered the construction costs of NZ$ 500. Even if the designed prototype is build, no actual testing was done to confirm the theoretically calculated power output.

Venetica M1 [4, 13] evaluation
The paper presents the planning and manufacturing step by step more generic than Al-Bahadly and does not present the theoretical background. Also the estimation of the turbine power coefficient of 0,3 is quiet optimistic. The measured power output of less than 50 % of the estimation documented at the website underlines this, also if there are other influences on the output like the electrical system. Another question, also mentioned by the author, which has to be answered is how the cloth behaves in the rain.

Generally the vertical axis wind turbines are more suitable than horizontal axis wind turbines for turbu-

lent airflows. Due to their prototype status and low power output both described turbines are currently not recommandable for electrification projects.

4.2 Horizontal axis

Rotor
The original manual is a hands on guide and enables people to build a small wind turbine with little technical knowledge. On the one hand the blades Hosmann [7] recommends improve the rotor efficiency and simplifiy the blade production. On the other hand the airfoil is thinner so the strength of the blades has to be evaluated. The PVC blades Melendez-Vega et al. [9] introduced are relatively easy to produce and have a significantly higher power output at wind speeds over 6 m/s but also have to be evaluated in respect to their strength. The paper by Latoufis [8] shows a big impact of the blade condition on the performance. They doesn't describe which wood they used or which could be a better alternative.

Generator
Due to the absence of field test data, Sumanik-Leary et al. [10] couldn't verify the laboratory results. The reduction of magnets Shea and Ludois [11] propose is associated with a cogging torque of 4 to 7 Nm while a similar generator which was tested by Hosmann [7] had a cogging torque of 0,05 Nm. The paper hasn't examined whether this increase would lead to start up problems or not.

To sum up the airfoil alternative described by Hos could be a good alternative for regions with low wind speed and where noise does not play a mayor role and building a bigger turbine is not possible. The design presented by Melendez-Vega et al. can be useful in regions with higher average wind speeds and where the availability of PVC pipes is not critical. Sumanik-Leary et al. [10] showed that the originally used neodymium are more efficient as the less corrosion sensitive ferrite ones. If it is useful to replace them even so, the difference in lifetime has to be evaluated. The use of iron fillings in the stator windings Shea and Ludois [11] proposed to reduce the mass of magnet increase the the cogging torque extensively to 4 Nm to 7 Nm which can be critical to the start up behavior of the turbine.

5 Outlook

In the evaluated set of papers, studies dealing with technical aspects as defined earlier in connection with self build small wind turbines are not really widely represented. For further research the search string should be extended or varied with typical and specific searching keys e.g. "VAWT" or "HAWT" which were not possible to include in this due to limited resources. Furthermore online forums where ideas are shared and discussed should be taken into account. To name only some there is the solar-electric forum with a wind power category [15] or one in Germany called "Kleinwindanlagen" [16].

References

[1] J. Sumanik-Leary. "Small wind turbines for decentralised rural electrification: Case studies in Peru, Nicaragua, and Scotland". PhD thesis. Sheffield: University of Sheffield, June 2013.

[2] C. Wohlin. "Guidelines for snowballing in systematic literature studies and a replication in software engineering". *18th International Conference on Evaluation and Assessment in Software Engineering*. London, England, UK, 2014.

[3] I. Al-Bahadly. "Building a wind turbine for rural home". *Energy for Sustainable Development* 13 (2009), 159–165.

[4] K. Bassett and I. Fleischmann. "An open source licensed vertical axis wind turbine for rural electrification and sustainability". *6th International Conference on Energy Sustainability*. San Diego, California, USA, 2012".

[5] K. Bassett, R. Carriveau, and D.-K. Ting. "3D printed wind turbines part 1: Design considerations and rapid manufacture potential". *Sustainable Energy Technologies and Assessments* 11 (2015), 186–193.

[6] H. Piggott. *A wind turbine recipe book*. Scoraig, Scotland: Scoraig Wind Electric, 2013.

[7] N. Hosmann. "Performance analysis and improvement of a small locally produced wind turbine for developing countries". MA thesis. Delft, NL: Technical University of Delft, Sept. 2012.

[8] K. Latoufis, V. Riziotis, S. Voutsinas, and N. Hatziargyriou. "Effects of leading edge erosion on the power performance and acoustic noise emissions of locally manufactured small wind turbine blades". *Journal of Physics: Conference Series* (2014).

[9] P. Melendez-Vega, G. Venkataramanan, D. Ludois, and J. Reed. "Low-cost lightweight quick-manufacturable blades for human-scale wind turbines". *IEEE Global Humanitarian Technology Conference*. Seattle, Washington, USA, 2011.

[10] J. Sumanik-Leary, K. Silwal, and T. Wastling. 2013.

[11] A. Shea and D. Ludois. "Reduction of permanent magnets in small-scale wind turbines". *IEEE Energy Conversion Congress and Exposition*. Denver, Colorado, USA, 2013.

https://doi.org/10.25974/ren_rev_2021_10

[12] H. Louie. "Experiences in the construction of open source low technology off-grid wind turbines". Aug. 2011, pp. 1 –7. DOI: 10.1109/PES.2011.6038924.

[13] K. Bassett. *Venecia M1 wind turbine: a low-cost wind turbine for rural electrification*. https://sites.google.com/site/veneciam1windturbine/. Accessed: 2021-01-02. 2010.

[14] D. Bartmann. *Homebrew wind power: a hands-on guide to harnessing the wind*. Buckville Publications, 2013.

[15] *Northern Arizona Wind Sun Solar Forum*. https://forum.solar-electric.com/categories/wind-power-generation. Accessed: 2021-01-02. 2021.

[16] U. Hallenga. *kleinwindanlagen.de*. https://www.kleinwindanlagen.de/Forum/cf3/index.php. Accessed: 2020-01-02. 2021.

Low-Cost Hydropower Turbines for Developing Countries

*Mark Scheffler**

Münster University of Applied Sciences, Stegerwaldstraße 39, 48565 Steinfurt, Germany

Abstract

There are many hydropower turbines for low heads or low flows on a small scale. Many technologies are unsuitable for developing countries because equipment or materials are limited, high-tech machines are to expensive or spare parts are not readily available. This review combines currently available technologies with the requirements of developing countries in small, micro and pico hydropower. In small hydropower a propeller turbine from Thailand has a high efficiency of 70 to 80 percent at calculated production costs of around $ 513 per kW. Pumps as turbines are suitable for developing countries in micro hydropower due to readily availability, low price and an large number of standard sizes. In pico-scale, a low-cost Turgo wheel can be made of spoons for $ 48 and yields acceptable values in comparison to a 3D printed Pelton wheel for $ 822. While the Turgo wheel is suitable for high heads, a homemade siphon turbine can be used for low heads. The siphon turbine generates up to 200 W, is made of materials that are available anywhere in the world, and costs less than $ 50.

Keywords: hydropower, developing countries, low-cost, micro hydro, small hydro, pico hydro

1 Introduction

Hydropower is a major source of renewable energy. In 2019, the total global hydropower installed capacity increased by 15.6 GW and reached 1,308 GW. That corresponds to a rise of 1.2 percent. Nevertheless, this is below the required carbon reduction targets outlined at the Paris Agreement, which requires an estimated growth rate of 2.0 percent. For comparison, 21.8 GW were added in 2018 [1].

The construction of large and medium-sized dams is decreasing worldwide. Reasons for this are environmental protection, decreasing returns on investment, concerns about resettlement of residents and decreasing availability of suitable new locations. Conversely, small hydropower still has potential wordwide and does not have the cost and environmental problems associated with dams [2].

Basically, the kinetic and potential energy of the water is converted into mechanical energy by hydro turbines to rotate generators or other machinery for power generation [3]. In a nutshell, any hydroppower system´s output is based on equation 1. The decisive factors are head, flow and efficiency [4].

$$P = \eta \cdot \rho \cdot g \cdot Q \cdot H \tag{1}$$

where

P:	mechanical power (W)
η:	hydraulic efficiency of the turbine
ρ:	density of water (kg/m^3)
g:	gravitational force (m/s^2)
Q:	volume flow rate (m^3/s)
H:	effective pressure head (m)

Hydropower plants can be differed based on several criteria, such as the power output, head or the type of turbine running. However, the classifications are not always uniform worldwide. Therefore, this paper uses the definition of the European Small Hydropower Association (ESHA) to classify the pressure head [4, 5]. Basically, pressure head is classified into ultra-low (<3 m), low (2 - 30 m), medium (30 - 100 m) and high head hydropower (>100 m) [6]. The subdivision of the hydropower potential is mostly country-dependent. Here the potential is divided into pico (<5 kW) , micro (<100 kW), mini (<1,000 kW), small (<10,000 kW) and large (>10,000 kW) hydropower [7].

Rural areas in developing countries with low population density need local and low cost electricity generation. Large hydropower plants are often not feasible as it requires high investments and a grid infrastructure [8] but there are still many potential locations for pico, micro, mini and small hydropower plants [2]. Those small-scale hydropower systems allow an economically viable electrification especially for small localities and remote areas [9].

Not all new technologies can be used in developing countries. Some are unsuitable due to the high development cost, operating costs or transport to the rural areas. This short review is intended to present examples of suitable solutions for developing countries in different performance classes.

*Corresponding author: m.scheffler@fh-muenster.de.

https://doi.org/10.25974/ren_rev_2021_11

2 Components of Hydropower Plants

The main components of a hydropower scheme are listed below [8]:

- Intake structure: Water exits from a dam or comes from a river bypass to the turbine through a pipeline (penstock)
- Turbine: Energy is converted from the water into a rotary motion by the turbine blades.
- Generator: The rotary motion of the turbine is converted into electrical energy in the generator.
- Outflow: The water exiting the turbine is transported back into the river trough pipelines.

Another distinction of the hydropower plants is the type of water withdrawal. Water is taken directly from a river (run-of-river) or dammed up as a reservoir. In run-of-river schemes, a bypass flows to the turbine and back to the course of the river. This system is more flexible and more environmentally friendly. The main costs of the hydropower plant are the turbine and the piping framework (penstock) since the construction of a dam is not required. On the one hand, dams are cost-intensive large-scale projects, therefore seldom practicable in developing countries, and have a negative impact on the environment. On the other hand, reservoirs enable storage for dry periods and provide flood protection through regulation [8].

There are two working principles for turbines. On the one hand, there are reaction turbines in which the rotor is completely immersed in the water in a closed pressure system. The profile of the runner blades creates pressure differences as well as lift forces thereupon form the rotary movement. On the other hand, there are impulse turbines that rotates under atmospheric pressure. The runner blades driven by a jet (or jets) operate in contact with the air [4] .

Generators convert the mechanical energy from the shaft to the electrical energy. Synchronous, asynchronous and permanent magnet generators are possible. Synchronous generators or alternators have a constant voltage, constant frequency, and supply active and reactive power. These are preferred in large and grid-connected systems. Induction generators are smaller size, lower cost and have a rugged construction with ease of maintenance as alternators. Permanent magnet systems with direct drive are often used for smaller projects [7].

The speed of the generator and hence output frequency can be regulated via the water input or the load. High-head systems with narrow penstock tubes can be easily control the water volume by mechanical governors. The electronic control, however, is more simple, less expensive, requires less maintance and responds faster at low heads [10]. Low speed turbines require low speed generators. These are bigger in size and costlier due to the higher number of poles [11].

3 Suitable Technologies for Developing Countries

There are many different types of turbines available for various situations. The selection of the most suitable turbine depends on the performance characteristics, power capacity, site conditions and cost of the turbine set. In addition, there are some difficulties in developing countries that should be taken into account [12].

The availability of high-tech equipment such as 3D printers or certain materials is limited, especially in rural areas. The delivery of new machines from other countries is sometimes not affordable or uneconomical. In addition, high-tech devices require the corresponding qualifications of people to operate and maintain the machines. Therefore, the construction of a plant should be simple in order to be able to exchange parts. Basically, low maintenance with low operating costs is required [5].

3.1 Small Hydropower

Axial blade machines are most suitable for low head and low flow conditions [13]. The best known types are Kaplan and propeller impeller turbines, which use the axial flow of water to rotate the runner blades. Both are reaction turbines that operates completely immersed in water. In contrast to the propeller impeller turbine, the Kaplan turbine can adjust the runner blades. Therefore, fluctuating water quantities can be optimally adjusted for a high degree of efficiency. In front of the impeller are the guide vanes that give the water a swirl. Guide vanes improves efficiency because the swirl is absorbed by the runner. With good adjustment, the emerging water only has a little residual angular momentum. Behind the impeller is the diffusor, also known as draft tube, through which the water discharges. The draft tube has a larger diameter and slows down the water velocity. This reduces the static pressure and increases the effective head of the turbine [4].

The manufacture of reaction turbines is demanding due to the complex blades and housing. Because of the manufacturing restrictions, these turbines are less common in developing countries [4]. The following example is different. There is a propeller turbine from Thailand, which is designed for a head range of 10 to 20 m. It´s power output is 160 kW by an SIEMENS induction motor with 1,000 rpm. Figure 1 shows the runner blade and guide vanes of the turbine.

The technical data are summarized in table 1. The production cost of this turbine are estimated at about

https://doi.org/10.25974/ren_rev_2021_11

Fig. 1: Runner blade (top) and guide vane (bottom) of the small hydro propeller turbine [3]

$ 513 per kW. The estimate is based on a 1000 kW low head turbine (0-30 m) from Hydro Tasmania Company in Australia that costs approximately $ 900 per kW. Comparable turbines installed in Sri Lanka, Nepal, Peru, Zimbabwe, and Mozambique cost approximately $ 615 - 1,911 per kW [3]. A reason for the wide price range is unknown. Nevertheless, the turbine prices are from the year 2000 and are therefore out of date.

Tab. 1: Conditions and results of the axial propeller turbine [3]

Head range	10 - 20	m
Diameter	0.4	m
Guide vanes	12	pieces (0° - 90°)
Turbine blades	4	pieces (40° radial)
Generator	160	kW
Efficiency	70 - 80	%
Cost	∼ 513	$/kW

The propeller impeller turbine from Thailand is a comparatively economical turbine in the micro hydropower, which is simply controlled via the guide vanes. Due to its low cost and easy operability, this turbine is suitable for use in developing countries. Nevertheless, there are areas that are dependent on self-sufficiency and need solutions on a smaller scale [3].

3.2 Micro Hydropower

Standard pumps as turbines are a attractive option for micro hydropower in developing countries. Centrifugal pumps running in reverse acts as a turbine. As it´s mass-produced, it is readily available an generally cheaper than turbines. Here are some advantages compared with purpose-made turbines [14]:

- Available for a wide range of head and flows
- Available in a number of standard sizes
- Low cost
- Spare parts such as seals and bearings are easy available
- Easy installation - uses standard pipe fittings

The testing of several pump types has shown that end-suction centrifugal pumps are most suitable. Other types of centrifugal pumps such as in-line or double suction centrifugal pumps are less efficient. It is important that the pump has a spiral volute, as a simple round casing with an angled outlet pipe is inefficient as a turbine. Centrifugal pumps are generally the most easily available and cheapest type. Alternatively, dry-motor submersible pumps are also possible, in which the pumped water flows through a casing and thus cools the motor. On the other hand, dry-motor submersible pumps with fin-cooling are useless because they will overheat. Furthermore, all positive displacement pumps are unsuitable [14].

It is particularly important in less industrialized countries to check the quality of a pump. Pumps from large manufacturers are often copied with poor quality in small workshops. This has a bad impact on performance and lifetime. The parts to be checked are Impeller eye clearance, casting quality, impeller material, shaft material and bearing quality [14].

Background: A pump has a specific performance curve and a best efficiency point. The best efficiency point depends on head and flow. These data are usually available from the pump manufacturer [14].

A suitable pump is selected based on the specific head and minimal available flow conditions of a site. (The head is the vertical head difference between the intake of the stream and the turbine outlet minus the loss from the penstock.) However, the best efficiency point (of head and flow) of a pump should be as close as possible to the site conditions in order to select the most suitable pump [14].

https://doi.org/10.25974/ren_rev_2021_11

3.3 Pico Hydropower

Spoon-Based Turgo Turbine

In high head and low flow conditions, a Pelton turbine is likely more efficient but not more expensive than a pump [14]. On the outside of a Pelton wheel, split buckets are arranged around one behind the other. The jet of high speed water hits the middle and splits into both buckets. The halved jets turn and deflect back almost through 180° in the bucket. Therefore nearly all of the energy goes into the rotation of the wheel.[5][4]

The Turgo turbine works on a similar principle. It differs mainly in the shape of the bucket and the direction of the incoming jet. Instead of two curved structures (Pelton) the buckets of a Turgo turbine consists of only one curved structure.[15] In addition, the jet hits at an angle of (typically) 20 °. Therefor the jet enters on one side and exits the other. The advantage is that the reflected water does not interfere with the jet, which reduces the flow rate. Consequently the Turgo turbine can be smaller than the Pelton turbine with equivalent power.[4]

In an experiment, a low-cost Turgo wheel was compared with a 3D printed Pelton wheel. Figure 2 shows the Turgo and Pelton Turbie that were tested. The bucket structure of the Turgo wheel is formed by spoons. The spoons are shortened and welded onto a steel plate that is wrapped around a wooden runner. The geometry of the Turgo wheel depends on the jet velocity and nozzle diameter. For example, the optimal ratio of wheel diameter to jet diameter is 11-16.

Fig. 2: Spoon-Based Turgo wheel (left) and 3D printed Pelton wheel (right) [15]

The main advantages of the Spoon-Based Turgo Turbine are easy availability and low cost. Spoons are easy to get in developing countries, unlike 3D printers, which are very rare and expansive. The low construction costs of $ 42 are suitable for rural areas with a low-income population. The experiment has proven that the Turgo turbine provides acceptable performance and efficiency in pico scale. Tabular 2 shows the most important results of the comparison between Turgo and Pelton wheel [15].

Tab. 2: Comparison of a low cost spoon-based Turgo wheel and a 3D printed Pelton wheel [15]

	Pelton	**Turgo**	
Flow rate	2.40	2.37	l/s
Hydraulic power	117.72	116.25	W
Generated power	30.42	32.80	W
Mechanical efficiency	26	28	%
Investment cost	822	48	$

Homemade Siphon Turbine

There are in the pico hydropower many approaches to build hydropower plants with simple objects, such as the Spoon-Based Turgo turbine. Many hobbyists explain their self-made turbines in videos and upload them to media platforms. These have not been tested under laboratory conditions, documented and published, so this does not represent a good scientific source. The functionality is often based on established techniques that are tested and applied on a larger scale. The difference are mainly the objects used for the construction, which are adopted from other applications. For example, Daniel Connell designed a 200 watt siphon turbine that costs around $ 50 and can be replicated anywhere in the world [16].

A siphon turbine has the advantage in small-scale hydropower that it can be retrofitted in existing structures. For example, suitable places are non-powered dams, irrigation canals, water diversion structures, water distribution systems, water or wastewater treatment plants and others. The siphon conveys the water from the upper reservoir over the dam into the lower reservoir [17].

Conell´s pico hydropower plant consists of the following materials:

- Penstock: PVC pipes and fittings (diameter: 125 mm and 160 mm)
- Turbine wheel: computer power supply plastic fan (diameter: 120 mm)
- Alternator: hoverboard wheel or motorcycle alternator
- Accessories: glue, nuts, bolts and washers

The U-shaped penstock consists of PVC pipes, PVC elbows and an PVC Y-piece. The PVC Y-piece is the upper part of the drop side. The water flows in through the side inlet and out on the straight side

https://doi.org/10.25974/ren_rev_2021_11

downwards in regular flow direction. The inlet on the straight side is closed airtight by a lid. A plastic fan serves as an impeller, which is centrally positioned at the outlet of the PVC Y-piece (Fig 3).

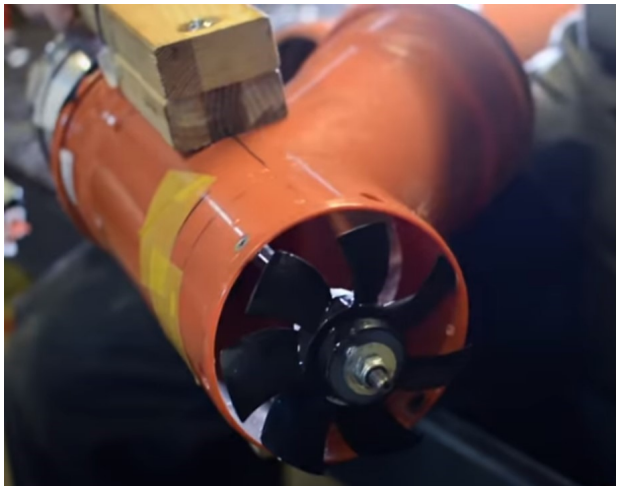

Fig. 3: Computer power supply PVC plastic fan as impeller [16]

The alternator is positioned centrally on the outside above the lid (Fig 4). Impeller and alternator are directly connected via a threaded rod through the lid. Behind the impeller, the diameter increases from 125 mm to 160 mm. The outlet can be extended as required to the lower reservoir by pieces of pipe. The pipes must end below the water surface, so no air enters from below and interrupts the siphon effect.

Fig. 4: Hoverboard wheel used as alternator [16]

A hoverboard wheel is available in western countries in secound hand or online shops for low budget. Alternatively, a motorcycle alternator can be used, which are widely used and available in developing countries.

The performance of the Pico hydropower plant was measured in a workshop with an ammeter and a voltmeter. The data are listed in Table 3.

Tab. 3: Conditions and results of the siphon turbine [16]

Head range	$\sim$ 2.5	m
Flow rate	$\sim$ 35	l/s
Power generated	$\sim$ 192	W
Investment cost	$\sim$ 50	$

4 Conclusion

The selection of the most suitable type of turbine for a site depends on various parameters. In addition, there are difficulties in developing countries. For example, equipment or materials are limited, high-tech machines are to expensive or spare parts are not readily available. Rural electrification requires a robust, low cost solution.

In small hydropower ($>$ 10,000 kW) a propeller turbine manufactured in Thailand is a suitable solution in head range 10 to 20 m. This turbine operates with a simple propeller and adjustable guide vanes, is low-priced at around $ 513 per KW compared to other manufacturers and has a high efficiency of 70 to 80 %.

Standard pumps running in reverse act as turbines. This is usable in micro hydropower ($>$ 100 kW) due to readily availability, lower price than turbines and a large number of standard sizes as pumps are mass-produced.

In pico-scale ($>$ 5 kW), a low cost spoon-based Turgo turbine yields an acceptable value of mechanical of power and efficiency in comparison to a 3D printed Pelton wheel. The Turbine wheel can easily be copied and is suitable for developing countries in high head and low flow conditions. A homemade siphon turbine is a suitable solution for low head and high flow. This generates up to 200 W, is made from materials that are available anywhere in the world, and costs less than $ 50.

These are just a few selected examples of the many possibilities that were presented due to their efficiency, low cost or simple construction. Further reviews could describe the installation of the presented technologies, problems occurring in operation and solutions for these.

References

[1] I. H. Association **et al.**. *Hydropower Status Report. Retrieved 26 April 2020.* 2019. URL: https://hydropower-assets.s3.eu-west-2.amazonaws.com/publications-docs/2020_hydropower_status_report.pdf.

https://doi.org/10.25974/ren_rev_2021_11

[2] D. Zhou, J. Gui, Z. D. Deng, H. Chen, Y. Yu, Yu, and C. Yang. "Development of an ultra-low head siphon hydro turbine using computational fluid dynamics". *Energy* 181 (2019), pp. 43–50. ISSN: 03605442. DOI: 10.1016/j.energy.2019.05.060.

[3] S. Phitaksurachai, R. Pan-Aram, N. Sritrakul, and Y. Tiaple. "Performance Testing of Low Head Small Hydro Power Development in Thailand". *Energy Procedia* 138 (2017), pp. 1140–1146. ISSN: 18766102. DOI: 10.1016/j.egypro.2017.10.221.

[4] O. Paish. "Micro-hydropower: Status and prospects". *Proceedings of the Institution of Mechanical Engineers, Part A: Journal of Power and Energy* 216.1 (2002), pp. 31–40. ISSN: 0957-6509. DOI: 10.1243/095765002760024827.

[5] I. Loots, M. van Dijk, B. Barta, S. J. van Vuuren, and J. N. Bhagwan. "A review of low head hydropower technologies and applications in a South African context". *Renewable and Sustainable Energy Reviews* 50 (2015), pp. 1254–1268. ISSN: 13640321. DOI: 10.1016/j.rser.2015.05.064.

[6] European Small Hydropower Association. "Guide on How to Develop a Small Hydropower Plant" (2004), pp. 1–151. URL: http://www.canyonhydro.com/images/Part_1_ESHA_Guide_on_how_to_develop_a_small_hydropower_plant.pdf.

[7] A. B. Timilsina, S. Mulligan, and T. R. Bajracharya. "Water vortex hydropower technology: a state-of-the-art review of developmental trends". *Clean Technologies and Environmental Policy* 20.8 (2018), pp. 1737–1760. ISSN: 1618-954X. DOI: 10.1007/s10098-018-1589-0.

[8] P. Narrain. *Low Head Hydropower for Local Energy Solutions*. 1st ed. Milton: CRC Press, 2017. ISBN: 978-0-8153-9612-3. URL: https://ebookcentral.proquest.com/lib/gbv/detail.action?docID=5145772.

[9] K. S. Balkhair and K. U. Rahman. "Sustainable and economical small-scale and low-head hydropower generation: A promising alternative potential solution for energy generation at local and regional scale". *Applied Energy* 188 (2017), pp. 378–391. ISSN: 03062619. DOI: 10.1016/j.apenergy.2016.12.012.

[10] V. J. Alzamora Guzmán, J. A. Glasscock, and F. Whitehouse. "Design and construction of an off-grid gravitational vortex hydropower plant: A case study in rural Peru". *Sustainable Energy Technologies and Assessments* 35 (2019), pp. 131–138. ISSN: 22131388. DOI: 10.1016/j.seta.2019.06.004.

[11] S. K. Singal, R. P. Saini, and C. S. Raghuvanshi. "Analysis for cost estimation of low head run-of-river small hydropower schemes". *Energy for Sustainable Development* 14.2 (2010), pp. 117–126. ISSN: 09730826. DOI: 10.1016/j.esd.2010.04.001.

[12] A. H. Elbatran, O. B. Yaakob, Y. M. Ahmed, and H. M. Shabara. "Operation, performance and economic analysis of low head micro-hydropower turbines for rural and remote areas: A review". *Renewable and Sustainable Energy Reviews* 43 (2015), pp. 40–50. ISSN: 13640321. DOI: 10.1016/j.rser.2014.11.045.

[13] K. V. Anisimov, A. V. Dub, S. K. Kolpakov, A. V. Lisitsa, A. N. Petrov, V. P. Polukarov, O. S. Popel, and V. A. Vinokurov, eds. *Proceedings of the Scientific-Practical Conference Research and Development - 2016*. Cham: Springer International Publishing, 2018. ISBN: 978-3-319-62869-1. DOI: 10.1007/978-3-319-62870-7.

[14] A. Williams. *Pumps as turbines: A user's guide*. Reprint. London: Intermediate Technology Publ, 1997. ISBN: 1853392855.

[15] Budiarso, Warjito, M. N. Lubis, and D. Adanta. "Performance of a Low Cost Spoon-Based Turgo Turbine for Pico Hydro Installation". *Energy Procedia* 156 (2019), pp. 447–451. ISSN: 18766102. DOI: 10.1016/j.egypro.2018.11.087.

[16] D. Connell [OpenSourceLowTech]. *The $50 Water Turbine Part 2 [Video]: Power Results - DIY, Portable, Powerful, and Open Source*. 2020. URL: [Youtube]https://www.youtube.com/watch?v=ibCu0PxIZA4.

[17] J. J. Martinez, Z. Daniel Deng, E.-M. Klopries, R. P. Mueller, P. Scott Titzler, D. Zhou, B. Beirao, and A. W. Hansten. "Characterization of a siphon turbine to accelerate low-head hydropower deployment". *Journal of Cleaner Production* 210 (2019), pp. 35–42. ISSN: 09596526. DOI: 10.1016/j.jclepro.2018.10.345.

Wells turbine: the state of the art

*Michael Hinse**

Münster University of Applied Sciences, Stegerwaldstraße 39, 48565 Steinfurt, Germany

Abstract

The first oscillating water column was invented in 1940. In the past decades the need of wave energy systems has significantly increased. This article quickly describes the Wells turbine and possibilities to enhance its performance and should answer the question: what are the design parameters that can be optimized? Furthermore it gives a small outlook about the history of oscillating Water Columns.

Keywords: wells turbine, owc, energy, oscillating water column, optimization

1 Introduction

In comparison to wind and solar power, ocean waves are continuously produced around the day. They vary in height and by that in potential of power. The ocean as a source of renewable energy has big potential regarding the fact that energy can be produced around the clock. Furthermore waves travel large distances without loosing significant amounts of power, which makes them efficient as an energy transport mechanism. To make use of this potential different devices were invented using the converting the wave energy to drive electrical generators. The devices are differentiated by the water depth in which they used to be built. Another way to sort the devices is to differentiate them by their principle of working.
Most of the devices, named as oscillating water columns, short OWC, are installed near the shore or on the shoreline. The benefits are easier installation and maintenance, because of the fact that long underwater cables are not necessary. Its also possible to built floating or fully submerged devices to use the most powerful wave systems available. The downside is the more complex part of the installation, maintenance and the problem of mooring the device.
To use the power of waves properly there needs to be an efficient and economical way. The solution is the Wells turbine [1].

*Corresponding author: hinse@fh-muenster.de.

2 Oscillating water columns

2.1 What is an oscillating water column?

Oscillating Water Columns, or short OWC, are devices which mainly convert wave energy. They use the absorption of wave energy and convert it into air pressure to infuse a generator with power, through a linked turbine. OWC functions as followed: a hollowed shell below the sea traps the inner water surface. Through wave energy, the air inside the shell compresses and decompresses. The air now moves through a turbine which is linked with a generator. The operating chain behind this process is shown in Figure 1 and Figure 2.

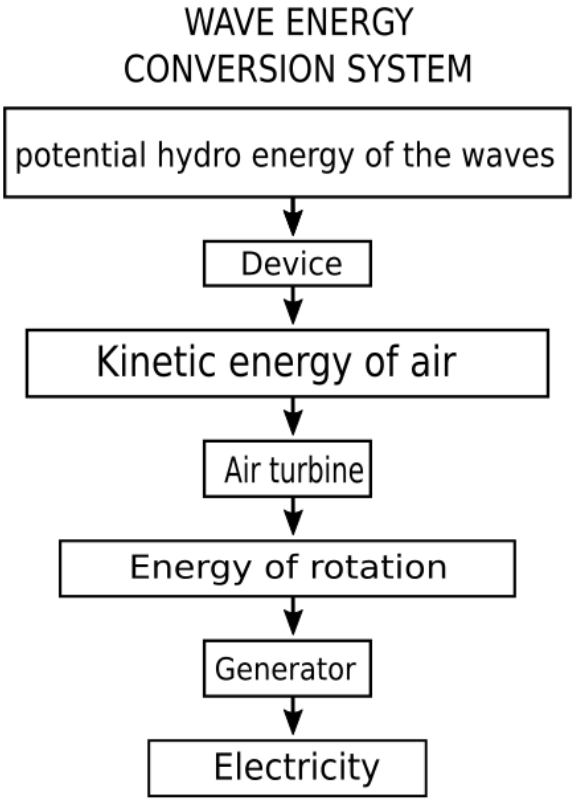

Fig. 1: Example of wave energy conversion operation chain

.

https://doi.org/10.25974/ren_rev_2021_12

2.2 History of Oscillating Water Columns

The first appearance of wave energy conversion (WEC) was published by Yohsio Masuda, born in 1925 and died in 2009, a navy officer from Japan, in the second half of 1940. Masuda invented a navigation buoy powered by wave energy. It was later named as a (floating) OWC. Buoys like these used an unidirectional air turbine with a system of rectifying valves. These kind of Buoys have been used in Japan, since 1965, and later in the USA. An example of this buoy is shown in Figure 3.
The first big water energy converter which was deployed into the sea was Kaimei, also invented by Masuda. It was built by the Japan Marine Science and Technnology Centre (JAMSTEC), weighing 820 ton with dimensions of a length of 80 m and a width of 12 m. It consists of thirteen OWC open bottom chambers each having a water plane area of 42 m^3-50 m^3 and was set off the western coast of Japan in 1978-1980.
After the oil crisis about 1973, Europe studies to develop large scale WECs. The aim was to build a large two GW wave energy plant, but without success. The National Engineering Laboratory (NEL) from Scotland was invented different concepts for one big OWC Plant. Without any built prototype the british programme was terminated in 1982. With the decision, made in in 1991 by the European Commission, of including wave energy in the research and development program on renewable energies the situation changed and lead to studies, followed by construction of two OWC plants. One was built in Portugal on the island of Pico, the other in Scotland on the Island of Islay. Both plants utilizes Wells turbines to drive the generator. Pico plant was completed in 1999 with a rating of 400 kW and still operational. Islay plant was completed in 2000 with a rating of 500 kW [2].

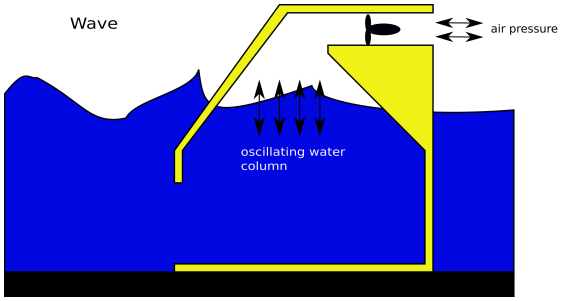

Fig. 2: Principle of the OWC

2.3 Wells Turbine

The Wells turbine, named by the inventor Professor Alan Wells of the Queens University of Belfast in the 1980s, is an axial flow turbine. It's used as an economical and efficient solution to convert the energy of oscillating flow motion to drive an electrical generator. It contains a rotor with untwisted airfoil blades. Because of this the turbine rotates in one direction, regardless the bi-directional air flow [1]. The simplest form of the Wells turbine consists of symmetrical aerofoil blades around a hub with their chord planes normal to the axis of rotation. The turbine can have guide vanes on both sides of the rotor [3]. The operation cycle of Wells turbine is differentiated into two stages because of the mechanism of OWC. The first stage is the compression. The water level inside the housing rises and pushes the air inside through the turbine. The aerodynamic force F_R due to push and pull forces is given by

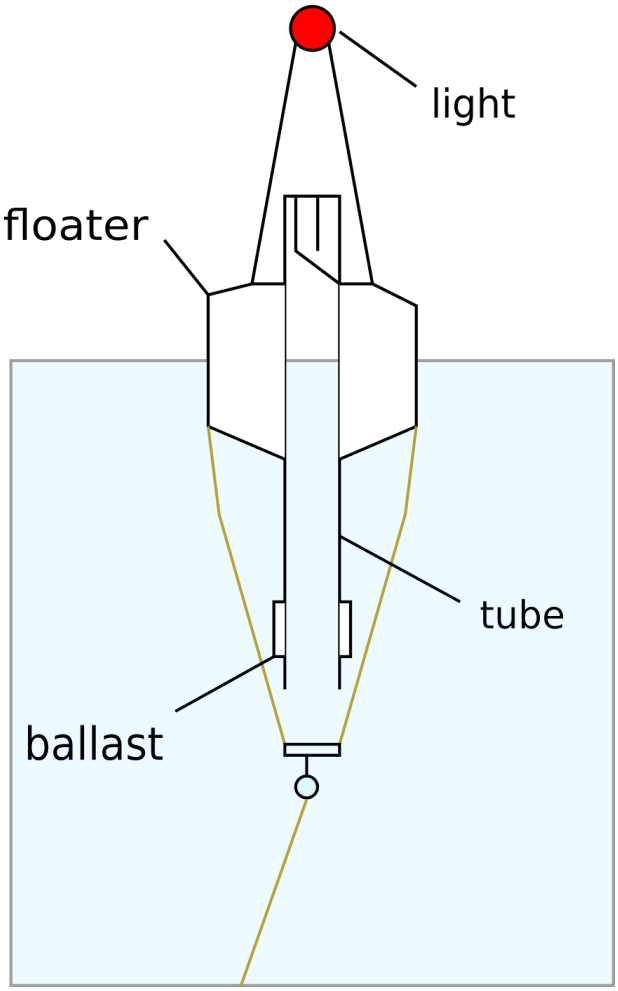

Fig. 3: Example of Masudas floating buoy.

$$F_R = \sqrt{L^2 + D^2} \tag{1}$$

This force can be seperated in two components, axial and tangential directions as

$$F_A = L\ cos\ \alpha + D\ sin\ \alpha \tag{2}$$

$$F_t = L\ sin\ \alpha - D\ cos\ \alpha \tag{3}$$

https://doi.org/10.25974/ren_rev_2021_12

where F_A and F_t are the axial and tangential forces. In the stage of pulling, in which the water level drops, air is sucked into the duct. It's also shown that in either stage there is just one direction for the rotor to move. That's because of the tangential Force. It remains in the same direction for both positive and negative values of α [1].

3 Performance parameters

There are several parameters that affect and influence the design and performance of Wells turbines. Typical drawbacks of Wells turbines are low tangential force, which are leading to low power output. Another one is the low aerodynamic efficiency.This section deals with solutions to overcome disadvantages and aims at improving the performance.

3.1 Guide Vanes

One option to improve the performance of a wells turbine is to delay the airfoil stall. To achieve this, guide vanes can be installed on the rotors hub. These vanes are used to reduce the swirl losses at the turbine exit. [1].

3.2 Hysteretic behaviour

Because of reciprocating flow there is a hysteretic loop in the performance of the Wells turbine. Those Characteristics are produced and affected by the differential pressure caused by different behaviour of waves between push and pull stage [1].

3.3 Multi-plane Wells turbine

It's possible to use multi-planes for Wells turbine. This is useful for high pressure values. These kind of concepts avoid using guide vanes, which results in less maintenance and repair. A multiplane turbine without guide vanes is simple to design but less efficient than with it. There is the possibility to build a turbine with two twin rotors rotating in opposite direction to use the swirl energy at the exit. It also has no guide vanes. [1].

3.4 Flow through Wells turbine

The aim is to design a turbine that has high aerodynamic efficiency and is matched with the OWC system for pressure drop and flow rate, regarding the wide range of sea conditions. The efficiency of aerodynamics increases with flow ratio up to a critical value. It decreases at a turning point. To avoid transonic effects the maximum Mach number on the blades should be less than the critical Mach number.

4 Comparison with other turbines

A lot of self-rectifying air turbines have been improved over the years. Another yet potent turbine is the impulse turbine. It has the potential to be superior to the Wells turbine in overall performancs under irregular flow conditions. Simulations show, that the new biradial impulse turbine has exhibit an overall device performance (71 % efficiency) better than that of a multi stage Wells turbine. It also got the advantage of smaller rotor diameter.

5 Optimization of design

This sections aim is to show methods to optimize the design of Wells turbine to enhance overall performance. Methods are: blade dimension or position, adding a plate on the blade or by creating new blades. Examples of optimization methods are shown in Figure 4.

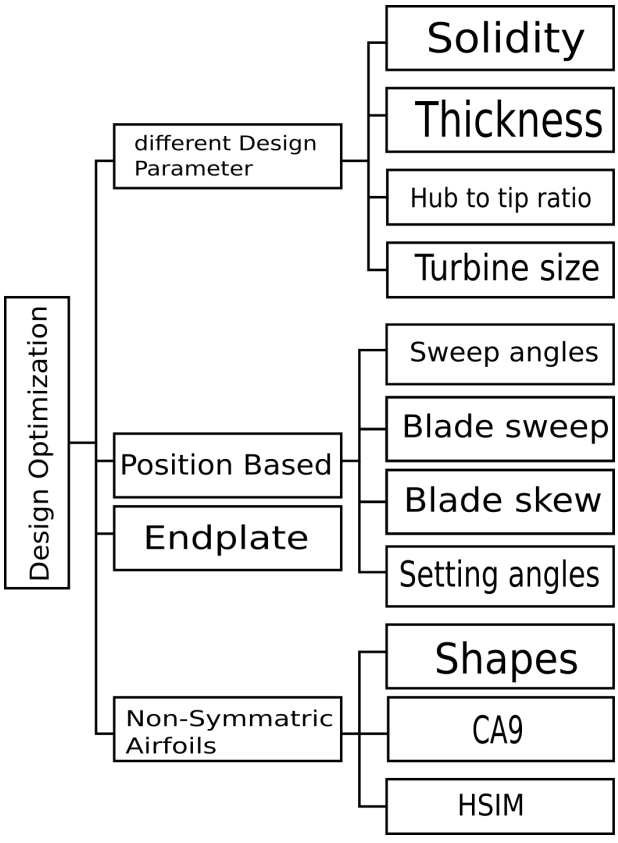

Fig. 4: Design optimisation categories and subcategories.

5.1 Solidity

The prediction methods and the variables that affect the aerodynamic performance of a Wells turbine are discussed in [4]. The increase in blade thickness leads to a larger negative value of torque coefficient, but has

https://doi.org/10.25974/ren_rev_2021_12

a favorable effect on starting. Thicker blade profiles are preferred for small scale turbines, whether thinner profiles are for large-scale turbines. A large solidity is need to self-start the turbine. With the optimal size of turbine, the simulation results in an improvement of 5 % in power output.

5.2 Position based parameter

Changing the position of blade according to the hub center line has a direct effect on performance.
A comparison was made to investigate the aerodynamic performance of backward swept and unswept angle blade for different solidities (σ=0.64 and σ=0.32) for the pitch angles 0° and 20°in [5]. In result: 0° setting pitch angles have shown that the swept back angle blade produces a more positive value of efficiency but at an expense of peak efficiency.

There was an experiment to investigate the influence of the blade sweep ratio on the performance of Wells turbine. In a quasi-steady analysis found in [6], it was found out that blade sweep influenced the performance of Wells turbine. A suitable choice for sweep ratio is 35%.

5.3 End plate

To improve the performance even more there is the option to install an end plate on the blade. Using an experimental model and CFD method [7], results in that the optimal position of the plate is a forward type. It results in an enhancement of peak efficiency of 4 % in comparison to a Wells turbine without the end plate on the blade.

6 Conclusion

This article is a short summary of the state of the art of the Wells turbine. Within this article it's shown, that there are a lot of parameters to look for, which improve and impact the overall performance of the Wells turbine. Most of them are design parameters that have lot of potential for optimization. The following remarks can be concluded:

- Components of Wells turbine are important for performance and efficiency. To harvest the most out of this turbine a lot of optimization in parts is needed
- Guide Vanes and multistage Wells turbines which rotate unidirectional are used to increase the efficiency
- Optimum position of an end plate, optimum value of blade sweep ratio, blade skew and pitch angle increase the efficiency even more

References

[1] A. S. Shehata, Q. Xiao, K. M. Saqr, and D. Alexander. "Wells turbine for wave energy conversion: a review". *International Journal of Energy Research* 41.1 (2017), pp. 6–38. ISSN: 0363907X. DOI: 10.1002/er.3583.

[2] A. F. Falcão and J. C. Henriques. "Oscillating-water-column wave energy converters and air turbines: A review". *Renewable Energy* 85 (2016), pp. 1391–1424. ISSN: 09601481. DOI: 10.1016/j.renene.2015.07.086.

[3] S. Raghunathan. "The wells air turbine for wave energy conversion". *Progress in Aerospace Sciences* 31.4 (1995), pp. 335–386. ISSN: 03760421. DOI: 10.1016/0376-0421(95)00001-F.

[4] S. Raghunathan. "A Methodology for Wells Turbine Design for Wave Energy Conversion". *Proceedings of the Institution of Mechanical Engineers, Part A: Journal of Power and Energy* 209.3 (1995), pp. 221–232. ISSN: 0957-6509. DOI: 10.1243/PIME_PROC_1995_209_040_02.

[5] L. M. C. Gato and M. Webster. "An experimental investigation into the effect of rotor blade sweep on the performance of the variable-pitch Wells turbine". *Proceedings of the Institution of Mechanical Engineers, Part A: Journal of Power and Energy* 215.5 (2001), pp. 611–622. ISSN: 0957-6509. DOI: 10.1243/0957650011538848.

[6] T. Setoguchi, T. W. Kim, M. Takao, A. Thakker, and S. Raghunathan. "The effect of rotor geometry on the performance of a Wells turbine for wave energy conversion". *International Journal of Ambient Energy* 25.3 (2004), pp. 137–150. ISSN: 0143-0750. DOI: 10.1080/01430750.2004.9674953.

[7] M. Takao, T. Setoguchi, Y. Kinoue, and K. Kaneko. "Wells turbine with end plates for wave energy conversion". *Ocean Engineering* 34.11-12 (2007), pp. 1790–1795. ISSN: 00298018. DOI: 10.1016/j.oceaneng.2006.10.009.

Sustainable hydro-power plants with focus on fish-friendly turbine design

*Niklas Olbertz**

Münster University of Applied Sciences, Stegerwaldstraße 39, 48565 Steinfurt, Germany

Abstract

The impact of hydro-power plants on the ecosystem was studied with focus on the fish mortality and types of damage for many years. The fish mortality have a wide range of causes. Types of damage can be different and are caused by different parts of the power plant. The most dangerous part of the system are the fast moving turbine blades. They can cause blade strike and barotrauma due to the high speeds. Different types of turbines were developed for a better survival rate. Five different types of different research groups and manufacturers are presented in this paper. By considering those newly developed turbine designs, a fish survival rate from 96 % to 100 % is achieved.

Keywords: fish-friendly turbine, fish injury, sustainable hydro-power, Alden turbine, Minimum Gap Runner

1 Introduction

Hydro-power stations are an important part of renewable energies. Moreover, they are built in an existing ecosystem and bring about changes. For a good interaction between efficient power station and low harm in the ecosystem they have to be well tested. Fish protection is one big topic for eco-friendly hydro-power stations. If possible, fish are led past the hydro-power plant via a bypass. However, some of the fish is passed through the power plant. To improve a fish-friendly turbine design, we have to understand the way of damage a turbine can cause, so that fish mortality is increased. Mortality can be caused by different parts of the turbine structure and by physical effects in the whole passage.

2 State of the art

2.1 Research methods

To investigate the impact of hydro turbine to different fish species, field and laboratory experiments must be conducted. Three methods provide the common investigation method.

The first method is used in field studies which analyzes the research on balloon-tagged fish [1]. For this method the fish is equipped with an external attachment of a small uninflated balloon-type tag. Injected with a small volume of water the balloon gets inflated with gas. This tag inflates after an adjusted time between 2 to 60 minutes depending on outer parameters e.g. water temperature or configuration of the study site. Preferably the inflation is set to the time the fish passed the turbine passage. The inflated balloon floats on the surface and the fish can be caught and analyzed. This examination method has the disadvantage that the component of the hydro-power station which caused the injury cannot be detected. Another aspect is that the fish has to be handled to attach the balloon-tag, with the result that they are more susceptible to injury.

The use of biotelemetry is another method to study the use of acoustic telemetry. Upstream and downstream sensors can be attached to determine the number of fish that passed the hydro-power plant [2].

Lastly, to study the effect of turbine passage is the use of a sensor fish. This sensor fish is a device which collects data during passing the hydro-power station. It is a small, neutrally buoyant autonomous sensor package [3]. The parameter can be collected are for example the pressure, acceleration and velocity. The sensor fish itself does not conclude that the fish has been injured but in laboratory experiments the measured data can correlated to fish injury [4].

2.2 General problems

Figure 1 shows the possible position for injury in a hydro-power station. At the beginning of the plant passage is the gradually increasing pressure. After this the stay vanes and wicket gates cause strike, collision and shear stress. The turbine itself causes additionally strike, rapidly decreasing pressures and cavitation. In the draft tube and the following underwater passage turbulence causes confusion. Examination of fish have indicated that the ratio of fish length to blade thickness (L/t) is an very important factor to measure

*Corresponding author: niklas.olbertz@fh-muenster.de.

https://doi.org/10.25974/ren_rev_2021_13

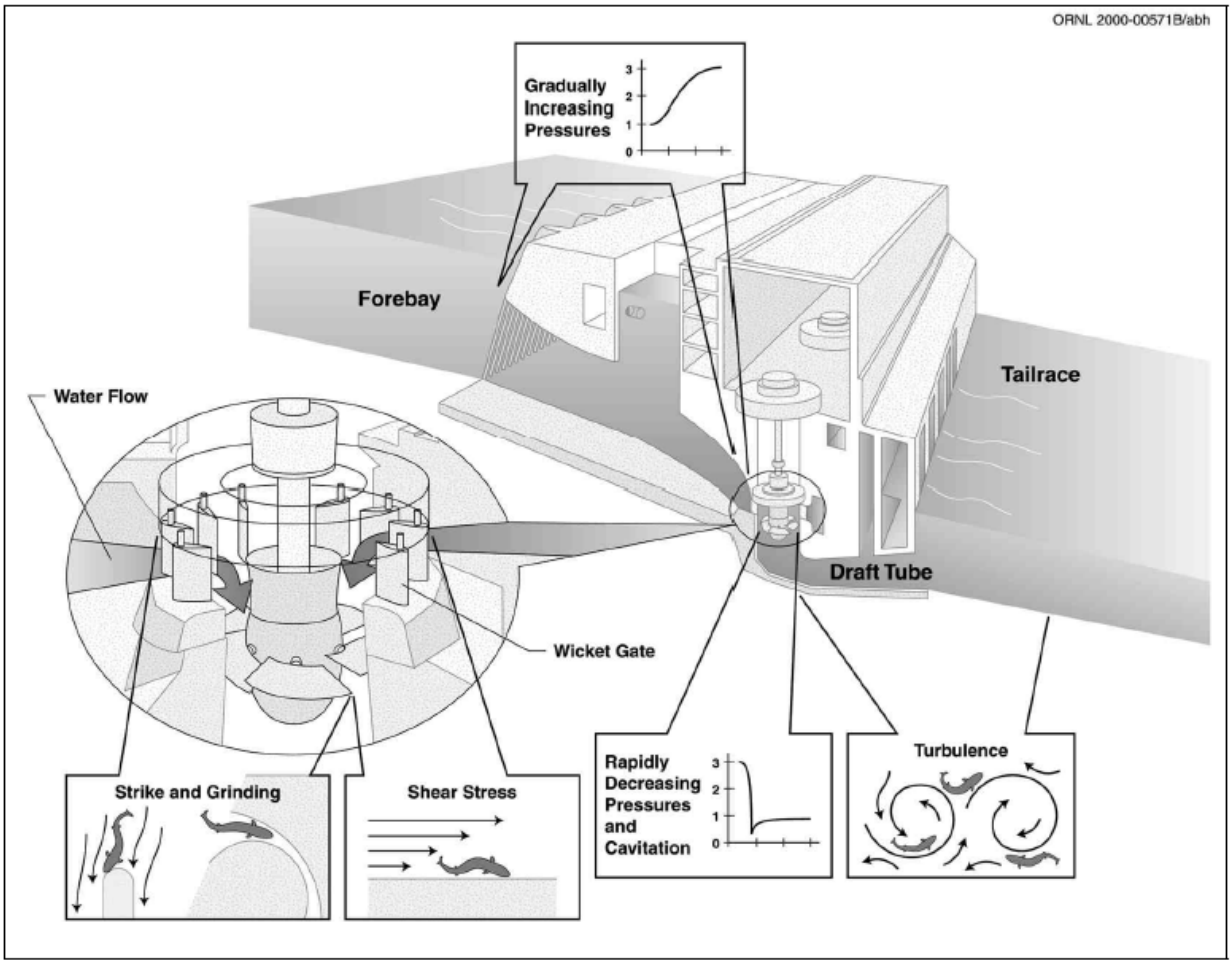

Fig. 1: Possible locations of fish injury passing a hydro-power station [5]

fish mortality [6]. Decreasing the ratio increases the fish survival. Additionally, a higher blade velocity decreases the fish survival. The fish mortality is nearly 0 % with blade velocities of about 5 m/s or less for all fish length-to-blade thickness ratios. Also the slant angle and the position of strike along the body has an effect on the survival rate [7, 8]. Another problem is that the type of turbine, e.g. a Francis or a Kaplan turbine, have different mortality rates.

2.3 Pressure changes

Pressure changes are not always dangerous for fish. If the pressure were slowly decompressed from 101 kPa to 13.8 kPa in more than 3.3 min the fish could expel gas from their swim bladder [9]. The time of decompression is the crucial factor. The intake and stay vane/wicket gate region show a minor change of pressure [3]. When fish pass between turbine blades, there is a sudden drop of pressure, in less than 0.5 s. Martinez et al. [3] measured a wide range of pressure changes between 253 and 860 kPa. The pressure changes below 300 kPa were measured with a fish-friendly turbine. Past the turbine, the pressure slowly increases again in the drafttube.

The rapid decompression can lead to barotrauma, which arises from two different pathways [9]. The first way can be explained by Boyle's Law, shown in equation 1.

$$P_1 \cdot V_1 = P_2 \cdot V_2 \tag{1}$$

The volume of gas is inversely proportional to the pressure. If the surrounding pressure of the fish decreases, the volume will increase. The fast decompression in less than 0.5 s causes ruptured swim bladders, exopthalmia (eyes popped outward), everted stomach or intestine.

The second approach can be explained with Henry's law [9]. Gas can dissolve in body fluids. If the pressure decreases, the solubility will decrease, too. The gas comes out of solution and resulting a bubble formation [10]. Temporarily grown bubbles can lead to great damage of organs and as the gas bubbles increase, they lead to massive internal rupture of vasculature.

https://doi.org/10.25974/ren_rev_2021_13

2.4 Strike and collision

Another cause of injury and mortality for fish is the collision and strike with the turbine blades. Typical characteristics of conventional low head hydro-power turbine are the high rotational speeds, high strike velocities and thin leading edges [7]. The primary source of mortality for fish is collision with the leading edge of turbine blades [11] Mentioned in chapter 2.2 the fish length to blade thickness ratio (L/t) is a good indicator for fish mortality.

The foreseeability of blade-strike injury is higher at low discharge than at high discharge [8]. The probability of strike can be described with equation 2 established by Von Raben (1957) [12].

$$P = \frac{l \cdot cos\theta \cdot n \cdot N}{V_{\text{axial}} \cdot 60} \tag{2}$$

Where l is the length of the fish, θ the angle between the velocity between V_{axial} and $V_{absolute}$, n the number of blades and N the runner speed in revolutions per minute (RPM).

2.5 Grinding, shear stress, cavitation and turbulence

Grinding occurs when a fish is squeezed between narrow gaps of two components of the power plant. In a conventional turbine this happened between the turbine blade and the fixed structures [5]. Shear stress is caused by two parallel bodies of water from different velocities or moving water near a solid structure [13]. The research on shear stress is difficult because in a controlled laboratory environment the reproduction is limited. In up-scaled hydro-power plants the distinction between the different sources of mechanical injury is not straightforward. Turbulence are irregular motions of the water caused by different static and moving components. These turbulence cause localized injuries or disorientation. Cavitation is formation of vapor bubbles caused by extremely low water pressures. The low water pressure is caused by fast rotating turbines.

3 Examples for fish friendly turbine design

3.1 Universal design

In general the turbine efficiency has great effects on fish survival [5]. The cause of physical injury is clearly visible in pressure changes, shear stresses, and turbulence as previously explained. A low operating efficiency caused by adversed turbulence and other losses for example frictional resistance. Those turbulences constitute one particular source of high fish mortality. Optimizing the operating efficiency can improve the survival rate of fish.

Beside the turbine design itself the other components of the whole power station influence the fish mortality. Components, for example the wicket gates or the stay vanes, can be modified in position and geometry: is a minimal spacing between the wicket gate leading edges and stay vane trailing edges important [14]. Otherwise the fish could pass between these components and physical injury are possible. Odeh [15] set up criteria for a fish friendly turbine design. He named a flow rate of 28.3 m^3/s and a head of 23 - 30 m. The minimum pressure is 68.8 kPa with a maximize rate of change of 550.3 kPa/s. The acceptable velocity is about 12 m/s.

3.2 Restoration Hydro Turbine

The Restoration Hydro Turbine (RHT) developed by *Natel Energy* is a turbine with high performance, safe fish passage and a short draft tube [16]. It is optimized for low head between 2 - 10 m with, a single units capacities from 32 kW to 1,400 kW and a flow between 1 and 200 m^3/s. The fish-friendly character is created by special curved turbine blades. With those thick leading edges the turbine reaches an L/t ratio of 2 or less with body lengths up to 400 mm. Additionally the number of blades is reduced compared to conventional turbines. The blunt, slanted leading edge reduces the severity of strike and collision and allowing high runner rpm. According to the manufacturer the most appropriate candidates for RHT retrofit are high-speed, low-head Francis turbines. A RHT prototype unit was tested by Jim Walsh of Rennasonic Inc. with a peak hydraulic efficiency above 90.5 % and good correlation to CFD simulation results. Amaral et al. [7] tested different configurations of the RHT turbine. With a slant angle of 45° and 30° and an L/t of 2 at 10 m/s the survival rate was around 96 % and 98 %.

3.3 Alden turbine

The Alden turbine is a newly developed turbine by the *Voith* company which also provides a fish-friendly system. It was initially developed using two- and three- dimensional Computational Fluid Dynamics (CFD) models [6]. The main changes of the Alden turbine constitute the reduced number of blades, a slower rotational speed and the number of stay vanes and wicket gates was reduced from eighteen, nineteen or twenty to fourteen (each). The Alden turbine is designed with just three runner blades. The other improvement is the slower rotational speed. These two factors provide the main reason for an estimated approximately fish passage survival of 98 % for 200 mm fish and the predicted survival rate of 100 % for fish 100 mm and less in length [14].

https://doi.org/10.25974/ren_rev_2021_13

3.4 Minimum Gap Runner

The Minimum Gap Runner (MGR) is a modified version of the Kaplan turbine in which the gaps between the moving and the static parts are reduced to a minimum at all blade positions. The conventional Kaplan turbine reaches survival rates about 88 % [5]. This modified version can achieve about 98 % to 100 % of survival rates. The first MGR Turbine was installed at the Bonneville Dam between the U.S. states of Washington and Oregon. Beside the good results of fish survival the expected efficiency gain is about 15 % compared to to the old Kaplan turbine [6]. Because of that benefit the Bonneville First Powerhouse replaced all 10 of the old Kaplan turbines with MGRs.

3.5 Very low head

The Very Low Head Turbine (VLH-Turbine) is a developed turbine for net head ranges between 1.5 and 3.4 m [17]. The flow range extends from 10 to 27 m^3/s and the range of power is between 100 and 500 kW per unit. A VLH-Turbine is shown in figure 2. The velocities are between 4.5 and 8 m/s and are

Fig. 2: VLH-Turbine in operation position [17]

lower than the acceptable velocity for the fish friendly design.

3.6 Screw Turbine

Archimedes Screw Turbines are naturally fish-friendly. The normal rotational speed is about 4 m/s. This speed causes no significant pressure changes or damaging shear forces. However, the uses and electrical performances of Archimedes screws are limited. They are suitable for sites with a head of 10 m or less [6]. Rohmer et al. [18] names the following common parameters, shown in table 1, for the application area of screw turbines:

Tab. 1: Most common field application of screw turbines [18]

Parameter	Value
head in m	1 to 6.5
flow rater in m^3/s	0.25 to 6.5
capacity in kW	1.7 to 300
overall efficiency in %	69 - 75

4 Conclusion

The different types of damage at fish show that a fish friendly turbine design is not the single factor to reduce fish mortality. Fish mortality is influenced by different characteristics of the whole power-plant. In addition to the moving components, the static components are also a cause. The different types of damage are rapid pressure changes, strike, grinding, shear stress, turbulence and cavitation. Strike, grinding and shear stress can influenced by different turbine designs. The number of stay vanes and wicket gates or the gap between these are an example for parameters which can be varied. Turbulence and cavitation can be reduced with a good overall efficiency. A lower radial velocity reduce the rapid pressure change. In this case, the best balance must be found between turbine efficiency and fish mortality. The examples of various fish-friendly turbines, that have already been developed, show that it is technically possible to build an economical and efficient turbine. They also show, that different operating places have different requirements to the turbine design for example for different head ranges.

References

[1] P. G. Heisey, D. Mathur, and T. Rineer. “A reliable tag–recapture technique for estimating turbine passage survival: application to young-of-the-year American shad (Alosa sapidissima)”. *Canadian Journal of Fisheries and Aquatic Sciences* 49.9 (1992), pp. 1826–1834.

[2] G. A. McMichael, M. B. Eppard, T. J. Carlson, J. A. Carter, B. D. Ebberts, R. S. Brown, M. Weiland, G. R. Ploskey, R. A. Harnish, and Z. D. Deng. “The juvenile salmon acoustic telemetry system: a new tool”. *Fisheries* 35.1 (2010), pp. 9–22.

[3] J. Martinez, Z. D. Deng, C. Tian, R. Mueller, O. Phonekhampheng, D. Singhanouvong, G. Thorncraft, T. Phommavong, and K. Phommachan. “In situ characterization of turbine hydraulic environment to support development of fish-friendly hydropower guidelines in the lower Mekong River region”. *Ecological engineering* 133 (2019), pp. 88–97.

https://doi.org/10.25974/ren_rev_2021_13

[4] R. S. Brown, T. J. Carlson, A. J. Gingerich, J. R. Stephenson, B. D. Pflugrath, A. E. Welch, M. J. Langeslay, M. L. Ahmann, R. L. Johnson, J. R. Skalski, **et al.**. "Quantifying mortal injury of juvenile Chinook salmon exposed to simulated hydro-turbine passage". *Transactions of the American Fisheries Society* 141.1 (2012), pp. 147–157.

[5] G. F. Čada. "The development of advanced hydroelectric turbines to improve fish passage survival". *Fisheries* 26.9 (2001), pp. 14–23.

[6] T. W. Hogan, G. F. Cada, and S. V. Amaral. "The status of environmentally enhanced hydropower turbines". *Fisheries* 39.4 (2014), pp. 164–172.

[7] S. V. Amaral, S. M. Watson, A. D. Schneider, J. Rackovan, and A. Baumgartner. "Improving survival: injury and mortality of fish struck by blades with slanted, blunt leading edges". *Journal of Ecohydraulics* (2020), pp. 1–9.

[8] Z. Deng, T. J. Carlson, G. R. Ploskey, M. C. Richmond, and D. D. Dauble. "Evaluation of blade-strike models for estimating the biological performance of Kaplan turbines". *Ecological Modelling* 208.2-4 (2007), pp. 165–176.

[9] R. S. Brown, A. H. Colotelo, B. D. Pflugrath, C. A. Boys, L. J. Baumgartner, Z. D. Deng, L. G. Silva, C. J. Brauner, M. Mallen-Cooper, O. Phonekhampeng, **et al.**. "Understanding barotrauma in fish passing hydro structures: a global strategy for sustainable development of water resources". *Fisheries* 39.3 (2014), pp. 108–122.

[10] R. S. Brown, B. D. Pflugrath, A. H. Colotelo, C. J. Brauner, T. J. Carlson, Z. D. Deng, and A. G. Seaburg. "Pathways of barotrauma in juvenile salmonids exposed to simulated hydro-turbine passage: Boyle's law vs. Henry's law". *Fisheries Research* 121 (2012), pp. 43–50.

[11] G. F. Franke, D. Webb, and R. Fisher Jr. *Development of environmentally advanced hydropower turbine system design concepts*. Tech. rep. Lockheed Idaho Technologies Co., 1997.

[12] K Von Raben. "Zur Frage der Beschädigung von Fischen durch Turbinen". *Die Wasserwirtschaft* 4 (1957), pp. 97–100.

[13] G. F. Cada, L. A. Garrison, and R. K. Fisher. "Determining the effect of shear stress on fish mortality during turbine passage". *Hydro Review* 26.7 (2007), p. 52.

[14] D Dixon. *" Fish Friendly" Hydropower Turbine Development and Deployment. Alden Turbine Preliminary Engineering and Model Testing*. Tech. rep. Electric Power Research Institute, Palo Alto, CA (United States), 2011.

[15] M. Odeh. "A summary of environmentally friendly turbine design concepts". *US Department of Energy Idaho Operations Office* (1999).

[16] *Restoration Hydro*. URL: https://www.natelenergy.com/turbines/.

[17] *VLH Turbine*. URL: http://www.vlh-turbine.com/products/vlh-turbine/.

[18] J. Rohmer, D. Knittel, G. Sturtzer, D. Flieller, and J. Renaud. "Modeling and experimental results of an Archimedes screw turbine". *Renewable energy* 94 (2016), pp. 136–146.

A comparison of reverse electrodialysis and pressure retarded osmosis as technologies for salinity gradient power

*Janik Budde**

Münster University of Applied Sciences, Stegerwaldstraße 39, 48565 Steinfurt, Germany

Abstract

The global salinity gradient power (SGP) potential is between 1 650 - 2 000 $\frac{\text{TWH}}{\text{a}}$ and can be converted by mixing two solutions with different salinities. The harnessing of SGP for conversion into power can be accomplished by means of pressure retarded osmosis (PRO) and reverse electrodialysis (RED). PRO and RED are membrane-based technologies and have different working principles. PRO uses a semipermeable membrane to seperate a concentrated salt solution from a diluted solution. The diluted solution flows through the semipermeable membrane towards the concentrated solution, which increases the pressure within the concentrated solution chamber. The pressure is balanced by a turbine and electricity is generated. RED uses the transport of ions through cation and anion exchange membranes. The chambers between the membranes are alternately filled with a concentrated and diluted solution. The salinity gradient difference is the driving force in transporting ions that results in an electric potential, which is then converted to electricity. The comparison shows that there are two different fields of application for PRO and RED. PRO is especially suitable at extracting salinity energy from large concentration differences. In contrast, RED are not effect by increasing concentration differences. So PRO are supposed to focus on applications with brines or waste water and RED on applications with river water and seawater. Moreover, just a few measured values from processes under real conditions are available, which makes it difficult to compare PRO and RED.

Keywords: osmotic power, salinity gradient power, salinity gradient energy, blue energy, pressure retarded osmosis, reverse electrodialysis

1 Introduction

The Covid-19 pandemic has caused high disruption to the energy sector. It is estimated that global energy demand is expected to fall by 5 % and energy-related CO_2 emissions by 7 %. The estimated decline of 8 % in oil demand and 7 % in coal use contrasts with a slight rise in the contribution of renewable energies. Especially an increase of solar and wind power is predicted [1] but both technologies are dependent on the present weather conditions, hence require back up supplies from other sources. Unlike wind and solar power, salinity gradient power (SGP)[1] has the characteristic of a base load source of renewable energy. Therefore SGP is able to generate a constant and reliable supply of power and has also a low environmental impact [2, 3].

SGP is generated by converting the chemical potential difference between two salt solutions with different concentrations into electrical or mechanical energy. It is a clean and sustainable energy source with no toxic gas emissions. SGP is available where salt solutions of different salinity mix, for example where fresh river water flows into the sea, or where industrial brine is discharged [3, 4]. The global energy potential is estimated to be between 1 650 - 2 000 $\frac{\text{TWH}}{\text{a}}$ [2, 4]. The harnessing of this energy for conversion into power can be accomplished by means of pressure retarded osmosis (PRO) and reverse electrodialysis (RED). PRO and RED are the two promising technologies which are at the most advanced stage of development [4].

This short review analyses technical, economical and other aspects in order to show which technology has more promising future prospects. At first PRO and RED are briefly explained. Then follows the comparison with focus on the literature. After that pilot power plants are presented and a conclusion is drawn.

2 Pressure Retarded Osmosis

The energy released through the mixing of fresh water and salt water can be explained using the osmosis effect. Osmosis is the transport of water across a semipermeable membrane from a solution of a lower salt concentration (feed solution) to a solution of a higher salt concentration (draw solution) [2]. The semipermeable membrane retains the passage of salts.

*Corresponding author: janik.budde@fh-muenster.de.

[1] Also known as salinity gradient energy, osmotic power, blue energy

https://doi.org/10.25974/ren_rev_2021_14

The chemical potential difference between both solutions creates a driving force. The water of the feed solution diffuses through the membrane toward the draw solution in order to equalize the chemical potential difference [3]. In PRO, an external hydraulic pressure is applied to the draw solution side. The transport of water molecules into draw solution side leads to the increase of flow rate since the volume is controlled. Then a turbine and generator can be introduced to generate power using the pressurized flow of the diluted draw solution (Figure 1) [5]. The osmotic pressure of a solution can be calculated using the van't Hoff equation, as shown below [3]:

$$\Pi = i \cdot c \cdot R \cdot T \tag{1}$$

Π	Osmotic pressure (Pa)
i	Number of osmotically active particles
c_j	Molar Concentration ($\frac{\text{kmol}}{\text{m}^3}$)
R	Universal gas constant (8314 $\frac{\text{Nm}}{\text{kmol·K}}$)
T	Absolute temperature (K)

For sea water, for example, where the sodium chloride (NaCl) solution ranges from 0.51 - 0.68 $\frac{\text{kmol}}{\text{m}^3}$ and $i = 2$, the osmotic pressure, for a temperature of 25 °C, is between 2.5 and 3.4 MPa [2].

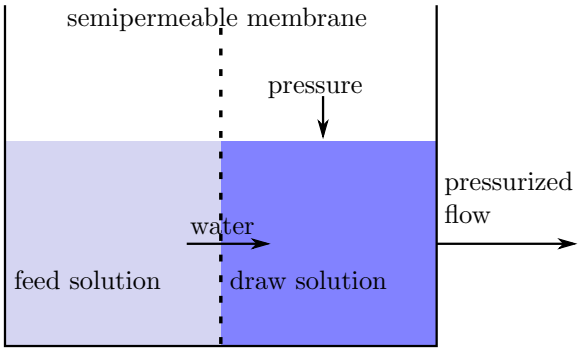

Fig. 1: Pressure retarded osmosis process [5].

3 Reverse Electrodialysis

In RED, the energy of mixing two solutions with different salinity is extracted through the transport of ions. Figure 2 shows the schematic illustration of RED. A concentrated salt solution (e.g. sea water) and a diluted salt solution (e.g. river water) are separated by an alternating series of cation and anion exchange membranes (CEM and AEM). The AEM contain fixed positive charges only allow the selective transport of anions toward the anode, whereas the CEM contain fixed negative charges only allow the selective passage of cations towards the cathode [3]. Salinity gradient and charge segregation induced by ion exchange membranes generate an electrochemical potential. The electrochemical potential difference causes the transport of ions through the membranes. For a sodium chloride solution, sodium ions permeate through the CEM in the direction of the cathode, and chloride ions permeate through the AEM in the direction of the anode. The ionic current is converted into electrical current by redox reactions that occur at the electrodes at the outside of the stack. The redox couple is used to reduce the transfer of electrons. The electrons released at the anode are subsequently transported through an external circuit containing an external load, to the cathode [3, 5].

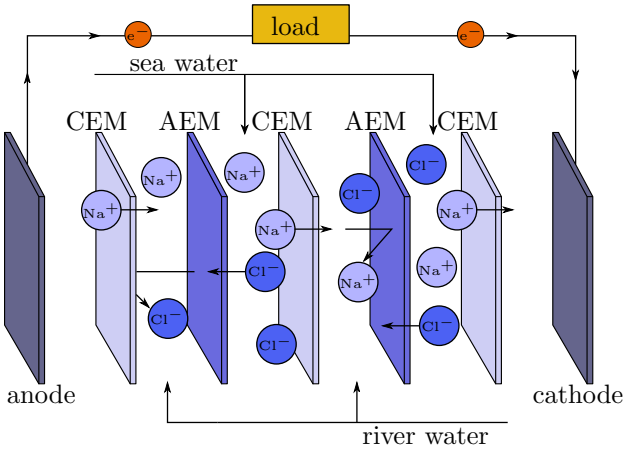

Fig. 2: Schematic illustration of RED. The redox pair helping ionic current to electron flows in the wire, the electrode rinse solution and the brackish water are not depicted [3, 5]. Acronyms: CEM (cation exchange membrane), AEM (anion exchange membrane), Na^+ (sodium-ion), Cl^- (chloride-ion), e^- (electron).

4 Comparison of PRO and RED

In the literature are several publications which only focus on PRO or RED [2, 4, 6, 7] but only a few articles compare these two processes [8, 9]. If only one technology is considered in an article, a comparison is not that easy. There are several reasons for this, for example

- efficiency losses,
- salinities and
- comparative values

are dealt with differently. For PRO the efficiency losses due to conversion of hydrostatic potential energy to electrical energy by a turbine and generator have taken into account. For RED the efficiency losses due to electrode reactions have taken into account. Furthermore, it is important to use the same mixtures of sodium chloride solutions. For PRO the salt concentrations of the diluted solutions are often kept considerably low whereas for RED the salt concentrations of the diluted solutions are higher. Moreover,

https://doi.org/10.25974/ren_rev_2021_14

the only reported measure of performance for each process is often the power density. However, for a comparison several variables have to be considered [8].
Based on this, Post et al. [8] and Yip and Elimelech [9] developed methods which allows a comparison of PRO and RED under equal conditions. In addition to the power density the authors considered the efficiency. The power density ($\frac{W}{m^2}$) is defined as the power produced per unit membrane area and is a measure of how quickly the membranes convert salinity energy to useful work. The efficiency (%) is the ratio of power produced to the amount of free energy which can be obtained from mixing two solutions with different salinities [8, 9].
The study by Post et al. [8] refers to the state-of-the art of PRO and RED in 2006. For power generation from mixing river water and seawater, the results show a higher power density and a higher efficiency for RED. For power generation from mixing a brine and less concentrated water, both are higher for PRO. In further steps the future potential of PRO and RED was considered. Higher performances was achieved for both techniques. According to Post et al., the development should focus on

- membrane characteristics for PRO (i.e. increasing the water permeability of the membrane skin and optimization of the porous support) and
- system characteristics for RED (i.e. optimization of the internal resistance, which is mainly determined by the width of the spacers) [8]

in order to achieve the potential performances. Referring to economic aspects, they assumed two to three times higher membrane costs for RED. However, the installed costs (including membranes, pumps, turbines) were estimated in the same order of magnitude but they assumed decreasing membrane costs for RED. Post et al. assumed in their model a co-current system which is not necessarily applied in practical operation. They also neglected efficiency losses (e.g. friction losses, pump and turbine efficiencies) which have different kinds of effect to PRO than RED [8].
The method of Yip and Elimelech [9] centers on membrane-based performance and was published in 2014. According to the authors, PRO is able to achieve greater efficiency and higher power density performance for a range of salinity gradients, compared to RED. PRO is especially suitable at extracting salinity energy from large concentration differences because PRO effectively uses larger salinity differences for driving force augmentation. As reported by Yip end Elimelech, RED is unable to gain appreciable power density benefits from salinity gradient increases, regardless of membrane transport properties. Furthermore the authors mention that the selectivity of the ion exchange membranes decrease at high solution concentrations, which leads to low efficiencies. So the application of RED energy production is restricted to relatively small salinity gradients. Referring to the economic aspects, Yip and Elimelch calculated higher costs for the ion exchange membranes employed in RED stacks than the semipermeable membranes in PRO modules. According to Yip and Elimelch the development should focus on greater permselectivity and higher conductivity for RED. For PRO, the authors see insufficient membrane robustness to withstand the high pressures due to large salinity gradients. In the study by Yip and Elimelch components like water turbines and pumps were neglected for PRO. This components are significant for converting mechanical energy to electrical energy. In comparison, RED employ a redox couple to convert salinity energy to electrical without mechanical components but also require pumping energy to circulate the solutions through the stack. In addition, foulants were not considered in the input streams, although this reduces the productivity [9].
Both studies come to similar results. However, a closer comparison is achieved when PRO and RED are considered under real operating conditions in pilot power plants.

4.1 PRO pilot power plant

In 2009, the first PRO pilot power plant was opened by the company Statkraft in Tofte (Norway). The pilot plant is equipped with 2 000 m^2 of membranes and has a power density of 1 $\frac{W}{m^2}$. The plant is described to utilize 20 $\frac{l}{s}$ seawater and 13 $\frac{l}{s}$ river water. Crucial for the power performance and reduction of membrane fouling is the pre-treatment of the incoming solutions. Rivers contain significant amounts of organic matter and silt, which contents vary considerably during the seasons. Therefore the pre-treatment for river water consists of a 50-µm pore size filter and a ultrafiltration plant. The pre-treatment of river water is more complex than with seawater because the seawater is supplied through water pipes approximately 35 m below sea level. The pre-treatment based solely on a 50 µm pore size filter. Due to the filtrations and standard maintenance cycle of the membranes, the performance is sustained for 7 - 10 years. The goal of the Statkraft power plant is to reach a power density of 5 $\frac{W}{m^2}$. A power density of 1 $\frac{W}{m^2}$ is not economical. This low power density requires a large area of membranes in order to produce an appreciable power output. For instance, the total membrane area for a 2 MW power plant would have to be 2 km^2 which results in high costs so the business is not financially profitable [2].
The goal of Statkraft, a power density of 5 $\frac{W}{m^2}$, could not be achieved so the pilot power plant was closed in December 2013. Statkraft justified that the technology was not sufficiently developed to become competitive at that time [10].

https://doi.org/10.25974/ren_rev_2021_14

4.2 RED pilot power plant

The Ettore-Infersa saltworks in Marsala (Italy) is one of the most important areas in the Mediterranean Sea for the production of sea salt. Since 2014 the first RED pilot power plant for power production from saline waters and concentrated brines is located in this area. Figure 3 shows the schematic overview of the RED power plant. The seawater flows into brine basins. Due to evaporation, salt concentration increases along the basins ending with a brine saturated in NaCl. The use of brine for RED power production does not compromise the salt production process of the saltworks. The daily volumes required for the RED

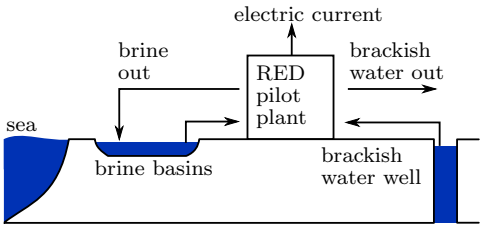

Fig. 3: Schematic overview of the RED power plant in Marsala (Italy) [7].

plant are negligible compared to the total volume of the basins and used brine can be recycled to the basins. A process-scale up of 3 - 4 orders of magnitude in this site considered technologically feasible and well integrated within the conventional production cycle. The installed RED module is equipped with 125 cell pairs and has a total membrane area of 48 m^2. The experimental campaign was from May 2014 to September 2014. The results are shown in Table 1. The yield and efficiency in Table 1 refer to the feed

power (W)	power density ($\frac{W}{m^2}$)	yield $\frac{kWh}{m^3}$	efficiency (%)
35 - 40	1,5 - 1,7	0,03 - 0,06	2 - 3

Tab. 1: Performance indicators of the RED pilot power plant [7].

solution. The net power output oscillated around an average of 25 W. The efficiency is relatively lower than commonly presented values for the RED process (i.e. a range from 10 to 20 %). This is due to the use of highly concentrated brine which leads to a reduction of the membranes permselectivity. The future target was a power capacity of the plant with a magnitude of 1 kW and more than 400 m^2 membrane area [7]. In 2016 a power capacity of 700 W was extracted when using artificial solutions, whereas 50 % decrease in power density was observed when using real solutions like brines seen above [11].
In 2013 started another project at Breezanddijk on the Afsluitsdijk (The Netherlands). In this project a RED pilot power plant with a capacity of 50 kW was build. The installed plant generates electricity by mixing salt water from the North Sea and fresh water from Lake Issel. One goal of the project is to upscale the power plant to 1 MW [4].

5 Discussion and conclusion

In Figure 4 and Figure 5 the results of the studies by Post et al. as well as Yip and Elimelech are quantified. However, the results are not supposed to be overestimated, because the studies were published in different years and the authors applied different models. In another study, a model was developed

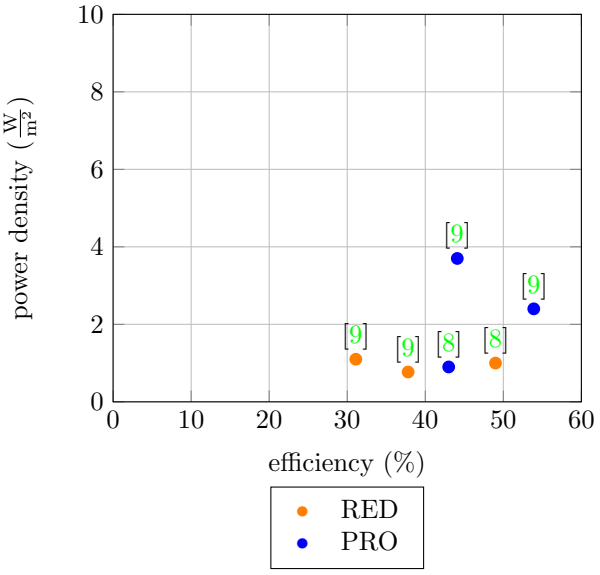

Fig. 4: PRO and RED with seawater and river water as solutions. Diluted solution in the range of 0,0015 - 0,05 $\frac{mol}{l}$ and the concentrated solution in range of 0,5 - 0,6 $\frac{mol}{l}$ [8, 9].

in which full-scale system losses were considered for PRO and RED. The authors wanted to achieve practical values for power density and efficiency. Table 2 shows that the power densities are in range with the results shown in Figure 4 but the efficiencies are lower.
The initial task was to enable a comparison between

technology	power density ($\frac{W}{m^2}$)	efficiency (%)
PRO	2,5	10 - 30
RED	2,0	10 - 20

Tab. 2: Power densities and efficiencies referring to the calculation of Feinberg et al. for river water and seawater [12].

PRO and RED. In this context, the power density and efficiency was considered by analyzing studies. However, PRO and RED have a trade-off between

https://doi.org/10.25974/ren_rev_2021_14

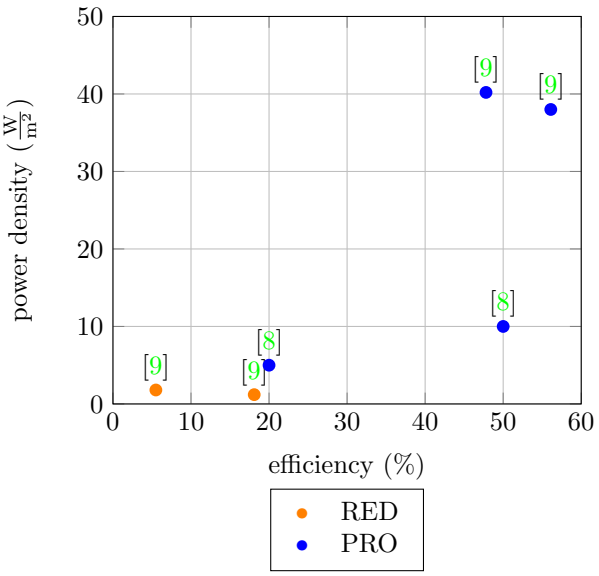

Fig. 5: PRO and RED for higher differences. Diluted solution in the range of 0,017 - 0,05 $\frac{mol}{l}$ and the concentrated solution in range of 4 - 5 $\frac{mol}{l}$ [8, 9].

efficiency and power density. For example, the use of more permeable but less selective membranes increase power density. But due to the uncontrolled mixing, the entropy production increases as well and efficiency is sacrificed [9]. Therefore, power densities and efficiencies vary depending on the selected membranes. Moreover the power density seems to be an unsuitable parameter for comparing PRO and RED. For example both technologies could produce the same power density, yet exhibit different power outputs, efficiencies and system sizes [12].
Finally, the energy costs and the capital cost are the most important factors in comparison between PRO and RED and, ultimately, between SGP and other forms of electricity generation. Since it would not be economically viable to seek complete mixing, the most cost-effective system lengths will lie somewhere between the maximum power density and efficiency [12]. Helfer et al. and Tufa et al. elaborated the costs from the literature (Table 3)[2]. The costs depending on the membrane costs, the solutions and other aspects which specify a wide range [2, 4]. For

technology	capital costs ($\frac{EUR}{kW}$)	energy costs ($\frac{EUR}{kWh}$)
PRO	3 093 - 309 334	0,05 - 0,94
RED	4 500	0,07 - 0,18

Tab. 3: Capital and energy costs for PRO and RED [2, 4].

RED, the capital costs were estimated within the project on the Afsluitsdijk and refer to a 200 kW plant. A calculation for a 200 MW plant resulted in same capital costs ($\frac{EUR}{kW}$). With a load factor of round about 90 %, such a RED plant delivers 1,6 million MWh to the public network. This amount of energy requires between 140 - 240 wind turbines (3 - 5 MW per plant, load factor between 25 - 30 %). The capital costs for wind turbines can be estimated between 1 000 - 2 000 $\frac{EUR}{kW}$, so the investment costs are 700 - 1 400 million euro. The investment costs for the 200 MW RED plant are 900 million euro, so both technologies are comparable [13].
However it is just as difficult to compare the costs as it is difficult to compare power densities and efficiencies because the values referring to different studies with different parameters. Measured values under real operating conditions are required for a comparison of PRO and RED. However, there are only a few power plants running under real operating conditions. An evaluation based on the current number is not sufficient to allow a good evaluation of the technologies. Considering only pilot plants, two promising projects exist for RED. But both projects are still in the testing stage and not commercial. Referring to PRO, the largest power plant has already been closed for economic reasons.
Despite all the challenges, a field of application for SGP will be found because of the need of base-load energy sources. This study has shown that there are different fields of application for PRO and RED. PRO is especially suitable at extracting salinity energy from large concentration differences. In contrast, the power density of RED does not increase strongly with increasing concentration differences. So PRO are supposed to focus on application with brines and RED on applications with river and seawater.

6 Outlook

In this work, only PRO and RED were considered in order to harness salinity gradient power. However, PRO and RED are not the only technologies for salinity gradient power. Future work should also focus on other technologies. For example, researchers of the university of Stanford presented a mixing entropy battery (MEB) in 2019. MEB uses battery electrodes to convert salinity gradient energy into electricity. MEB does not need membranes or turbines and have passed a practical test with waste water and seawater [14].
In addition, the use of hybrid systems can be very efficient. For example, a hybrid RED/ED system can harness salinity gradient power and enable desalination in the process of wastewater treatment [15].
Results from previous studies showed that for PRO and RED the membranes are the key factor. In 2019, researchers of the Rutgers University may have achieved a breakthrough in membrane science. They have found a solution how to use the potential of a

[2] The costs were converted from dollar to euro.

membrane with a boron nitride nanotube (BNNT). One square centimeter of such membrane could produce 30 MWh per year [16].
Following studies should always keep an eye on current developments. As soon as improvements are achieved in membrane science, the possibility of economic power supply due to PRO and RED increases.

References

[1] International Energy Agency. *World energy outlook 2020*. 1. Auflg. Paris: International Energy Agency, 2020. ISBN: 978-92-64-44923-7. URL: https://www.iea.org/reports/world-energy-outlook-2020.

[2] F. Helfer, C. Lemckert, and Y. G. Anissimov. "Osmotic power with Pressure Retarded Osmosis: Theory, performance and trends – A review". *Journal of Membrane Science* 453 (2014), pp. 337–358. ISSN: 0376-7388. DOI: 10.1016/j.memsci.2013.10.053.

[3] K. Nijmeijer and S. Metz. "Chapter 5 Salinity Gradient Energy". *Sustainability Science and Engineering : Sustainable Water for the Future: Water Recycling versus Desalination*. Ed. by I. C. Escobar and A. I. Schäfer. Vol. 2. Elsevier, 2010, pp. 95–139. ISBN: 1871-2711. DOI: 10.1016/S1871-2711(09)00205-0. URL: http://www.sciencedirect.com/science/article/pii/S1871271109002050.

[4] Ramato Ashu, S. Pawlowski, J. Veerman, K. Bouzek, E. Fontananova, G. Di Profio, S. Velizarov, J. Goulão Crespo, K. Nijmeijer, and E. Curcio. "Progress and prospects in reverse electrodialysis for salinity gradient energy conversion and storage". *Applied Energy* 225 (2018), pp. 290–331. ISSN: 0306-2619. DOI: 10.1016/j.apenergy.2018.04.111. URL: http://www.sciencedirect.com/science/article/pii/S0306261918306792.

[5] A. B. Basile, A. Figoli, and A. Cassano, eds. *Current Trends and Future Developments on (Bio-) Membranes: Renewable Energy Integrated with Membrane Operations: Chapter 6 - Pressure Retarded Osmosis and Reverse Electrodialysis*. San Diego: Elsevier, 2018. ISBN: 9780128135457.

[6] A. Achilli, T. Y. Cath, and A. E. Childress. "Power generation with pressure retarded osmosis: An experimental and theoretical investigation". *Journal of Membrane Science* 343.1-2 (2009), pp. 42–52. ISSN: 0376-7388. DOI: 10.1016/j.memsci.2009.07.006. URL: http://www.sciencedirect.com/science/article/pii/S0376738809005134.

[7] M. Tedesco, C. Scalici, D. Vaccari, A. Cipollina, A. Tamburini, and G. Micale. "Performance of the first reverse electrodialysis pilot plant for power production from saline waters and concentrated brines". *Journal of Membrane Science* 500 (2016), pp. 33–45. ISSN: 0376-7388. DOI: 10.1016/j.memsci.2015.10.057. URL: http://www.sciencedirect.com/science/article/pii/S0376738815302878.

[8] J. W. Post, J. Veerman, H. V. Hamelers, G. J. Euverink, S. J. Metz, K. Nymeijer, and C. J. Buisman. "Salinity-gradient power: Evaluation of pressure-retarded osmosis and reverse electrodialysis". *Journal of Membrane Science* 288.1-2 (2007), pp. 218–230. ISSN: 0376-7388. DOI: 10.1016/j.memsci.2006.11.018. URL: http://www.sciencedirect.com/science/article/pii/S0376738806007575.

[9] N. Y. Yip and M. Elimelech. "Comparison of energy efficiency and power density in pressure retarded osmosis and reverse electrodialysis". *Environmental science & technology* 48.18 (2014), pp. 11002–11012. DOI: 10.1021/es5029316.

[10] Statkraft. *Statkraft halts osmotic power investments*. 20.12.2013. URL: https://www.statkraft.com/newsroom/news-and-stories/archive/2013/Statkraft-halts-osmotic-power-investments/ (visited on 12/05/2020).

[11] M. Tedesco, A. Cipollina, A. Tamburini, and G. Micale. "Towards 1 kW power production in a reverse electrodialysis pilot plant with saline waters and concentrated brines". *Journal of Membrane Science* 522 (2017), pp. 226–236. ISSN: 0376-7388. DOI: 10.1016/j.memsci.2016.09.015.

[12] B. J. Feinberg, G. Z. Ramon, and E. M. Hoek. "Scale-up characteristics of membrane-based salinity-gradient power production". *Journal of Membrane Science* 476 (2015), pp. 311–320. ISSN: 0376-7388. DOI: 10.1016/j.memsci.2014.10.023.

[13] J. W. Post, C. H. Goeting, J. Valk, S. Goinga, J. Veerman, H. V. M. Hamelers, and P. J. F. M. Hack. "Towards implementation of reverse electrodialysis for power generation from salinity gradients". *Desalination and Water Treatment* 16.1-3 (2010), pp. 182–193. ISSN: 1944-3994. DOI: 10.5004/dwt.2010.1093.

[14] M. Ye, M. Pasta, X. Xie, K. L. Dubrawski, J. Xu, C. Liu, Y. Cui, and C. S. Criddle. "Charge-Free Mixing Entropy Battery Enabled by Low-Cost Electrode Materials". *ACS omega* 4.7 (2019), pp. 11785–11790. DOI: 10.1021/acsomega.9b00863.

[15] Q. Wang, X. Gao, Y. Zhang, Z. He, Z. Ji, X. Wang, and C. Gao. "Hybrid RED/ED system: Simultaneous osmotic energy recovery and desalination of high-salinity wastewater". *Desalination* 405 (2017), pp. 59–67. ISSN: 00119164. DOI: 10.1016/j.desal.2016.12.005.

[16] R. Service. "Rivers could generate thousands of nuclear power plants worth of energy, thanks to a new 'blue' membrane". *Science* (2019). ISSN: 0036-8075. DOI: 10.1126/science.aba4523. URL: https://www.sciencemag.org/news/2019/12/rivers-could-generate-thousands-nuclear-power-plants-worth-energy-thanks-new-blue.